Institute of Mathematics and Informatics
Bulgarian Academy of Sciences

APPLICATION OF STOCHASTIC AND OPTIMIZATION METHODS FOR RISK MANAGEMENT AND PRICING OF FINANCIAL INSTRUMENTS

Dragomir Colev Nedeltchev

THESIS

for conferring the academic and scientific degree

DOCTOR

in professional field 4.5 Mathematics

(Probability Theory and Mathematical Statistics)

Scientific Advisor:

Associate Professor DSc. Tsvetelin Zaevski

Sofia, 2025

Declaration of Originality

Hereby I declare that the present thesis has been developed by me. I have clearly referenced in the text and the bibliography all sources used in the dissertation.

Preface

The Market Risk holds a special rank among the financial risks since it is located at the cross-road of both exogenous and endogenous factors. It is worth mentioning the role of the supervisory entities among the exogenous factors and the interactions of various risk factors on the contemporary financial markets. An example of endogenous factor is the risk measure that the market participant applies and the interpretation given to the value of the risk measure. The market participants vary in their freedom to select the market measure. The more the market is regulated, the less the freedom. Hence, the exogenous and the endogenous factors intertwingle.

Which risk measure to apply is a choice that depends where we put our focus. If we are interested in a single dot on the left-hand tail of the returns distribution or if we must comply with financial regulations, then we select the Value-at-Risk (VaR) as the risk measure. In case we need information how the left-hand tail behaves beyond a certain threshold and we do not need to back-test the performance of the risk measure, then we pick up the Expected Shortfall (ES). The Expectile VaR (ERM) is selected when the risk measure is expected to bring information about both tails simultaneously and when we need a risk measure that is both coherent and back-testable. The Entropic VaR ($EVaR$) is the preferred risk measure when we have to identify the upper VaR bound at relatively low computations costs and the risk measure must be coherent. The ever enriching family of risk measures comprises members that are designed to capture the particular needs of the market participants.

But selecting the risk measure is not sufficient to mitigate the market risk. The market participant operates on a particular market that is marked with certain patterns. Hence, the risk management toolkit has to adequately reflect the stylized facts of that market. Here, the models for describing the returns dynamics enter the game. A multitude of stochastic processes might

be leveraged to produce the necessary price evolution (some examples – the Black-Scholes model, the exponent tempered stable model, the Heston model, the Bates model, the stochastic volatility tempered stable model, etc.). Most importantly, the financial maturity supposes an optimal mix of returns model and risk measure, for example the underlying asset price follows the Heston model while the market risk is measured via the ERM.

The plan of the dissertation is as follows. The motivation of this study is presented in Chapter 1. Chapter 2 describes the main elements of the risk measures discussed and the stochastic processes applied. The models used to describe the log-returns dynamics are explored in Chapter 3. Currently the supervisors require the banks to apply two quantile-based risk measures (the VaR and the ES) that are discussed in Chapter 4. Chapter 5 presents the expectile-based VaR as a risk measure that remedies the flaws of the VaR and the ES since it is both coherent and elicitable. When we use the Heston model we deal with an unobservable parameter (the initial volatility). Chapter 6 is dedicated to the way we proceed with this model when this parameter is not measurable. During the recent years we witness an increasing number of risk measures designed to meet specific requirements. The Entropic VaR has been created with the purpose to indicate the upper VaR bound at relatively low computational costs. It is presented in Chapter 7. The dissertation combines theoretical and practical aspects of the market risk measurement. In Chapter 8 we empirically challenge the theoretical topics discussed in previous chapters. The constitution of new stylized facts requires the elaboration of the supporting theoretical models. Chapter 9 discusses the Rough Volatility as a feature of the financial markets of the last decade. We conclude by Chapter 10.

Table of Contents

Chapter 1

Introduction

1.1 Aim of the dissertation

The dissertation aims at exploring the application of sophisticated market risk measures to asset log-returns models that capture various patterns of the market realities. At the background of the dissertation are the traditionally applied risk measures like the VaR and the ES, and the pros/cons of these measures that we witness during the last decades. The dissertation contributes to the current quest of risk measures that meet the augmenting business requirements. Recently the ERM and the $EVaR$ drew the attention of the academic community thanks to some advantages, like combining the coherence with the elicitability (in the ERM case) or representing the upper VaR bound (in the $EVaR$ case).

To achieve its goals, the dissertation introduces several theoretical innovations which are empirically challenged via S&P500 index data for a large time period. These data are used to calibrate five stochastic models: the Black-Scholes model, the exponential tempered stable model, the Heston model, the Bates model, the stochastic volatility tempered stable model.

1.2 Actuality of the topic

Risk Measures appear on the agenda of financial mathematicians for two main reasons: providing capital buffers against crises and optimizing portfolio via minimizing its market risk exposure. Regulatory entities issue obligatory for the credit institutions recommendation regarding the capital reserves based

on regulator's acceptance set (see Definition 2.2). Such approach enables the application of multiple ways to measure the risk. Hence, the question arises what is the most appropriate risk measure and, as a consequence, the most conservative one among the various available choices. Risk managers are required to be aware of the ultimate scenario that a portfolio should be ready to face.

The main driver for the risk measures evolution is rules issued by regulatory entities, not the business practice. The beginning was marked by the Basel Accord that the Basel Committee for Banking Supervision (BCBS) enacted in 1988 to regulate the capital requirements (aka Basel I) (on Banking Regulations and Supervisory Practices [148]). The act constitutes the international response to the Latin American debt crisis of 1982. This version of the Accord coined the concept of "risk-weighted" assets but was focused on the Credit Risk until an update in 1996 that added the market risk to the regulatory framework.

The Asian Debt Crisis of 1997 revealed the weaknesses of Basel I and this is why the BCBS issued in 2004 a new version of the Accord known as Basel II. The new Accord recognized and defined the credit risk, the market risk, and the operational risk. It permits banks to use their internal models.

Basel II was severely criticized during the Global Financing Crisis of 2008 (the GFC) and this is why the BCBS published in July 2009 the so-called Basel 2.5 to help the banks mitigate the GFC consequences.

The BCBS adopted Basel III in 2010 (on Banking Supervision[149]). A consultative paper issued in October 2013 announced the fundamental review of the trading books (FRTB) (Committee et al.[50]) and a related Quantitative Impact Study was published in November 2015. In December 2017 the BCBS published amendments to the Basel III framework which is referred to as "Basel IV".

The FRTB (see for example Neisen and Röth[142]) allows the banks to apply either the Standardized Approach (SA) where the supervisor describes the models the banks are allowed to apply or the Internal Model Approach (IMA) where the banks are free to develop and apply their own sophisticated models. Among other things, this overhaul got necessary to solve some drawbacks of the VaR as risk measure: the regulatory bodies and the credit institutions became aware of the inability of VaR to capture the risk accumulated in the returns distribution tail beyond the confidence level. Also, the VaR is not subadditive which means that this measure ignores the portfolio diversification effects. A problematic became the holding period

used for VaR-purposes especially for complex and structured products with long holding period which require many days to be secured or hedged. The applied regulatory framework resulted in a pro-cyclicality since it required calibrating the VaR model for one year. Last but not least, the gap between the SA and IMA widened and the IMA generated disproportionally heavy capital allocation requirements which was contrary to the initial intention of the BCBS.

The FRTB deals with several risk measures. Some capital requirements were based on the 99% VaR with 10 days holding period. The rule to convert the 1-day VaR into a 10-days VaR is overthrown. The Stressed VaR follows the VaR computation algorithm but it covers a one year stress period since 2005 when the portfolio loss reached its maximum. The ES with confidence level of 97.5% was introduced and the holding period varies for the different asset types and might be adjusted for the liquidity of the position. The Incremental Risk Charge was adopted to capture the default and the migration risk, and might be replaced by the Default Risk Charge. Backtesting at trading desk level is used to determine the quality of the applied models for the risk measures.

In the period 2023-2024 the business was looking forward to having the regulators finalizing the FRTB. On the eve of the presidential elections in the USA by the end of 2024, the US supervisors retrieved the Internal Model Approach and left the banks rely on the Standardized Approach which approach leaves no chance to the banks to elaborate and run sophisticated market risk models. Soon, the regulators from the UK and the EU postponed the FRTB-related activities. The dissertation appears in a moment when dominates the uncertainty which direction shall the supervisors take as a next step.

1.3 Methodology

The methodology of the dissertation is based on admitting that the future value of a financial position is a random variable. We consider five stochastic models that capture various features of the position's returns distribution. We extend the modeling toolkit with the Rough Volatility model since this model reflects an emblematic stylized fact of the nowadays financial markets and this way we add the fractional Brownian Motion to the stochastic processes that secure the randomness of the asset returns.

The future value of a financial position produces the returns distribution

which we leverage to figure out what market risk are we exposed to when investing in the position. To this end, we apply a Risk Measure. There is plenty of risk measures and we need some criteria to select the one that meets our particular needs. We agree that the risk measure might be coherent and/or elicitable (i.e. back-testable). We introduce sophisticated risk measures (the ERM and the $EVaR$) based on their features and potential to outperform the currently dominating risk measures: the quantile VaR and the ES.

Alternatively to the established practice, we approach the risk measurement in a different manner. We assume that the considered object, particularly the S&P500 index, is driven by a stochastic process instead of investigating its statistical properties from the empirical data. Once we have chosen the particular stochastic process, we calibrate it to the historical data. There are several important advantages of this approach. First, in this way we can capture some inherent features like fat-tailed and asymmetric distributions, frequent sudden jump movements, leverage effect, volatility clustering, long range dependence, etc., which, directly or indirectly, influence the risk characteristics. On the other hand, the risk is mainly affected by extreme events, i.e. the tail observations. The extreme events are not so many and often it is hard to distinguish them from the so-called statistical errors. This way the used stochastic process treats the missing observations since it filters out the statistical error from the empirical data. Another advantage the dissertation exhibits is the possibility to incorporate an additional information from the real markets. The standard risk measuring approach is based on its historical movements and misses the information available at the derivative markets. Our approach allows extracting this information by a joint calibration to the historical data as well as to the available derivatives – see Zaevski et al.[188]. It is well known that contrary to the main asset, whose behavior is measured by the real-life probability measure, the derivative prices obey to the so-called risk-neutral measure. These two measures are related to each other by some non-changeable parameters – for example in the Black-Scholes model the volatility remains the same under the real world measure and the risk-neutral measure. This way, based on both the asset history and its derivatives' prices, we can describe more realistically the asset and thus more precisely measure its risk. However, this aspect is not the subject of the dissertation and is topic for further researches. We base our approach on five major models which we use to describe the S&P500 index namely the famous Black and Scholes[35] model, exponential tempered stable model (Koponen[116], Rachev et al.[161], Küchler and Tappe[118]) and the models of

Heston[100], Bates[20], and Zaevski et al.[188]. The first two of them are with stationary and independent increments – Gaussian and Lévy style, respectively. Differently to the Gaussian assumption, tempered stable one allows an asymmetry, jumps, and a more mass in the tails. The rest of the models exhibit stochastic volatility – this way we can capture the phenomena of leverage effect, volatility clustering, and long range dependence. In addition, the models of Bates[20] and Zaevski et al.[188] combine all mentioned above market characteristics adding jumps to the Heston framework – the first one by a compound Poisson process with normally distributed innovations, whereas the second one uses infinite activity Lévy processes, particularly tempered stable. A main feature of these models, except the Black and Scholes[35] one, is that they do not have probability density functions in a closed form – only the characteristic functions are available. This requires leveraging Fourier inversion methods.[1]

Our approach to measuring the market risk is based on the assumption that the studied object (asset, stocks, commodity, index) is driven by a stochastic process. We faced the choice to select which models will be the subject of our study. We solved the dilemma by picking up models based on their capability to match the stylized facts such as sudden jumps, strong asymmetry in log-returns' distributions, volatility clustering, leverage effect, long-range dependence, etc. – see Cont[51]. The Gaussian assumptions that lay the ground of the Black and Scholes[35] model do not meet the stylized facts but serve a solid ground to compare the rest of the models. We would like to see asset price dynamics different from the log-normal one and this is why we leveraged the exponential tempered stable model which is closer to the market realities since the asset price dynamics is driven by a process of infinitely small-size jumps – see the survey of Küchler and Tappe[118] as well as the fundamental works of Rachev et al.[161] and Cont and Tankov[53]. It is a stylized fact that the asset returns volatility is a stochastic process and hence the Heston[100] model was added to the set of models we deal with. The dissertation captures the combination of stochastic volatility and asset returns jumps, and this is how we enlarged the set with the model of Bates[20] that use compound Poisson jumps. Last but not least, we selected a stochastic volatility/tempered stable model since this model replaces the finite-number Bates jumps with jumps of infinite activity –see Zaevski

[1]Some similar approaches can be found in Kim et al.[115], Bormetti et al.[36], Rachev et al.[162], and Nguyen and Nguyen[144] .

et al.[188].

The approach we follow has several outstanding advantages over working directly with the empirical observations. First, using an appropriate model we may introduce the well-observed in the markets inherent features into the asset model. Second, the financial risks influence mainly the distributions' tails but these observations are rare or even extremely rare. This does not allow a proper deriving of the risk measures. This is almost true when we work with a moving window with relatively small size. Third, we may use the extracted stochastic process that drive the corresponding model for other financial purpose such as option pricing (see for example Popchev and Velinova[157] and Zaevski and Kounchev[185]), portfolio optimization, etc. Last but not least, the stochastic process introduces a proper structure and fills the gap of limited observations.

The $EVaR$ formula is based on the Moment Generating Function (the MGF) and we derive the MGF for the five models discussed. Three of the considered models (the Heston Model, the Bates Model, and the Stochastic Volatility Tempered Stable) depend on an unobservable state variable (the initial variance). We solve this conundrum by averaging the variance process over its stationary distribution. Also, we identify the diapason where the MGF is well defined.

We leverage the elicitability coined by Gneiting[93] as the necessary condition for the back-testability of measures. The applied approach is based on the idea that the elicitability requires a strictly consistent scoring function with the risk measure. The topic of risk measure elicitability goes beyond the aim of this dissertation and this is why we will complete the discussion by mentioning that Bellini and Bignozzi[23] extended the Gneiting's approach to the risk measure area.

Our methodology deals with risk measures calculation via backward-looking application of several stochastic models. It is worth mentioning this is not the only way to use these models. Financial instruments (incl. derivatives) are priced by a forward-looking run of the same models to the risk factors that drive the instrument's price. In this way we get the future price and its distribution under a new risk measure (the risk-neutral measure). Among other things, we have to verify that the new measure exists, is it unique or there is a multitude of such measures in the case of incomplete markets. To complete the pricing, we have to estimate the expectation of the future price under the risk-neutral measure, discount the future price to the valuation moment (observing the time value of money), and close the

gap between the risk-neutral measure and the real measure by deriving the pricing kernel.

1.4 Original findings

The dissertation contains the following novelties:

1. The considered risk measures are examined under the assumption that the studied object is driven by one of the following five stochastic models – Black-Scholes, Exponential Tempered Stable, Heston, Stochastic Volatility with Compound Poisson Jumps (Bates, SV/CP), and Stochastic Volatility with Tempered Stable Jumps.

2. the ES and the ERM are derived via the usage of truncated expectation;

3. determined is the diapason where the MGF is defined for the Heston returns averaged w.r.t. the initial volatility;

4. derived are the $EVaR$ equations and proved are the conditions for the existence and the uniqueness of the solutions;

5. performed is a detailed empirical research based on historical S&P500 data and the results analyzed per risk measure and per stochastic process;

6. we found that the S&P500 volatility is rough since the Hurst index value is $H < \frac{1}{2}$ and the profile of this value varies within a certain range and moves in packages with transition period between the packages.

7. we found that the relationship between the scaling factor and the Hurst index value is not linear for three indexes (the STOXX50E index, the FTSE index, and the KSE index) while the originating study (Gatheral[87]) concluded this relationship is linear for the S&P500 index.

1.5 Review of the contemporary scientific literature

Before delving into the risk measurement approaches we suggest, let us summarize what is the *status-quo* in this area. Authors from various academic fields have contributed to the base which we will leverage in the next chapters (see for example Popchev et al.[158], Georgieva and Popchev[90]). This chapter reveals some main theoretical findings reached so far.

1.5.1 Quantile Value at Risk and Expected Shortfall

Nowadays, the research on VaR and ES remains a high priority for the academic community. Machine learning approaches based on *Mogrifier* recurrent neural networks are applied to improve the VaR and ES estimation accuracy in Wang et al.[180]. One the other hand, a better estimate of VaR and ES necessitates to leverage different novel sophisticated techniques, for example quantum computing – see Adegbola et al.[4] and Dri et al.[73]. Lévy–VaR and ES are used as alternative to the generalized Pareto VaR and ES, to better comprehend the tail behavior – see Mozumder et al.[139]. Ortega-Jiménez et al.[151] propose to compute the VaR and ES by considering the possible interactions with other observable risks.

Raising the ability to forecast VaR and ES is another domain of contemporary researches. A better forecast is possible for Chinese stock markets when normal and non-normal GARCH-type filters are combined with the extreme value theory – see Tong et al.[177]. On the other hand, Lyu et al.[128] combine the extreme value theory with GARCH-mixed data sampling to forecast the VaR on the crude oil market. VaR and ES forecast improvement is possible when applying machine learning methods like Recurrent Neural Networks and Feed-Forward Neural Networks – see Qiu et al.[159]). There are evidences that the dynamic Gerber model results in better VaR and ES forecasts than alternative parametric, non-parametric and semi-parametric methods for estimating the covariance matrix of returns – see Leccadito et al.[120]. Furthermore, there is a heightened current interest in VaR and ES research for crypto currency markets – see Kamal and Bouri[112]. Also, the portfolio selection and optimization remain a preferred area of researching the VaR and ES during the last couple of years (see for example Gulliksson et al.[96]).

1.5.2 Expectile Value at Risk

Recently published articles (Ziegel[193] and Bellini and Bernardino[22]) mention the drawbacks of the dominating risk measures (discussed in Chapter 4) as arguments to introduce an expectile based risk measure (ERM) - see Chapter 5. A benefactor for selecting it as the next risk measure is the clear economic interpretation of the expectile, see for example Kuan et al.[117]. The closely related notion of *gain-loss ratio* and *omega ratio* are considered in Chen[44]. Adopting the ERM produces some innovations like the application of new ratios to measure the portfolio performance, see for example Lin et al.[122], Avci and Avci[17], Hu and Zheng[103] and Bellini et al.[25]. The expectile captures information about both the left-hand tail of the returns distribution and the right-hand tail thereof which means that a risk measure based on the expectile will reflect both the loss potential and the profit capacity of the position in question; from this viewpoint, an expectile-based risk measure resembles the Rachev ratio (see Biglova et al.[34] and pp. 322-323 of Rachev et al.[160]). The reinsurance business uses the expectile measure under the name *optimal retention*, see Cai and Tan[40], Gerber et al.[91], and Indah and Fadilla[106]. The need to capture the stylized facts of return tails entails attempts to apply heavy tails methods – see Daouia et al.[61], Hu et al.[102], Liu and Wang[123], Opschoor and Lucas[150], Davison et al.[62]. Alternatively, Mihoci et al.[137] use mixing Gaussian and Laplace densities to calculate the ERM and explore its sensitivity and robustness. Tadese and Drapeau[174] demonstrate how to characterize the expectile via the ES, and how to derive the lower and upper bounds of the expectile in terms of the ES. Bellini et al.[26] compare time series of the S&P 500 index through inter-expectile shortfall differences. Based on the VaR, ES, and ERM, Marcin and Schmidt[133] introduce an efficient way to reduce the backtesting bias in the case of heavy-tailed and heteroscedastic data. On the other hand, the authors claim that the expectile might become sensitive to the magnitude of extreme losses by the introduction of the conditional ERM – see Ren et al.[164].

Reliable risk measures are at the core of banks' efforts to correctly estimate the capital reserves (Righi et al.[165]); hence, the asset type (Ahelegbey et al.[5]) and potential asset mispricing (Yang and Ma[183]) have impact on selecting the risk measure. Despite the progress in describing the risk market phenomena, not considered were the possibilities to remedy the drawbacks of the traditional risk measures like the VaR and the ES.

1.5.3 Entropic Value at Risk

Two streams mark the genesis of the $EVaR$: the invention of the Entropic Risk Measure and its adoption in the financial area, and the introduction of the $EVaR$ in the field of operations research. Föllmer and Schied[81] introduced the entropic risk measure and later studied its properties in Föllmer and Schied[82]. Rockafellar et al.[167] elaborated deviation measures and the so-called risk envelopes. Föllmer and Knispel[79] further developed the $EVaR$ concept. Special attention is paid to studying the coherence and the convexity of the new risk measure in Föllmer and Knispel[80] and Brandtner et al.[37]. This theoretical field was expanded further by introducing new entropy-based risk measures. Chengli and Yan[45] elaborated the isoentropic risk measure. Assa et al.[16] introduced the so-called cumulative risk measure. The Weighted Entropic Risk Measure that is consistent with the second-order stochastic dominance and additive for sums of independent random variables is considered in Xia[182]. Zhou et al.[192] discuss the risk measures based on some generalizations of the entropy concept: information entropy, cumulative residual entropy, fuzzy entropy, credibility entropy, sine entropy and hybrid entropy. Generally said, the portfolio optimization is the dominant area of applying the entropic risk measures - see (Zhong[191]).

The $EVaR$ was introduced by Ahmadi-Javid[6] and Ahmadi-Javid[7] as a measure based on the generalized relative entropy where $\ln(\cdot)$ plays the role of a convex function. Delbaen[64] extends the measure as he used Kullback-Leiber divergence for the Kusuoka representation of the $EVaR$. Ahmadi-Javid and Fallah-Tafti[8] prove that contrary to the VaR and the ES, the $EVaR$ is strongly monotone over its domain and strictly monotone over a broad sub-domain including all continuous distributions. Ahmed et al.[10] adjust the new measure to the market realities by adding Rayleigh distribution to the normal one. Mishura et al.[138] elaborate a close form $EVaR$ formula for numerous continuous distributions. Ahmadi-Javid and Pichler[9] leverage the bilateral links between $EVaR$ and norms, and study the metric induced by Banach spaces. Axelrod and Chowdhary[18] prove that the $EVaR$ can be finitely-valued dynamic risk measure if the moment generating function exists.

Substantial efforts are paid to generalize the $EVaR$. For example, Ahmadi-Javid[7] introduces the g-entropic risk measures which include the ES and the $EVaR$, and proves that the $EVaR$ is computationally more efficient than the ES. Pichler and Schlotter[155] extend and generalize the $EVaR$ towards

the Rényi entropies. Furthermore, they replaced the relative entropy in the dual representation with different divergences and so created the f-$EVaR$. Also, Zou et al.[194] challenge the capabilities of the Adjusted Rényi $EVaR$ to deal with different parts of the tail distribution. Jia[109] extends the $EVaR$ into a new coherent uncertain entropic risk measure and verifies the properties of $EVaR$ under uncertain measure (positive homogeneity, translation invariance, monotonicity and subadditivity under independence). The $EVaR$ served the base for the introduction of other risk measures. Chennaf and Amor[46] coin the mean-$EVaR$ model that deals with uncertain random returns. Liu et al.[124] apply the mean-$EVaR$ results in a distributionally robust optimization model. Ardakani[13] develops the multivariate $EVaR$ as a coherent entropic risk measure that encapsulates the integrated risk of various assets in a portfolio. Zou et al.[195] explore the $EVaR$ based on the Tsallis relative entropy and derive explicit formula for the dual Tsallis VaR norm. Yoshioka and Yoshioka[184] apply the Tsallis $EVaR$ to identify the reversion measure when modeling and identifying time series are with a long memory.

The $EVaR$ is calculated through the infimum of the moment generating function. Its dual representation (like every coherent risk measure - see Definition 2.1) is based on finding the optimal probability measure in some sense. Our approach is close to academic articles that deal with the Risk Measure Optimization. For example, Ruszczyński and Shapiro[170] present the optimization by the probability measure and an equivalent solution for optimizing by the decision vector.

1.5.4 Rough Volatility

In 2001 Cont[51] defined the stylized facts as '*A set of properties, common across many instruments, markets and time periods, has been observed by independent studies and classified as "stylized facts"*' and solved the "model vs. data" dilemma in favor of the latter. Also, he introduced the challenges created by the availability of high-frequency data and underlined how important is to have processing power.

Cont explored the qualitative properties of the asset returns while the volatility remains subordinated to the returns in his research. Only four of totally eleven stylized facts deal with volatility features (Intermittency, Volatility clustering, Volume/volatility correlation, Asymmetry in time scales). A separate group of stylized facts comprises interactions between the returns

and the volatility (Conditional heavy tails, Leverage effect).

Since 2001 the majority of the academic efforts remains constrained in verifying that the above stylized facts are still valid. This approach underestimates an important market innovation: the volatility itself became an asset with the introduction of trading derivatives on the VIX Index (in 2004 for VIX futures and in 2006 for VIX options). The basic way to estimate the volatility via returns reinforces the importance of returns-related stylized facts.

Some recent researches establish volatility-related stylized facts when the volatility is estimated from returns. For example, Masset[134] identifies several volatility stylized facts (Horizontal dependence, Extreme events, leverage effects, Vertical dependence) for bull and bear market in emerging and mature markets. Ghosh and co-authors explore the stylized facts for crypto currencies (see Ghosh et al.[92]).

Other studies establish stylized facts for the realized volatility or the historic volatility. For example, Baillie and co-authors focus on the long-memory of the realized volatility (see Baillie et al.[19]). Zumbach[196] explored several stylized facts about the volatility and the volatility increments (Probability Density Function, Moments Scaling, Relative Excess Kurtosis, Lagged Correlation, Realized-Historical Volatility Correlation, Trend and Leverage Effects).

Also, some researchers check the stylized facts of the implied volatility, like the mean-reversion property (Ielpo and Simon[105]), the path-dependency (Wen et al.[181]), etc. which allows its prediction (Goncalves and Guidolin[94]). Sinclair[172] explores several stylized facts of the implied volatility - Volatility Level Dynamics, The Smile and its dynamics, Term Structure Dynamics.

It is emblematic to mention the numerous attempts to preserve the standard Brownian Motion (for the sBM see Section 2.2.1) as the pivotal tool to establish stylized facts: by end-2024 the book Malkiel[129] got its 13th edition. It seems reasonable to ask to what extent our understanding and the admitted stylized facts keep pace with the market evolution. Back in the 80s financial markets were expected to match the Efficient Market Hypothesis Fama[76]. Hence, random walk suffices to describe and forecast the market dynamics Malkiel[129]. A couple of decades later the market ecosystem required the invention of the Fractal Market Hypothesis Peters[153]. Stochastic tools more sophisticated than the random walk were necessary Lo and MacKinlay[126]. Hence, the sBM was replaced by the fBM (for the fBM see Section 2.2.2) even though the latter was added to the Financial

Mathematics' toolkit by Mandelbrot and Van Ness back in 1968 Mandelbrot and Ness[132]. Nowadays, there are attempts to apply the Adaptive Market Hypothesis to the current market realities Lo[125]. But still there is no complete set of stylized facts to adequately describe what we observe on the markets.

Last but not least, let us mention that the available stylized facts have been designed to grasp the market in its equilibrium mode. The financial crisis are considered a non-representative exception that appears unexpectedly and market's memory absorbs its echoes. Key elements of the Fractals Mandelbrot and Hudson[131] and the Chaos Theory Peters[154] were added to the financial toolkit but still no *vivant* set of turmoil stylized facts was nailed down from these theories.

The spillover of the COVID19 pandemic on financial markets exemplified the gaps in our understanding of the globalized markets in turbulence (especially the volatility). Consequently, attempts were done to close these gaps. Vera-Valdés[178] found that the pandemic resulted in a longer memory of the volatility for the VIX Index and the realized variance; also, some volatility measures got non-stationary. Bhattacharjee and co-authors (see Bhattacharjee et al.[31]) reported persistence and drop of the volatility for sectoral indexes on India's National Stock Exchange. Bentes[28] found increased volatility persistence in the G7 markets. Curto and Serrasqueiro[56] focused on three of the Cont's stylized facts (clustering, persistence and asymmetry) of the return volatility and observed differing reaction for eleven S&P500 sector sub-indices. Zhang and Fang[190] explored 5-min time series for CSI300 Index (China) and S&P500 (USA) and found that the multifractal characteristics increased during the pandemic period.

Chapter 2

Preliminaries

Let us introduce some notions common for all chapters of the dissertation. Let $(\Omega, \mathcal{F}, \mathcal{F}_t, \mathbb{P})$ be a filtered probability space, where Ω is a finite sample space, $\mathcal{F}$ is a σ-algebra on Ω, $\mathcal{F}_t$ is a filtration over $\mathcal{F}$, and $\mathbb{P}$ is the probability measure. In financial terms, the set Ω is a collection of all trajectories of the asset prices, $\mathcal{F}$ contains the possible events, and $\mathcal{F}_t$ models the information flow w.r.t. the time. $\mathbb{P}$ measures the probability of the non-sample events of $\mathcal{F}$. Let us denote by $\mathcal{Q}$ the set of the probability measures $\mathbb{Q}$ that are equivalent to $\mathbb{P}$. We denote by $\mathcal{G}$ the set of all random variables on $(\Omega, \mathcal{F}, \mathcal{F}_t, \mathbb{P})$ which in financial terms means the set of all risks. We shall use the notations $f(\cdot)$, $F(\cdot)$, $F^{-1}(\cdot)$, $q(\cdot)$, $\Psi(\cdot)$, and $M(\cdot)$ for the probability density function (PDF), the cumulative distribution function (CDF), the inverted cumulative distribution function (ICDF), the quantile function (QF), the characteristic function (CF), and the moment generating function (MGF) of a random variable ζ respectively. If we need a further clarification, we shall use a lower sub-script – $f_\zeta(\cdot)$, $F_\zeta(\cdot)$, $F_\zeta^{-1}(\cdot)$, $q_\zeta(\cdot)$, $\Psi_\zeta(\cdot)$ and $M_\zeta()$.

We shall use the notations x^+ and x^- for $\max(x, 0)$ and $\max(-x, 0)$.

2.1 Risk Measure

This dissertation deals with the risk measure ρ of position ζ as the mapping $\rho(\zeta) : \mathcal{G} \to \mathbb{R}$. For the discrete case of such mapping see Section 4.1 of Föllmer and Schied[82] and Artzner et al.[15]; for the general case we refer to Delbaen[65]. See also Georgieva and Popchev[89]. We will add structure and financial reasoning to this definition by introducing a special kind of

risk measures – the coherent ones – which the dissertation captures going onwards.

Definition 2.1. *Risk measure $\rho(\cdot)$ that satisfies the conditions below is coherent (see Artzner et al.[15]).*

1. *Translation Invariance: If ζ is a random variable and $x \in \mathbb{R}$, then $\rho(\zeta + x) = \rho(\zeta) - x$.*
2. *Subadditivity: If ζ_1 and ζ_2 are random variables, then $\rho(\zeta_1 + \zeta_2) \leq \rho(\zeta_1) + \rho(\zeta_2)$.*
3. *Monotonicity: If ζ_1 and ζ_2 are random variables and for all sample paths $\zeta_1 \leq \zeta_2$, then $\rho(\zeta_1) \geq \rho(\zeta_2)$.*
4. *Positive homogeneity: If ζ is a random variable and c is a positive constant, then $\rho(c\zeta) = c\rho(\zeta)$.*

What follows is the financial interpretation of the coherence conditions. The Translation Invariance property means that the amount x of a risk-free asset added to position ζ to make the position acceptable for the supervisor shall be reduced from the capital reserves. As a corollary, we get that $\rho(\zeta + \rho(\zeta)) = 0$ and $\rho(x) = \rho(0) - x$, $\forall x \in \mathbb{R}$. No capital reserves will be required, if we add risk-free asset of value equal to the risk measure to a risky position.

The subadditive property reflects the diversification effect according to which the risk of the portfolio $\{\zeta_1, \zeta_2\}$ is not greater than the sum of the risk of each position.

The monotonic property secures that the risk diminishes with the position increase. This conclusion might be exemplified by two call option positions D_1 and D_2 of the same parameters but different strikes $K_{D_1} > K_{D_2}$.

Thanks to the Positive homogeneity property, the risk of a position doubles, if we double the position value.

Following Definition 2.2 of Föllmer and Schied[82], we define the so-called acceptance set as:

Definition 2.2. *The Acceptance Set $\mathcal{A}_\rho$ for risk measure $\rho(\zeta)$ includes the set of positions for which*

$$\mathcal{A}_\rho = \{\zeta \in \mathcal{G} \mid \rho(\zeta) \leq 0\}. \tag{2.1}$$

In other words, the set of positions $\mathcal{A}$ contains acceptable for the supervisor positions since each position of the set poses acceptable for the supervisor level of risk. The supervisor might be a regulator who considers the impact of a risky position, like the national deposit insurance body; clearing firm of a stock exchange which secures the proper execution of financial transactions; or an investment company that instructs its traders when and how to execute fire trade exits.

From Definition 2.2 we conclude that the risk measure can be of negative sign which is not the case of the probability measure and hence the Theory of Measure is inapplicable here. A negative risk measure means that we can take out capital from the investment position and it will still remain safe from the viewpoint of the supervisor.

We can derive the risk measure $\rho(\zeta)$ from the acceptance set $\mathcal{A}$ in the following way:

Proposition 2.1. *The risk measure $\rho(\zeta)$ corresponding to the acceptance set $\mathcal{A}$ is*

$$\rho(\zeta) = \inf \{m \in \mathbb{R} | (m + \zeta) \in \mathcal{A}\}, \tag{2.2}$$

where m is the minimum amount of risk-free investment (default-free zero coupon bond for example - see Zaevski et al.[189]) which if added to the position ζ makes the joint position acceptable for the supervisor.

Proof: See the proof of Proposition 4.6 of Föllmer and Schied[82]. □

There stands a Dual Representation of a coherent risk measure:

Proposition 2.2. *A functional $\rho(\zeta) : \mathcal{G} \to \mathbb{R}$ is a coherent risk measure if and only if there exists a subset $\mathcal{S} \subset \mathcal{Q}$ such that*

$$\rho(\zeta) = \sup_{\mathbb{Q} \in \mathcal{S}} \mathbb{E}_{\mathbb{Q}}[-\zeta], \zeta \in \mathcal{G}. \tag{2.3}$$

Proof: See the proof of Proposition 4.15 of Föllmer and Schied[82]. □

As mentioned earlier, the coherent risk measure involves optimization by probability measure. Further details on such optimization are available in Dentcheva et al.[69], Dentcheva and Stock[68], and Dentcheva and Ruszczynski[67].

2.2 Stochastic Processes

In this section we discuss the stochastic processes covered by the dissertation.

2.2.1 Standard Brownian Motion

Following Definition 2.2.1 of Oksendal[147], we define the Standard Brownian Motion (sBM):

Definition 2.3. *Brownian Motion B_t is a stochastic process with the following properties:*

- $B_0 = 0$.
- *Given $t_1 < t_2 < ... < t_n$, the increments $B_{t_1}, B_{t_2} - B_{t_1}, ..., B_{t_n} - B_{t_{n-1}}$ are independent.*
- *The increments are normally distributed $B_t - B_s \sim N(0, t-s)$.*
- *The paths are continuous.*

2.2.2 Fractional Brownian Motion

Following pp. 5–6 of Biagini et al.[32], we define the Fractional Brownian Motion(fBM) as:

Definition 2.4. *The fBM B_t^H is a continuous and centered Gaussian process with covariance function:*

$$\mathbb{E}\left[B_t^H B_s^H\right] = \frac{1}{2}\left(t^{2H} + s^{2H} - |t-s|^{2H}\right), \tag{2.4}$$

where H is the Hurst index, $H \in (0,1)$, and $0 \leq s < t$.

We need some properties of this process for later chapters:

Property 2.1. *The fBM is marked with several properties:*

- $B_0^H = 0$ *and* $\mathbb{E}\left[B_t^H\right] = 0$ *for all* $t \geq 0$.
- B_t^H *has homogenous increments, i.e.* $B_{t+s}^H - B_s^H$ *has the same law as* B_t^H.

- $\mathbb{E}\left[\left(B_t^H\right)^2\right] = t^{2H}$.
- B_t^H *is a self-similar process, i.e. for all* $a > 0$ $Law\big(B_{at}^H, t \geq 0\big) = Law\big(a^H B_t^H, t \geq 0\big)$.
- *it is not semi-martingale for* $H \neq \frac{1}{2}$.
- *it is not Markovian process for* $H \neq \frac{1}{2}$.

The self-similarity property links two other fBM properties: the long-range dependence of increments and the Hölder continuity of any order less than the Hurst index. These two properties reflect the Hurst index value in the following way:

- when $H = \frac{1}{2}$, we are talking of sBM;
- when $H \in \big(\frac{1}{2}, 1\big)$, we have long-range dependence and smooth paths (smoother than the sBM);
- when $H \in \big(0, \frac{1}{2}\big)$, the process experiences counter-persistence and rough paths (rougher than the sBM).

2.2.3 Lévy Process

Following Chapter 4.6 of Rachev et al.[161], we define the Lévy Process as:

Definition 2.5. *A stochastic process* $X = (X_t)_{t \geq 0}$ *is called a Lévy Process if the following conditions are met:*

- $X_0 = 0$ *a.s.*
- X *has independent increments.*
- X *has stationary increments.*
- X *is stochastically continuous; that is* $\forall t \geq 0$ *and* $a > 0$

$$\lim_{s \to t} \mathbb{P}[|X_s - X_t| > a] = 0. \tag{2.5}$$

- X *is right continuous and has left limits (cadlag).*

2.2.4 Lévy Triplet

Following Proposition 3.2 of Cont and Tankov[53], the characteristic function of the Lévy Process X_t is

$$\Psi(x) = \mathbb{E}[e^{ixX_t}] = e^{t\psi(x)}, \tag{2.6}$$

where $x \in \Re$ and the function $\psi(\cdot)$ is the characteristic exponent. Each Lévy Process has a characteristic exponent of the form (see formula 3.16 of Rachev et al.[161])

$$\psi(x) = \frac{1}{2}\sigma^2 x^2 - i\mu x - \int_{-\infty}^{+\infty} (e^{izx} - 1 - izxI_{[-1,1]}(z))\nu(dz), \tag{2.7}$$

where ν meets the condition

$$\int_{-\infty}^{+\infty} \min\left\{z^2, 1\right\}\nu(dz) < \infty. \tag{2.8}$$

The triplet (μ, σ, ν) is called the Lévy triplet. Following the Lévy-Ito decomposition (see Proposition 3.7 of Cont and Tankov[53]), (μ, σ) reflects the Gaussian part of the process and ν is the Lévy measure which corresponds to the expected number of jumps per unit time. Every Lévy process can be defined by its triplet. On the other hand, each triplet generates a Lévy process.

Let us mention that the Standard Brownian Motion is a Lévy Process with $\mu = 0$, $\sigma = 1$, and $\nu = 0$.

2.2.5 Poisson Process and Compound Poisson Process

Following Proposition 3.5 of Cont and Tankov[53], the Lévy measure of Poisson Process is

$$\nu(A) = \lambda I_{1\in A}, \tag{2.9}$$

where $A \subset \mathbb{R}\backslash\{0\}$ and λ is a positive constant that reads the jump intensity. The characteristic exponent is $\psi(x) = \lambda(\exp(ix) - 1)$.

Compound Poisson Process consists of jumps with size that is $a-priori$ given by a random variable with density $f(\cdot)$. Its Lévy measure is

$$\nu(A) = \lambda \int_A f(u)\, du, \tag{2.10}$$

The characteristic exponent is

$$\psi(x) = \lambda \int_{-\infty}^{\infty} (\exp(ixu) - 1) f(u)\, du. \tag{2.11}$$

2.2.6 Stable Process

The Lévy measure of an α-Stable Process has density of the form (see formula 3.17 of Rachev et al.[161])

$$\nu(x) = \frac{c_1}{(-x)^{1+\alpha}} I_{x<0} + \frac{c_2}{x^{1+\alpha}} I_{x>0} \tag{2.12}$$

for some positive values of c_1 and c_2, and stability index $\alpha \in (0,2)$. The density of its distributions is available in closed form for the process of Cauchy ($\alpha = 1$) and Lévy ($\alpha = 0.5$). For the rest stable processes we apply the characteristic exponent of the form (see formula (11) and (13) of Jalal[107]):

$$\psi(x) = \begin{cases} -\sigma^\alpha |x|^\alpha \left(1 - i\beta \text{sgn}(x) \tan\left(\frac{\pi\alpha}{2}\right)\right) + i\mu x, & \alpha \neq 1 \\ -\sigma |x| \left(1 + i\beta \frac{2}{\pi} \text{sgn}(x) \log(|x|)\right) + i\mu x, & \alpha = 1. \end{cases} \tag{2.13}$$

where

$$\sigma = \begin{cases} \left(\frac{(c_1+c_2)}{\alpha} \Gamma(1-\alpha) \cos\left(\frac{\pi\alpha}{2}\right)\right)^{1/\alpha}, & \alpha \neq 1 \\ \frac{\pi}{2}(c_1 + c_2), & \alpha = 1, \end{cases} \tag{2.14}$$

$$\beta = \frac{c_2 - c_1}{c_1 + c_2} \tag{2.15}$$

$$\mu = \begin{cases} \frac{c_1 - c_2}{1-\alpha}, & \alpha \neq 1 \\ c(c_2 - c_1), & \alpha = 1, \end{cases} \tag{2.16}$$

$$c = \int_1^\infty \frac{\sin(r)}{r^2} dr + \int_0^1 \frac{\sin(r) - r}{r^2} dr \tag{2.17}$$

We have to add to this group the standard Brownian motion which has stability index $\alpha = 2$.

For the properties of the Stable Processes see p. 7 and pp. 61-62 of Rachev et al.[161].

2.2.7 Tempered Stable Process

A Tempered Stable Process is a Lévy process with drift μ and Lévy measure's density (see p. 79 of Rachev et al.[161])

$$\nu(x) = \frac{c_1}{(-x)^{1+\alpha_1}} e^{\lambda_1 x} I_{x<0} + \frac{c_2}{x^{1+\alpha_2}} e^{-\lambda_2 x} I_{x>0}, \tag{2.18}$$

for some positive constants $c_{1,2}$, $\lambda_{1,2}$, and $\alpha_{1,2} \in (0, 2)$. Parameters c_1, λ_1, and α_1 describe the negative jumps and c_2 λ_2, and α_2 are related to the positive ones. The characteristic exponent of this distribution can be written as

$$\psi_{TS}(x) = i\mu x + \psi_1(x) + \psi_2(x), \tag{2.19}$$

where

$$\begin{aligned}
\psi_1(x) &= \begin{cases} \Gamma(-\alpha_1)\lambda_1^{\alpha_1} c_1 \left(\left(1 + \frac{ix}{\lambda_1}\right)^{\alpha_1} - 1 - \frac{ix\alpha_1}{\lambda_1} \right), & if \quad \alpha_1 \neq 1 \\ -ixc_1 + c_1(\lambda_1 + ix) \ln\left(1 + \frac{ix}{\lambda_1}\right), & if \quad \alpha_1 = 1 \end{cases} \\
\psi_2(x) &= \begin{cases} \Gamma(-\alpha_2)\lambda_2^{\alpha_2} c_2 \left(\left(1 - \frac{ix}{\lambda_2}\right)^{\alpha_2} - 1 + \frac{ix\alpha_2}{\lambda_2} \right), & if \quad \alpha_2 \neq 1 \\ ixc_2 + c_2(\lambda_2 - ix) \ln\left(1 - \frac{ix}{\lambda_2}\right), & if \quad \alpha_2 = 1. \end{cases}
\end{aligned} \tag{2.20}$$

The Tempered Stable Process is mainly used in the Financial Mathematics (instead of Stable Process) because the asset returns have distributions with tails that are thinner than the stable distribution (see Grabchak and Samorodnitsky[95]). Also, this process does not have some disadvantages of the stable process: infinite variance and infinite exponential moments (see p. 266 of Bianchi et al.[33] and p. 8 of Rachev et al.[161]). Thanks to these properties, the tempered stable process can be applied to mean-variance portfolio optimization and modeling option prices.

Chapter 3

Models for stock log-returns

The dissertation utilizes several models to describe the stochastic dynamics of the asset returns since we are aware how important is to adequately capture the stylized facts. We shall index all studied terms by the used models instead of the random variables – Black-Scholes (BS), Exponential Tempered Stable (ETS), Heston, Stochastic Volatility with Compound Poisson Jumps (Bates, SV/CP), and Stochastic Volatility with Tempered Stable Jumps (SV/TS).

3.1 Constant Volatility Model

Black and Scholes[35] coined a model that presents the asset price dynamics by a log-normal process of the type

$$dS_t = \mu S_t dt + \sigma S_t dB_t, \tag{3.1}$$

where μ and σ are the asset return and volatility, respectively. B_t is a standard Brownian motion that secures the stochastic nature of the process. After applying Ito Lemma, the asset log-returns of the asset become

$$\zeta_t := \ln\left(\frac{S_t}{S_0}\right) = \left(\mu - \frac{\sigma^2}{2}\right) t + \sigma B_t. \tag{3.2}$$

They are normally distributed with parameters $\left\{\left(\mu - \frac{\sigma^2}{2}\right) t, \sigma\sqrt{t}\right\}$.

Note that the model is based on the assumption that the volatility σ is constant.

3.2 Exponential tempered stable model

In this model the asset dynamics is presented by $S_t = S_0 e^{\zeta_t}$, where ζ_t is a tempered stable process. The model treats the log-returns as a tempered stable process (for details see Cont and Tankov[53] and Rachev et al.[161] and also Section 2.2.7).

3.3 Stochastic Volatility Model of Heston

The Heston[100] model upgrades the Black-Scholes model (3.1) by adding stochasticity to the volatility. The asset is driven by the two-dimensional stochastic differential equation

$$\begin{aligned} dS_t &= \mu S_t dt + \sqrt{V_t} S_t dB_t \\ dV_t &= \xi\left(\eta - V_t\right) dt + \theta\sqrt{V_t} d\tilde{B}_t. \end{aligned} \tag{3.3}$$

The standard Brownian motions B_t and $\tilde{B}_t$ are correlated with the coefficient ρ. The initial volatility $V_0 = v$ is a hidden parameter, not directly observable at the market which we deal with in Section 6.2. The parameter ξ is the speed of reversion to the long-term mean value η and θ is the volatility of the volatility. Thus the Heston's model is driven by five parameters μ, ξ, η, θ, and ρ. If $2\xi\eta \geq \theta^2$, then the process V_t never touches the zero. On the contrary, this is possible when $2\xi\eta < \theta^2$. For more detail, see Feller[77] or Pitman and Yor[156]. The log-price can be written as

$$d\left(\ln\left(S_t\right)\right) = \left(\mu - \frac{V_t}{2}\right) dt + \sqrt{V_t} dB_t. \tag{3.4}$$

We denote $x = ln(S_0)$ and follow formula (15.13) of Cont and Tankov[53] to get the characteristic function of the log-returns

$$\Psi_{Heston}\left(t, x, v; u\right) = \mathbb{E}[e^{iu \ln S_t}] = e^{C(t,u) + vD(t,u) + iux}, \tag{3.5}$$

where

$$
\begin{aligned}
C(t,u) &= \mu u i t + \frac{\xi\eta}{\theta^2}\left[(\xi - \rho\theta u i + d(u))\,t - 2\log\left(\frac{1-g(u)\exp(d(u)t)}{1-g(u)}\right)\right] \\
D(t,u) &= \frac{\xi - \rho\theta u i + d(u)}{\theta^2}\,\frac{1-\exp(d(u)t)}{1-g(u)\exp(d(u)t)} \\
g(u) &= \frac{\xi - \rho\theta u i + d(u)}{\xi - \rho\theta u i - d(u)} \\
d(u) &= \sqrt{(\rho\theta u i - \xi)^2 + \theta^2(u i + u^2)}.
\end{aligned}
\tag{3.6}
$$

3.4 Stochastic volatility jump model of Bates

The Bates[20] model upgrades the Heston model by adding a compound Poisson process with log-normally distributed jumps. Let us denote the compound Poisson process by $\overline{X}_t$, then the asset dynamics is

$$
\begin{aligned}
dS_t &= \mu S_t dt + \sqrt{V_t} S_t dB_t + S_t d\overline{X}_t \\
dV_t &= \xi(\eta - V_t)\,dt + \theta\sqrt{V_t} d\tilde{B}_t.
\end{aligned}
\tag{3.7}
$$

The support of $\overline{X}_t$ is the interval $(-1, +\infty)$ which condition guarantees the positiveness of the asset price process S_t. The intensity of $\overline{X}_t$ is denoted by λ. The jump sizes have log-normal distribution and if $\overline{k}$ denotes the jump size, then $\ln\left(1+\overline{k}\right) \sim N\left(\ln(1+k) - \frac{\delta^2}{2}, \delta\right)$. Thus the model depends on eight parameters μ, ξ, η, θ, ρ, λ, k, and δ. The Bates log-price can be written as

$$
d(\log(S_t)) = \left(\mu - \frac{V_t}{2}\right)dt + \sqrt{V_t} dB_t + dX_t. \tag{3.8}
$$

The process X_t is a compound Poisson with intensity λ and (k, δ)-normally distributed jumps. The characteristic function of the log-price can be presented as a product of two parts – Heston term (3.5) multiplied by the jump characteristic function

$$
\Psi(t, x, v; u) = \Psi_{Heston}(t, x, v; u)\, e^{t\psi_J(u)}, \tag{3.9}
$$

where in this case $\psi_J(u)$

$$\psi_J(u) = \lambda\left(e^{-\frac{\delta^2 u^2}{2}+i\left(k-\frac{\delta^2}{2}\right)u}-1\right). \tag{3.10}$$

3.5 Stochastic volatility/tempered stable model

Contrary to the Bates model, this model contains jumps that are an infinite activity process (Zaevski et al.[188]). The formulas for the asset price and the log-returns, (3.7) and (3.8), still hold but X_t is a tempered stable process [1] with parameters $c_{1,2}$, $\lambda_{1,2}$, and $\alpha_{1,2}$. This way the characteristic function of the asset is presented by formula (3.5), but now the characteristic exponent of the jump process is

$$\psi_J(u) = i\mu x + \psi_1(u) + \psi_2(u), \tag{3.11}$$

where μ is the drift and $\psi_1(\cdot)$ and $\psi_2(\cdot)$ are given in formulas (2.20). This model is driven by eleven parameters μ, ξ, η, θ, ρ, $c_{1,2}$, $\lambda_{1,2}$, and $\alpha_{1,2}$.

[1] The form of $\overline{X}_t$ is available in appendix A of Zaevski et al.[188].

Chapter 4

Quantile-based Risk Measures

This chapter discusses two risk measures that are quantile-based. These are the measures currently used most of all, since Basel IV requires the banks to calculate the capital reserves via the VaR and the ES (see Section 1.2). We present the formulas that define these measures and check whether the measures have the coherence and the elicitability as property. Next, the chapter discusses the dual representation (if available) and the acceptance set. The *pros* and the *cons* of using these measures are also mentioned. We introduce a way to derive the ES via truncated expectation.

4.1 Value at Risk

We can compute the VaR for the discounted P&L distribution or for the (log)-returns distribution. We choose to proceed with the latter approach since the returns are measured in relative terms and therefore are comparable over long time periods, and also are summable (for details see p. 17 of Alexander[11]).

Following formula (6.5) of Rachev et al.[160], we define the VaR:

Definition 4.1. *The VaR is*

$$VaR(\epsilon;\zeta) = -\inf\{x \in \mathbb{R} : \mathbb{P}(\zeta < x) > \epsilon\} \equiv -F^{-1}(\epsilon) \equiv -q_{\zeta}(\epsilon), \quad (4.1)$$

where ζ is the log-returns of the position/portfolio. The significance level $\epsilon \in (0,1)$ and has small values – most common ones are 0.05, 0.025, and 0.01. Since VaR is the opposite of the quantile function, we can derive this

risk measure by computing the CDF, inverting it, and taking the opposite value.

The VaR has the following properties:

- coherence: The VaR is not a coherent risk measure as determined by Definition 2.1 (see for example Acerbi[1] for the argumentation), since it is not sub-additive, i.e. it does not correctly reflect the consequences of the portfolio diversification. However, some authors consider border cases when the VaR becomes a coherent risk measure. For example, Roccioletti[166] mentions that the properties of the loss distribution determine whether a risk measure is sub-additive:

  - The random variables are independent and identically distributed, as well as positively regularly varying. In other words, when the loss distribution is normal, VaR is a coherent risk measure. We find similar opinion in Chapter 4.4.3 of Daníelsson[58]: VaR is sub-additive under the normal distribution where VaR is proportional to volatility, which is sub-additive.
  - The random variables have an elliptical distribution.
  - The random variables have an Archimedean survival dependence structure.

  Also, Daníelsson et al.[60] prove that the VaR is subadditive when the tail index exceeds 2. In other words, the VaR subadditivity depends on the tails features.

- elicitability: The VaR is elicitable risk measure since there is a scoring function that is strictly consistent with the quantile (see formula 5.2 of Thomson[176]). Thanks to its elicitability, the VaR can be backtested (the regulatory requirement to backtest the VaR was discussed in Section 1.2 of the dissertation. Roccioletti[166] provides guidance on how to backtest the VaR).

- A drawback of the VaR is the incapacity to capture the tail behaviour beyond the quantile level (Daníelsson et al.[59]).

- Following Definition 2.2 and Definition 4.1 we conclude that the acceptance set of the VaR is $\mathcal{A}_{VaR_{(\epsilon;\zeta)}} = \{\zeta \in \mathcal{G} \mid q_\zeta(\epsilon) \geq 0\}$.

- There is no dual representation of the VaR since it is not a coherent risk measure - see Proposition 2.2.

4.2 Expected Shortfall

The Expected Shortfall (also known as the averaged VaR or the conditional VaR) compensates the incapability of the VaR to capture the risk beyond the quantile level: it measures the market risk by averaging the VaR beyond the related quantile. We define the ES as follows:

Definition 4.2. *The ES is*

$$ES(\epsilon;\zeta) = \frac{1}{\epsilon}\int_0^{\epsilon} VaR(x;\zeta)dx, \tag{4.2}$$

where ζ stands for the log-returns, and the significance level $\epsilon \in (0,1)$.

Definition 4.2 allows us to derive the ES via the returns CDF, if we leverage the connection between the quantile and the CDF: $ES(\epsilon;\zeta) = -\frac{1}{\epsilon}\int_{-\infty}^{q(\epsilon)} xdF(x)$. When we are given the returns PDF, we can derive the expected shortfall as $ES(\epsilon;\zeta) = -\frac{1}{\epsilon}\int_{-\infty}^{q(\epsilon)} xf_{\zeta}(x)dx$.

The shift stipulated by Basel III from VaR to ES requires to minimize the gap between the capital reserve requirements and hence it is worth knowing the confidence level at which the quantile risk measures produce similar values. It is known that $VaR_{0.01} \approx 2.326348$ (let us remind that Basel III discussed in Section 1.2 stipulates the usage of the 99-th quantile) for the standard normal distributions. To get a relatively similar value, we have to apply $\epsilon = 0.025$ to the ES ($ES_{0.025} \approx 2.337808$).

The quantile risk measures considered in the dissertation differ in the weights assigned to quantiles till ϵ. While the VaR assigns unit weight at ϵ, the ES might assign either equal weights (as in this dissertation; see also Hull[104]) or varying weights (see Storti and Wang[173]).

It is possible to derive the ES through truncated expectations:

Proposition 4.1. *The following statement holds*

$$ES(\epsilon;\zeta) = \frac{\mathbb{E}\left[(\zeta - q(\epsilon))^{-}\right]}{\epsilon} - q(\epsilon). \tag{4.3}$$

Proof: Using the change of variables $s = q(t)$ or equivalently $t = F(s)$, we derive

$$\begin{aligned} ES(\epsilon;\zeta) &= -\frac{1}{\epsilon}\int_0^{\epsilon} q(t)\,dt = -\frac{1}{\epsilon}\int_{-\infty}^{q(\epsilon)} s dF(s) = -\frac{\mathbb{E}\left[\zeta I_{\zeta<q(\epsilon)}\right]}{\epsilon} \\ &= \frac{\mathbb{E}\left[(\zeta - q(\epsilon))^{-} - q(\epsilon) I_{\zeta<q(\epsilon)}\right]}{\epsilon} \\ &= \frac{\mathbb{E}\left[(\zeta - q(\epsilon))^{-}\right]}{\epsilon} - q(\epsilon), \end{aligned} \tag{4.4}$$

which finishes the proof. □

The ES has the following properties:

- coherence: Acerbi and Tasche[3] prove that the ES meets the requirements of a coherent risk measure (see Definition 2.1).
- elicitability: The ES is not an elicitable risk measure (see Tasche[175] and Gneiting[93]), i.e. its point forecasts can't be back-tested. Ziegel[193] disagrees with the Gneiting's approach to proving the ES non-elicitability and proposes another way to verify the ES elicitability. Other authors question the admitted connection between elicitability and capacity to be backtested. Another stream of the academic publications claim that the ES is backtestable: for example, Acerbi and Szekely[2] introduce three model-free, nonparametric ES backtesting methodologies that are empirically tested by Roccioletti[166]. Arguments in favor of the ES backtestability can be found in pp. 58 - 59 of Roccioletti[166]. Chapter 8.4 of Daníelsson[58] suggests a ES backtesting methodology that is analogous to the use of violation ratios for VaR. Chapter 9.3.2 of McNeil et al.[135] proposes to use the magnitudes of VaR violations to backtest estimates of the ES. Christoffersen[49] recommends the application of an extreme value approach to estimate the tail-related risk measures for heteroscedastic financial time series. The non-elicitability of the ES can be remedied by applying two steps VaR-based algorithm (Storti and Wang[173]) or by forecasting the VaR-ES pair (Gao et al.[85]). See also Burzoni et al.[39] for other generalizations of how to solve the ES non-elicitability.

Some authors assume a certain "structure" of the returns distribution tail that allow to backtest the ES (see for example, Chapter 7.5 of Rachev et al.[160]. Two general approaches are feasible:

- Use the tails of the Lévy stable distributions (see Section 2.2.6 of the dissertation) as a proxy for the tail of the returns distribution and use certain semi-analytic formula for the ES to construct a statistical test. The approach is based on the good fit of Lévy stable distribution to returns data and thus the stable tail is a good approximation.
- Assume that the returns distribution belongs to the domain of attraction of a maxstable distribution. Hence, large negative returns are approximated by the limit maxstable distribution and a statistical test can be based on it. Let us mention that a maxstable distribution arises as the limit distribution of properly scaled and centered maxima of i.i.d. random variables.

Following Definition 2.2 and Definition 4.2 we conclude that the acceptance set of the ES is $\mathcal{A}_{ES(\epsilon;\,\zeta)} = \left\{ \zeta \in \mathcal{G} \mid \int_0^{\epsilon} q_\zeta(x)\,dx \geq 0 \right\}$.

Following Proposition 2.2, we may give the following dual representation for the ES:

Theorem 4.1. *The dual representation of the ES is*

$$ES(\epsilon;\zeta) = \sup_{\mathbb{Q}\in\mathcal{S}} \mathbb{E}_{\mathbb{Q}}[-\zeta]\ , \tag{4.5}$$

where the supremum is obtained amongst the set $\left\{\mathbb{Q} \in \mathcal{S} :\ \frac{d\mathbb{Q}}{d\mathbb{P}} \leq \frac{1}{\epsilon},\ \mathbb{P}\ a.s.\right\}$.

For more details see Herdegen and Munari[99], pp. (235, 237) of Föllmer and Schied[82], Hamel[98], Embrechts and Wang[74], or Fuchs et al.[83].

Chapter 5

Expectile-based Value at Risk

For the business it is of utmost importance the way it measures the market risks. This is more than true for supervised entities, like the credit institutions. Banks must obey the requirements of the local regulators. The national bank supervisor adopts the acts of the Basel Committee on Banking Supervision (see Section 1.2) and adjusts their implementation to the regulated entities. Hence, for banks matters the risk measurement approach recommended by the BCBS. Nevertheless, the Internal Model Approach of the FRTB leaves a room for the banks to elaborate and implement more sophisticated than the quantile VaR or ES models which freedom we take advantage of. The aptitude to forecast by a risk measure is important per se (Dai et al.[57], Hallin and Trucíos[97]) and for backtesting purposes – Argyropoulos and Panopoulou[14], Lazar and Xue[119], Brio et al.[38], Dimitriadis and Schnaitmann[70]. Also what matters for selecting a risk measure is the costs of estimating the measure – simple, tractable and transparent estimation are the preferred choice factors, see for example Catania and Luati[42]. We consider a new risk measure (the expectile-based VaR) which is both coherent and elicitable and thus compensates the drawbacks of its ancestors. Something more, the dissertation considers the ERM to be the only coherent and elicitable risk measure.

The invention of a new risk measure entails challenging consequences, like securing a smooth shift to the new measure, to avoid a substantial increase of the required capital reserves. It is currently accepted that this is done by a change of the level (the ϵ in the dissertation) for the new measure and the previous one. Based on the standard normal distribution and many historical observations, the BCBS enforces the 2.5-th percentile of the ES to replace

the 1-st percentile VaR. Later, Li and Wang[121] investigate the probability equivalent level that allows to shift among several risk measures. In the same vein Bellini and Bernardino[22] propose the 0.01 VaR and the 0.25 ES to be accompanied by the 0.00145 expectile. Also, Chen[44] provides further VaR-ES-expectile relations. Unfortunately, this approach can be seriously criticized due to the strongly non-Gaussian structure of the returns distribution observed at financial markets. Another shortcoming of this approach is that the quantile level change leads to adding or loosing some tail/risk information. To avoid these disadvantages, we suggest the use of correction coefficients between the measures – the values of the ES and the ERM are taken not themselves, but multiplied by some coefficients. This way different measures generate relatively similar values preserving the whole tail information. Last but not least, the approach we apply allows a large flexibility and changeability during the time.

This chapter introduces the ERM and its properties. We suggest to compute the ERM via truncated expectation. Contrary to the quantile-based VaR and ES, the ERM is expectile-based which requires us to discuss the expectile.

5.1 Expectiles

The expectile $\phi(\epsilon;\ \zeta)$ is defined firstly in Newey and Powell[143] as the solution of the following square optimization problem

$$\phi(\epsilon;\ \zeta) = \underset{x\in\mathbb{R}}{\arg\min} \left\{ \mathbb{E}\left[\epsilon \left((\zeta - x)^+ \right)^2 + (1-\epsilon) \left((\zeta - x)^- \right)^2 \right] \right\}, \tag{5.1}$$

where $x^- = max(-x, 0)$ and $x^+ = max(0, x)$.

Note that it is well defined only for random variables with finite second moments. For the bivariate and multivariate expectile see Cascos and Ochoa[41]. The analogies with the quantile function become evident when we present the quantile as the solution of the linear optimization problem

$$q(\epsilon;\ \zeta) = \underset{x\in\mathbb{R}}{\arg\min} \left\{ \mathbb{E}\left[\epsilon \left(\zeta - x \right)^+ + (1-\epsilon) \left(\zeta - x \right)^- \right] \right\}. \tag{5.2}$$

The following presentation gives us another viewpoint on the expectile:

Proposition 5.1. *(see formula (2) of Bellini and Bernardino[22]) The expectile is the solution of the equation*

$$\epsilon\mathbb{E}\left[(\zeta - x)^{+}\right] = (1-\epsilon)\,\mathbb{E}\left[(\zeta - x)^{-}\right]. \tag{5.3}$$

To verify that expectiles have properties similar to quantiles (see Newey and Powell[143]), we use an *anteriori* distribution with CDF $F(x)$ and PDF $f(x)$ to construct a *posteriori* distribution with CDF

$$G(x) = \frac{P(x) - xF(x)}{2(P(x) - xF(x)) + x - \mathbb{E}[x]} \tag{5.4}$$

and PDF

$$g(x) = \frac{\mathbb{E}[x]\ F(x) - P(x)}{[2(P(x) - xF(x) + x - \mathbb{E}[x]]^2}, \tag{5.5}$$

where the partial moment $P(x) = \int_{-\infty}^{x} yf(y)dy$.

Thanks to formulas (1.1) and (1.2) of Jones[111], we know that an expectile of the *anteriori* distribution is a quantile of the *posteriori* distribution.

5.2 ERM and its properties

We define the $ERM\,(\epsilon;\ \zeta)$ as follows:

Definition 5.1. *The* $ERM\,(\epsilon;\ \zeta)$ *is the opposite of the expectile* $\phi(\epsilon;\ \zeta)$ *given by formula* (5.1).

The ERM meets the requirements for a coherent and elicitable risk measure:

- coherence: Bellini et al.[24] and Bellini and Bernardino[22] prove that the ERM is law-invariant coherent risk measure for $\epsilon \in (0, 1/2]$.
- elicitability: the elicitability of the ERM is proved in Chapter 9 of McNeil et al.[135] and well presented in Chapter 3.4 of Roccioletti[166]. Nolde and Ziegel[145] and Chen[44] describe how to backtest the ERM.

Based on the above, we conclude that the ERM is both coherent and elicitable risk measure. There are authors who claim that this is the only

Table 5.1: Normally distributed VaR, ES, and ERM for various ϵ

ϵ	VaR_ϵ	ES_ϵ	ERM_ϵ
0.00135000	2.99998	3.28308	0.000127364
0.00353299	2.69372	3.00000	0.000401386
0.010000	2.32648	2.66521	0.00145241
0.025000	1.95996	2.33780	0.00477345
0.050000	1.64485	2.06271	0.0123873

risk measure that meets both criteria (see p. 903 of Ziegel[193]) as long as $\epsilon \leq \frac{1}{2}$.

Being a coherent risk measure, the ERM has a dual representation (see Proposition 2.2). Following formula (2.2) of Drapeau and Tadese[72], we introduce the ERM dual representation:

Proposition 5.2. *The dual representation of the ERM is:*

$$ERM(\epsilon;\ \zeta) = \sup_{\mathbb{Q}\in\mathcal{S}}\ \mathbb{E}_{\mathbb{Q}}[-\zeta], \tag{5.6}$$

where $\mathcal{S} = \left\{\mathbb{Q} \in \mathcal{Q} : \gamma \leq \frac{d\mathbb{Q}}{d\mathbb{P}} \leq \frac{(1-\epsilon)\gamma}{\epsilon}\right\}$ for some $\gamma \in [\frac{\epsilon}{1-\epsilon},\ 1]$.

Bellini et al.[24] give the following presentation of the ERM acceptance set:

$$\mathcal{A}_{ERM(\epsilon;\ \zeta)} = \left\{\zeta \in \mathcal{G} \mid \frac{\mathbb{E}\left[\zeta^+\right]}{\mathbb{E}\left[\zeta^-\right]} \geq \frac{1-\epsilon}{\epsilon}\right\}. \tag{5.7}$$

Following Chen[44], we present in Table 5.1 the values of VaR, ES, and ERM computed for normally distributed returns. We see what we have already mentioned: for normally distributed returns the $VaR_{0.01} \approx ES_{0.025}$. We need different values of the ERM to get the same value for the VaR and the ES: to get $VaR \approx 3$, for example, we need to take the 0.00135-th ERM; to obtain the same value for the ES, i.e. $ES \approx 3$, we have to consider the 0.0035329-th ERM.

Last but not least, let us mention the flaws of the ERM as a risk measure. Chapter 2.4 of Roccioletti[166] enumerates the following drawbacks of the ERM: the concept is less intuitive than the VaR or ES; the expectiles do not observe the comonotonic additive principle which implies that in applications they may fail to detect risk concentration due to non-linear dependencies.

5.3 Some necessary facts

We shall use the following form of the Fourier transform which agrees with the definition of the characteristic function

$$\hat{f}(u) \equiv (Ff)(x) = \int_{-\infty}^{\infty} e^{ixu} f(u)\, dx. \tag{5.8}$$

As usually, we shall notate the real and the imaginary part of a complex number by the symbols $\Re(\cdot)$ and $\Im(\cdot)$, respectively. Let us formulate the following version of the Fourier inverse formula:

Theorem 5.1. *Suppose that for some random variable ζ the constants $a_1 < a_2$ satisfy the condition*

$$\mathbb{E}\left[e^{-a_{1,2}\zeta}\right] < \infty. \tag{5.9}$$

Then for every $b \in (a_1, a_2)$, the PDF of ζ can be obtained by applying inverse Fourier transform to the characteristic function:

$$f_\zeta(x) = \left(F^{-1}\Psi_\zeta\right)(x) = \frac{1}{2\pi} \int_{ib-\infty}^{ib+\infty} e^{-ixu}\Psi_\zeta(u)\, du. \tag{5.10}$$

Proof: We refer to Theorem 7.1.1. of Lukacs[127]. □

Remark 5.1. *Note that the characteristic function $\Psi_\zeta(z)$ is analytical in the whole strip $a_1 < \Im(z) < a_2$ and hence we may use the Cauchy's contour theorem.*

Remark 5.2. *We can think that $a_1 \le 0 \le a_2$, since condition (5.9) holds for $a = 0$. Note that Theorem 5.1 can be rewritten for arbitrary function $f(\cdot)$, not only for PDF. In this case, the inequality $a_1 \le 0 \le a_2$ is not obligatory.*

We need the following lemma.

Lemma 5.1. *We have for arbitrary real v, x, and b*

$$\begin{aligned} \Re\left(\frac{e^{-ixv}\Psi_\zeta(v+ib)}{v+ib}\right) &= -\Re\left(\frac{e^{ixv}\Psi_\zeta(-v+ib)}{-v+ib}\right) \\ \Im\left(\frac{e^{-ixv}\Psi_\zeta(v+ib)}{v+ib}\right) &= \Im\left(\frac{e^{ixv}\Psi_\zeta(-v+ib)}{-v+ib}\right). \end{aligned} \tag{5.11}$$

Proof: The equations (5.11) follows from the fact that the pair

$$\left\{ i\frac{e^{-ixv}\Psi_\zeta\left(v+ib\right)}{v+ib}, i\frac{e^{ixv}\Psi_\zeta\left(-v+ib\right)}{-v+ib} \right\} \tag{5.12}$$

is complex conjugate due to the same fact for the pairs

- $\{e^{-ixv}, e^{ixv}\}$,
- $\{\Psi_\zeta\left(v+ib\right), \Psi_\zeta\left(-v+ib\right)\}$, or
- $\{i\left(v+ib\right), i\left(-v+ib\right)\}$.

□

5.4 Theoretical results

The following presentations for the CDF via the characteristic function is valid:

Proposition 5.3. *(Proposition 3.1 of Zaevski and Nedeltchev[186]) Let the constants $a_1 \leq 0 \leq a_2$ satisfy condition (5.9) and $b \in (a_1, a_2)$. The following three cases arise w.r.t. the sign of b:*

1. *If $b > 0$, then*

$$F_\zeta\left(x\right) = \frac{e^{bx}}{\pi}\int\limits_0^{+\infty} \Im\left(\frac{e^{-ixv}\Psi_\zeta\left(v+ib\right)}{-v-ib}\right)dv. \tag{5.13}$$

2. *If $b < 0$, then*

$$F_\zeta\left(x\right) = 1 - \frac{e^{bx}}{\pi}\int\limits_0^{+\infty} \Im\left(\frac{e^{-ixv}\Psi_\zeta\left(v+ib\right)}{v+ib}\right)dv. \tag{5.14}$$

3. *We have in the limiting case $b = 0$*

$$F_\zeta\left(x\right) = \frac{1}{2} + \frac{1}{\pi}\lim_{\epsilon\to 0}\int\limits_\epsilon^{+\infty} \Im\left(\frac{e^{-ixv}\Psi_\zeta\left(v\right)}{v}\right)dv. \tag{5.15}$$

Remark 5.3. *Additionally to the proof presented below, we refer to Kim et al.*[115] *and Park*[152].

Proof: See Section 5.5. □

Based on Proposition 5.3 for the CDF we can derive the VaR through inverting the CDF and taking the opposite sign.

The next notion we need is the truncated expectation. The following proposition describes it:

Proposition 5.4. *(Proposition 3.2 of Zaevski and Nedeltchev*[186]*) If the constants $a_1 \leq 0 \leq a_2$ satisfy condition (5.9) and $a_1 \leq b_1 < 0 < b_2 \leq a_2$, then*

$$\begin{aligned}
\mathbb{E}\left[(\zeta - x)^{-}\right] &= -\frac{1}{2\pi}\int_{ib_2-\infty}^{ib_2+\infty} \frac{\Psi_\zeta(u)\, e^{-ixu}}{u^2} du = -\frac{e^{b_2 x}}{\pi}\int_0^{+\infty} \Re\left(\frac{e^{-ixv}\Psi_\zeta(v+ib_2)}{(b_2-iv)^2}\right) dv \\
\mathbb{E}\left[(\zeta - x)^{+}\right] &= -\frac{1}{2\pi}\int_{ib_1-\infty}^{ib_1+\infty} \frac{\Psi_\zeta(u)\, e^{-ixu}}{u^2} du = -\frac{e^{b_1 x}}{\pi}\int_0^{+\infty} \Re\left(\frac{e^{-ixv}\Psi_\zeta(v+ib_1)}{(b_1-iv)^2}\right) dv,
\end{aligned} \tag{5.16}$$

where $\Psi(\cdot)$ is the characteristic function. Something more, the following presentations also hold:

$$\begin{aligned}
\mathbb{E}\left[(\zeta - x)^{-}\right] &= \frac{i\Psi'_\zeta(0) + x}{2} - \frac{1}{\pi}\lim_{\epsilon\to 0}\int_\epsilon^{+\infty} \Re\left(\frac{e^{-ixv}\Psi_\zeta(v)}{v^2}\right) dv \\
\mathbb{E}\left[(\zeta - x)^{+}\right] &= -\frac{i\Psi'_\zeta(0) + x}{2} - \frac{1}{\pi}\lim_{\epsilon\to 0}\int_\epsilon^{+\infty} \Re\left(\frac{e^{-ixv}\Psi_\zeta(v)}{v^2}\right) dv.
\end{aligned} \tag{5.17}$$

Proof: See Section 5.5. □

Using Proposition 5.4 for the truncated expectations, we shall prove the following theorem for the ES and ERM.

Theorem 5.2. *(Theorem 3.2 of Zaevski and Nedeltchev[186]) Let* $0 < b_2 < a_2$ *and* $\epsilon < \frac{1}{2}$*. Then the expected shortfall can be derived as*

$$\begin{aligned} ES(\epsilon;\zeta) &= -q_\zeta(\epsilon) - \frac{e^{b_2 q_\zeta(\epsilon)}}{\epsilon\pi} \int_0^{+\infty} \Re\left(\frac{e^{-iq_\zeta(v)v}\Psi_\zeta(v+ib_2)}{(b_2-iv)^2}\right) dv \\ &= \frac{(1-2\epsilon)\,q_\zeta(\epsilon) + i\Psi'_\zeta(0)}{2\epsilon} - \frac{1}{\epsilon\pi}\lim_{\delta\to 0}\int_\delta^{+\infty} \Re\left(\frac{e^{-iq_\zeta(\epsilon)v}\Psi_\zeta(v)}{v^2}\right) dv. \end{aligned} \tag{5.18}$$

The ϵ*-expectile can be obtained as the solution of the following equation w.r.t. the variable* x

$$x = \frac{2(1-2\epsilon)}{\pi}\lim_{\delta\to 0}\int_\delta^{+\infty} \Re\left(\frac{e^{-ixv}\Psi_\zeta(v)}{v^2}\right) dv. \tag{5.19}$$

Alternatively, if $a_1 < b_1 < 0 < b_2 < a_2$*, then we obtain an equivalent to* (5.19) *equation:*

$$\int_0^{+\infty} \Re\left(\frac{\begin{array}{l}(1-\epsilon)\,e^{(b_2-b_1)x}(b_1-iv)^2\Psi_\zeta(v+ib_2) \\ -\epsilon(b_2-iv)^2\Psi_\zeta(v+ib_1)\end{array}}{(b_1-iv)^2(b_2-iv)^2} e^{-ixv}\right) dv = 0. \tag{5.20}$$

Consequently and based on Definition 5.1, the expectile based risk measure, $ERM(\epsilon;\zeta)$*, is the opposite of the solution of equations* (5.19) *and* (5.20)*.*

Proof: Formula (5.18) for the expected shortfall follows from propositions 4.1 and 5.4. Equations (5.19) and (5.20) for the expectile can be obtained through equations (5.2), (5.16) and (5.17), respectively. □

5.5 Proofs

Proof: Proposition 5.3:

Suppose first that $b > 0$. We have

$$\begin{aligned} F_\zeta(x) &= \frac{1}{2\pi} \int_{-\infty}^{x} \int_{ib-\infty}^{ib+\infty} e^{-ivu} \Psi_\zeta(u)\, du dv \\ &= \frac{1}{2\pi} \int_{ib-\infty}^{ib+\infty} \Psi_\zeta(u) \int_{-\infty}^{x} e^{-ivu} dv du \\ &= \frac{i}{2\pi} \int_{ib-\infty}^{ib+\infty} \frac{e^{-ixu} \Psi_\zeta(u)}{u} du \\ &= \frac{i e^{bx}}{2\pi} \int_{-\infty}^{+\infty} \frac{e^{-ixv} \Psi_\zeta(v+ib)}{v+ib} dv \\ &= \frac{e^{bx}}{\pi} \int_{0}^{+\infty} \Im\left(\frac{e^{-ixv} \Psi_\zeta(v+ib)}{-v-ib} \right) dv. \end{aligned} \tag{5.21}$$

We have used above (A) Theorem 5.1, (B) the fact that condition (5.9) allows us to interchange the integration order, (C) $\lim_{v\to-\infty} \left| e^{-i(\beta+ib)v} \right| = \lim_{v\to-\infty} e^{vb} = 0$ for every $\beta \in \mathbb{R}$ and Lemma 5.1.

Let us turn to the case $b < 0$. Having in mind $\lim_{v\to\infty} \left| e^{-i(\beta+ib)v} \right| = \lim_{v\to\infty} e^{vb} = 0$ we analogously obtain for the complementary cumulative distribution function

Figure 5.1: Integration regions

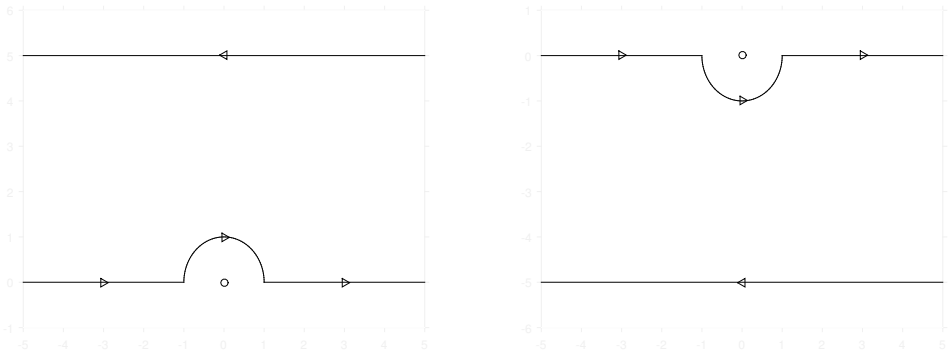

(a) Positive integration region

(b) Negative integration region

$$
\begin{aligned}
1 - F_{\zeta}(x) &= \frac{1}{2\pi} \int_{x}^{+\infty} \int_{ib-\infty}^{ib+\infty} e^{-ivu} \Psi_{\zeta}(u)\, du dv \\
&= \frac{1}{2\pi} \int_{ib-\infty}^{ib+\infty} \Psi_{\zeta}(u) \int_{x}^{+\infty} e^{-ivu} dv du \\
&= -\frac{i}{2\pi} \int_{ib-\infty}^{ib+\infty} \frac{e^{-ixu} \Psi_{\zeta}(u)}{u} du \\
&= \frac{e^{bx}}{\pi} \int_{0}^{+\infty} \Im\left(\frac{e^{-ixv} \Psi_{\zeta}(v+ib)}{v+ib} \right) dv.
\end{aligned}
\tag{5.22}
$$

Finally, let us consider the limiting case $b = 0$. We shall use the Cauchy integral theorem. Note that the integrated function has a singularity for $v = 0$ and hence we can choose an appropriate contour (with infinite endpoints). Let $b \in (a_1, a_2)$ and $b > 0$. We choose the region presented at Figure 5.1a. We have

$$\int\limits_{\overset{\frown}{(-\epsilon,\epsilon)}} \frac{e^{-ixv}\Psi_\zeta(v)}{v}dv = -\frac{1}{2}\oint \frac{e^{-ixv}\Psi_\zeta(v)}{v}dv = -\pi i \tag{5.23}$$

since

$$\operatorname{Res}\left(\frac{e^{-ixv}\Psi_\zeta(v)}{v}, 0\right) = 1. \tag{5.24}$$

Using equation (5.21) we derive

$$\begin{aligned} F_\zeta(x) &= \frac{i}{2\pi}\int\limits_{ib-\infty}^{ib+\infty} \frac{e^{-ixu}\Psi_\zeta(u)}{u}du \\ &= \lim_{\epsilon\to 0}\frac{i}{2\pi}\left(\int\limits_{(-\infty,-\epsilon)\cup(\epsilon,\infty)} \frac{e^{-ixv}\Psi_\zeta(v)}{v}dv + \int\limits_{\overset{\frown}{(-\epsilon,\epsilon)}} \frac{e^{-ixv}\Psi_\zeta(v)}{v}dv\right) \\ &= \frac{1}{2} + \frac{1}{\pi}\lim_{\epsilon\to 0}\int\limits_{\epsilon}^{+\infty} \Im\left(\frac{e^{-ixv}\Psi_\zeta(v)}{v}\right)dv. \end{aligned} \tag{5.25}$$

Analogously, suppose that $a_1 < b < 0$ and let us consider the negative contour at Figure 5.1b. We have

$$\int\limits_{\overset{\frown}{(-\epsilon,\epsilon)}} \frac{e^{-ixv}\Psi_\zeta(v)}{v}dv = \pi i \tag{5.26}$$

due to equation (5.24). Hence, using equation (5.22), we obtain

$$
\begin{aligned}
F_{\zeta}(x) &= 1 + \frac{i}{2\pi} \int_{ib-\infty}^{ib+\infty} \frac{e^{-ixu}\Psi_{\zeta}(u)}{u} du \\
&= 1 + \lim_{\epsilon \to 0} \frac{i}{2\pi} \left(\int_{(-\infty,-\epsilon)\cup(\epsilon,\infty)} \frac{e^{-ixv}\Psi_{\zeta}(v)}{v} dv + \int_{\widehat{(-\epsilon,\epsilon)}} \frac{e^{-ixv}\Psi_{\zeta}(v)}{v} dv \right) \\
&= \frac{1}{2} + \frac{1}{\pi} \lim_{\epsilon \to 0} \int_{\epsilon}^{+\infty} \Im \left(\frac{e^{-ixv}\Psi_{\zeta}(v)}{v} \right) dv.
\end{aligned}
\tag{5.27}
$$

□

Proof: Proposition 5.4: Let us remind the following integral

$$
I(v,u) := \frac{ivu+1}{u^2} e^{-ivu} = \int v e^{-ivu} dv. \tag{5.28}
$$

Having in mind $\lim_{v \to -\infty} |e^{-iuv}| = 0$ and $\lim_{v \to -\infty} |I(v,u)| = 0$ when $\Im(u) = b_2 > 0$ and integral (5.28), we obtain

$$\begin{aligned}
\mathbb{E}\left[(\zeta - x)^{-}\right] &= \frac{1}{2\pi}\int_{-\infty}^{x}(x-v)\int_{ib_2-\infty}^{ib_2+\infty} e^{-ivu}\Psi_\zeta(u)\,dudv \\
&= \frac{1}{2\pi}\int_{ib_2-\infty}^{ib_2+\infty}\Psi_\zeta(u)\int_{-\infty}^{x}(x-v)\,e^{-ivu}dvdu \\
&= \frac{1}{2\pi}\int_{ib_2-\infty}^{ib_2+\infty}\left(\Psi_\zeta(u)\left[ix\frac{e^{-ivu}}{u} - \frac{ivu+1}{u^2}e^{-ivu}\right]\Bigg|_{v=-\infty}^{v=x}\right)du \\
&= -\frac{1}{2\pi}\int_{ib_2-\infty}^{ib_2+\infty}\frac{\Psi_\zeta(u)\,e^{-ixu}}{u^2}du \\
&= \frac{e^{b_2x}}{2\pi}\int_{-\infty}^{+\infty}\frac{e^{-ixv}\Psi_\zeta(v+ib_2)}{(b_2-iv)^2}dv \\
&= \frac{e^{b_2x}}{\pi}\int_{0}^{+\infty}\Re\left(\frac{e^{-ixv}\Psi_\zeta(v+ib_2)}{(b_2-iv)^2}\right)dv
\end{aligned} \tag{5.29}$$

The second statement of formula (5.16) can be obtained similarly to Kim et al.[115], having in mind $\lim_{v\to\infty}|e^{-izv}| = 0$ and $\lim_{v\to\infty}|I(v,z)| = 0$ when $\Im(z) = b_1 < 0$.

The residual at the point zero is

$$\operatorname{Res}\left(\frac{e^{-ixv}\Psi_\zeta(v)}{v^2}, 0\right) = \left.\frac{d\left(e^{-ixv}\Psi_\zeta(v)\right)}{dv}\right|_{v=0} = \Psi_\zeta'(0) - ix. \tag{5.30}$$

Let us take the limit $b_2 \to 0$ in the first part of formula (5.17) and integrate on the contour presented at Figure 5.1a:

$$\begin{aligned}\mathbb{E}\left[(\zeta - x)^{-}\right] &= -\frac{1}{2\pi}\int_{ib_2-\infty}^{ib_2+\infty}\frac{e^{-ixv}\Psi_\zeta(v)}{v^2}dv \\ &= -\lim_{\epsilon\to 0}\frac{1}{2\pi}\left(\int_{(-\infty,-\epsilon)\cup(\epsilon,\infty)}\frac{e^{-ixv}\Psi_\zeta(v)}{v^2}dv + \int_{\overset{\frown}{(-\epsilon,\epsilon)}}\frac{e^{-ixv}\Psi_\zeta(v)}{v^2}dv\right) \\ &= \frac{i\Psi_\zeta^{'}(0)+x}{2} - \frac{1}{\pi}\lim_{\epsilon\to 0}\int_{\epsilon}^{+\infty}\Re\left(\frac{e^{-ixv}\Psi_\zeta(v)}{v^2}\right)dv.\end{aligned} \tag{5.31}$$

We obtain analogously the positive truncated expectation using the Cauchy theorem applied to the contour presented at Figure 5.1b:

$$\begin{aligned}\mathbb{E}\left[(\zeta - x)^{+}\right] &= -\frac{1}{2\pi}\int_{ib_1-\infty}^{ib_1+\infty}\frac{e^{-ixv}\Psi_\zeta(v)}{v^2}dv \\ &= -\lim_{\epsilon\to 0}\frac{1}{2\pi}\left(\int_{(-\infty,-\epsilon)\cup(\epsilon,\infty)}\frac{e^{-ixv}\Psi_\zeta(v)}{v^2}dv + \int_{\overset{\frown}{(-\epsilon,\epsilon)}}\frac{e^{-ixv}\Psi_\zeta(v)}{v^2}dv\right) \\ &= -\frac{i\Psi_\zeta^{'}(0)+x}{2} - \frac{1}{\pi}\lim_{\epsilon\to 0}\int_{\epsilon}^{+\infty}\Re\left(\frac{e^{-ixv}\Psi_\zeta(v)}{v^2}\right)dv.\end{aligned} \tag{5.32}$$

□

Chapter 6

Averaging over the volatility

Here we prepare the ground for the next chapter where we deal with the Moment Generating Function (MGF) of the Heston Model (see Section 3.3). The model poses the challenge to know the initial value of volatility V_t, i.e. v, which is not an observable process for the markets. The solution we suggest is to leverage the Cox-Ingersoll-Ross process that drives the volatility. It has a stationary Gamma distribution and we insert in v the integrated over this distribution volatility. Last but not least, we obtain the positions of the convergence abscissas for the Heston MGF.

6.1 Moment generating function of the Heston's log-returns

It is well-known that differently to the characteristic function, the MGF does not always exist. The following result, which can be found as Theorem 3.1 from del Baño Rollin et al.[63], provides its domain as well as its form:

Proposition 6.1. *(Proposition 2.1 of Zaevski and Nedeltchev[187]) Let the quadratic function $p(x)$ be defined as*

$$\begin{aligned} p(x) &= (\xi - \rho\theta x)^2 + \theta^2 \left(x - x^2\right) \\ &\equiv -x^2\theta^2 \left(1 - \rho^2\right) + x\theta \left(\theta - 2\rho\xi\right) + \xi^2. \end{aligned} \tag{6.1}$$

It has two real roots, possibly infinitely small (large), $-\infty \leq x_1 < 0 < x_2 \leq \infty$, $p(x) > 0$ when $x \in (x_1, x_2)$, and $p(x) < 0$ if $x < x_1$ or $x > x_2$:

$$x_{1,2} = \frac{\theta - 2\rho\xi \pm \sqrt{\theta^2 - 4\rho\theta\xi + 4\xi^2}}{2\theta\left(1-\rho^2\right)}. \tag{6.2}$$

Let $P(x) = \sqrt{|p(x)|}$ *and the function* $g(\cdot)$ *be defined as*

$$\begin{aligned} g(x) &= g_1(x) + (\xi - \rho\theta x)\, g_2(x) \\ g_1(x) &= \cosh\left(\frac{P(x)\,t}{2}\right) I_{x\in(x_1,x_2)} + \cos\left(\frac{P(x)\,t}{2}\right) I_{x\notin(x_1,x_2)} \\ g_2(x) &= \frac{1}{P(x)}\left[\sinh\left(\frac{P(x)\,t}{2}\right) I_{x\in(x_1,x_2)} + \sin\left(\frac{P(x)\,t}{2}\right) I_{x\notin(x_1,x_2)}\right]. \end{aligned} \tag{6.3}$$

The MGF of Heston log-returns can be written as

$$M(z;v) = e^{\omega(z)+v\kappa(z)}, \tag{6.4}$$

where v *is the initial value of the volatility and the functions* $\omega(\cdot)$ *and* $\kappa(\cdot)$ *are defined as*

$$\begin{aligned} \omega(z) &= \frac{2\xi\eta}{\theta^2}\left((\xi - \rho\theta z)\,\frac{t}{2} - \ln g(z)\right) + t\mu z \\ \kappa(z) &= \left(z^2 - z\right)\frac{g_2(z)}{g(z)}. \end{aligned} \tag{6.5}$$

If we need to mark the dependence on t*, we shall use the notations* $\omega(x;t)$ *and* $\kappa(x;t)$ *or* $\omega(\cdot;t)$ *and* $\kappa(\cdot;t)$*. Let us denote the domain of the MGF by* (x^-, x^+)*. The left abscissa of convergence* x^- *is the largest root of the equation* $g(x) = 0$ *smaller than* x_1*. The right abscissa* x^+ *can be obtained through the following statements.*

1. *If* $\xi \geq \rho\theta$*, then* x^+ *is the smallest root of* $g(x) = 0$ *larger than* x_2*.*

2. *If* $\rho = 1$ *and* $2\xi = \theta$*, then*

$$x^+ = \frac{1}{1 - e^{-\xi t}}. \tag{6.6}$$

3. *Let us consider* $\xi < \rho\theta$ *excluding the case* $\rho = 1$ *and* $2\xi = \theta$. *Let* $\bar{t}$ *be defined as*

$$\bar{t} = \frac{2}{\rho\theta x_2 - \xi}. \tag{6.7}$$

   (a) *If* $t < \bar{t}$, *then* x^+ *is the smallest zero of* $g(x)$ *larger than* x_2.

   (b) *If* $t \geq \bar{t}$, *then* x^+ *is the unique root of* $g(x)$ *in the interval* $(1, x_2)$.

We can observe the following immediate corollary:

Corollary 6.1. *(Corollary 2.1 of Zaevski and Nedeltchev[187]) The domain of the MGF of the Heston's log-returns is independent of the initial value of the volatility.*

6.2 Volatility Integration

It is well-known that the CIR process driving the volatility in SDE (3.3) (see Cox et al.[54]) admits a stationary distribution which is a Gamma one with parameters $\alpha = \frac{2\xi}{\theta^2}$ and $\beta = \frac{2\xi\eta}{\theta^2}$. Its density is

$$f_\gamma(u) = \frac{\alpha^\beta}{\Gamma(\beta)} u^{\beta-1} \exp(-\alpha u) I_{u\geq 0}, \tag{6.8}$$

where $\Gamma(\cdot)$ is the Gamma function. Before we continue, we need the following lemma:

Lemma 6.1. *The real part of the function* $D(u)$ *from the characteristic function* (3.5) *is non-positive.*

Proof: The Jensen's inequality leads to

$$|\Psi(u)|^2 = (\mathbb{E}[\cos(X_t u)])^2 + (\mathbb{E}[\sin(X_t u)])^2 \leq 1. \tag{6.9}$$

Suppose that for some u, $\Re D(u) > 0$. Using formula (3.5), we see that

$$|\Psi(u)|^2 = e^{\Re C(u) + v\Re D(u)} \tag{6.10}$$

is larger than one for large enough values of v. This contradicts inequality (6.9). □

As we mentioned in Section 3.3, the initial volatility v in the characteristic function (3.5) is unobservable and thus a natural approach to deal with this problem is to average via the stationary distribution (see for example Dragulescu and Yakovenko[71]). The following proposition allows this:

Proposition 6.2. *(Proposition 3.1 of Zaevski and Nedeltchev[187])*
There exists a random variable $\widetilde{V}$ with characteristic function

$$\begin{aligned}\widetilde{\Psi}(u) &= \int_0^\infty \Psi_{Heston}(u;v)\, f_\gamma(v)\, dv \\ &= \int_0^\infty e^{C(u)+D(u)v} f_\gamma(v)\, dv \\ &= e^{C(u)}\Psi_\gamma(-iD(u)),\end{aligned} \tag{6.11}$$

where $\Psi_\gamma(\cdot)$ is the characteristic function of the Gamma distribution

$$\Psi_\gamma(u) = \left(1-\frac{iu}{\alpha}\right)^{-\beta} \equiv \left(1-\frac{i\theta^2 u}{2\xi}\right)^{-\frac{2\xi\eta}{\theta^2}}. \tag{6.12}$$

Proof: The proof is based on the Bochner's theorem. To use it, we need $\Re D(u) < \alpha$ which is true due to Lemma 6.1. Note that the MGF of the Gamma distribution is well-defined for all values less than α. □

We are ready to investigate the main task of this chapter, namely the domain of the MGF of the random variable $\widetilde{V}$. Let us denote it by $\mathcal{D} \equiv (\widetilde{x}^-, \widetilde{x}^+)$. We shall prove first that $\mathcal{D}$ is a subset of the MGF's domain of the original Heston's log-returns.

Lemma 6.2. *(Lemma 3.2 of Zaevski and Nedeltchev[187]) We have the inclusion $\mathcal{D} \subset (x^-,\ x^+)$.*

Proof: Suppose that $x \in \mathcal{D}$ but $x \notin (x^-,\ x^+)$. Using formula (6.11), we see that the MGF of $\widetilde{V}$ at point x can be written as

$$\widetilde{M}(x) = \int_0^\infty \Psi_{Heston}(-ix;v)\, f_\gamma(v)\, dv. \tag{6.13}$$

On the other hand, Corollary 6.1 gives us that the MGF of the original Heston's log-returns $\Psi(-ix; v)$ diverges for all initial values of the volatility. Hence, integral (6.13) diverges too. □

Lemma 6.3. *(Lemma 3.3 of Zaevski and Nedeltchev[187]) For a fixed t, the function $\kappa(x)$ decreases in the interval $(x^-, 0)$ from $+\infty$ to zero and increases for $x \in (1, x^+)$ from zero to $+\infty$.*

Proof: Using the log-convexity of the MGF, we see that $\omega''(x) + v\kappa''(x) > 0$ for all positive values of v and thus $\kappa''(x)$ is always positive. Hence, the function $\kappa(\cdot)$ is convex in the interval $x \notin (x^-,\ x^+)$ and therefore it has at most two roots in this interval. Something more, the function decreases before the smaller root and increases after the larger one. We finish the proof mentioning that $\kappa(0) = \kappa(1) = 0$ and $\kappa(x^-) = \kappa(x^+) = +\infty$ due to $g(x^-) = g(x^+) = 0$ and formula (6.5). □

As a corollary, we can state our first result:

Theorem 6.1. *(Theorem 3.1 of Zaevski and Nedeltchev[187]) The abscissas of convergence $\widetilde{x}^-$ and $\widetilde{x}^+$ for the random variable $\widetilde{V}$ are the unique roots of the equation $\kappa(x) = \frac{2\xi}{\theta^2}$ in the intervals $(x^-, 0)$ and $(1, x^+)$, respectively. For every $x \in (\widetilde{x}^-, \widetilde{x}^+)$, the MGF is*

$$\widetilde{M}(x) = e^{\omega(x)} \left(1 - \frac{\theta^2 \kappa(x)}{2\xi}\right)^{-\frac{2\xi\eta}{\theta^2}}. \tag{6.14}$$

Proof: The theorem holds because $\kappa(x) < \frac{2\xi}{\theta^2}$ for $x \in (\widetilde{x}^-, \widetilde{x}^+)$ and the domain of the Gamma MGF consists of all points below $\alpha = \frac{2\xi}{\theta^2}$. □

6.3 Positions of the convergence abscissas

Next we discuss the position of $\widetilde{x}^-$ and $\widetilde{x}^+$ w.r.t. x_1 and x_2, where x_1 and x_2 are the roots of function (6.1) and are given by formulas (6.2). We shall investigate separately the cases $|\rho| < 1$ and $|\rho| = 1$.

6.3.1 Main case, $|\rho| < 1$

We need the following lemma:

Lemma 6.4. *(Lemma 3.4 of Zaevski and Nedeltchev[187]) The inequality $\xi - \rho\theta x_1 > 0$ holds. Something more, if $\xi \geq \rho\theta$, then $\xi - \rho\theta x_2 > 0$ too.*

Proof: First we shall prove the result for the lower root x_1. If $\rho \geq 0$, then the inequality holds since $x_1 < 0$. Suppose that $\rho < 0$. Hence, the desired inequality is equivalent to the following ones

$$\begin{aligned}
&\xi > \rho\frac{\theta - 2\rho\xi - \sqrt{\theta^2 - 4\rho\theta\xi + 4\xi^2}}{2\left(1-\rho^2\right)} \text{ due to (6.2)} \\
&\sqrt{\theta^2 - 4\rho\theta\xi + 4\xi^2} < -2\frac{\xi}{\rho} + \theta \\
&\theta^2 - 4\rho\theta\xi + 4\xi^2 < \left(2\frac{\xi}{\rho} - \theta\right)^2 \\
&0 < \left(1-\rho^2\right)(\xi - \theta\rho).
\end{aligned} \tag{6.15}$$

The last equation is true again due to $\rho < 0$.

Let us turn to the statement related to x_2 supposing $\xi \geq \rho\theta$. If $\rho \leq 0$, then the desired result holds since $x_2 > 0$. Assume now that $\rho > 0$. The inequality $\xi - \rho\theta x_2 > 0$ is equivalent to

$$\sqrt{\theta^2 - 4\rho\theta\xi + 4\xi^2} < 2\frac{\xi}{\rho} - \theta. \tag{6.16}$$

Having in mind that the right hand-side of inequality (6.16) is positive (due to $\xi \geq \rho\theta$), we find that it is equivalent to $0 < (1-\rho^2)(\xi - \theta\rho)$ which is true. □

We are ready now to prove the next main results for the position of $\widetilde{x}^-$ and $\widetilde{x}^+$ w.r.t. x_1 and x_2. Let the constants $y_{1,2}$ and $t_{1,2}$ be defined as

$$\begin{aligned}
y_{1,2} &= \pm\frac{2\rho^2 - 1}{\rho} \\
t_{1,2} &= \frac{4\xi}{\theta^2\left(x_{1,2}^2 - x_{1,2}\right) - 2\xi\left(\xi - \theta\rho x_{1,2}\right)}.
\end{aligned} \tag{6.17}$$

Theorem 6.2. *(Theorem 3.2 of Zaevski and Nedeltchev[187])*

We have $\widetilde{x}^- \in (x^-, x_1)$ *in the following cases:* $\left\{\rho \leq \frac{1}{2}\right\}$, $\left\{\rho > \frac{1}{2},\ \frac{\theta}{\xi} \geq y_1 + 2\rho\right\}$, *and* $\left\{\rho > \frac{1}{2},\ \frac{\theta}{\xi} < y_1 + 2\rho, t < t_1\right\}$. *If* $\left\{\rho > \frac{1}{2},\ \frac{\theta}{\xi} < y_1 + 2\rho, t > t_1\right\}$, *then* $\widetilde{x}^- \in (x_1, 0)$. *The equality* $\widetilde{x}^- = x_1$ *holds when* $\left\{\rho > \frac{1}{2},\ \frac{\theta}{\xi} < y_1 + 2\rho, t = t_1\right\}$.

Proof: We shall investigate when $\widetilde{x}^- \in (x^-, x_1)$. This happens when the following equivalent inequalities hold:

$$\begin{aligned} &\kappa(x_1; t) < \frac{2\xi}{\theta^2} \\ &\left(x_1^2 - x_1\right)\frac{g_2(x_1)}{g(x_1)} < \frac{2\xi}{\theta^2} \text{ due to (6.5)} \\ &\frac{x_1^2 - x_1}{\frac{2}{t} + \zeta - \theta\rho x_1} < \frac{2\xi}{\theta^2} \text{ due to } \lim_{x\to 0} x\cot x = 1. \end{aligned} \tag{6.18}$$

Note that the function

$$H(t) = \frac{x_1^2 - x_1}{\frac{2}{t} + \xi - \theta\rho x_1} \tag{6.19}$$

increases from $H(0) = 0$ to $H(\infty) = \frac{x_1^2 - x_1}{\xi - \theta\rho x_1} > 0$ due to Lemma 6.4. We shall check when $H(\infty) \leq \frac{2\xi}{\theta^2}$ or equivalently $-\rho\theta x_1 \leq \xi$ due to Definition (6.1). If $\rho \leq 0$, then the inequality holds since its left hand-side is non-positive. Suppose now that $\rho > 0$. Using formula (6.2) for x_1, we see that $-\rho\theta x_1 \leq \xi$ is equivalent to

$$h\left(\frac{\theta}{\xi} - 2\rho\right) \leq 2\frac{1-\rho^2}{\rho}, \tag{6.20}$$

where function $h(\cdot)$ is defined as

$$h(y) = \sqrt{y^2 + 4\left(1 - \rho^2\right)} - y. \tag{6.21}$$

It decreases from $+\infty$ to zero since its derivative $h'(y) = \frac{y}{\sqrt{y^2 + 4(1-\rho^2)}} - 1$ is always negative. Hence, the equation $h(y) = 2\frac{1-\rho^2}{\rho}$ has a unique root which is namely y_1. Also, $y_1 + 2\rho > 0$ when $\rho > \frac{1}{2}$. Hence, inequality (6.20) holds when $\rho \leq \frac{1}{2}$ or when $\left\{\rho > \frac{1}{2},\ \frac{\theta}{\xi} \geq y_1 + 2\rho\right\}$.

Suppose that $\left\{\rho > \frac{1}{2},\ \frac{\theta}{\xi} < y_1 + 2\rho\right\}$. Therefore, $H(\infty) > \frac{2\xi}{\theta^2}$ and thus the equation $H(t) = \frac{2\xi}{\theta^2}$ has a unique positive root and it is t_1. Thus we conclude that inequalities (6.18) hold when $t < t_1$. The opposite inequalities are true for $t > t_1$. This finishes the proof. □

We turn now to the position of x^+.

Theorem 6.3. *(Theorem 3.3 of Zaevski and Nedeltchev[187]) The following statements characterize the position of $\widetilde{x}^+$ w.r.t. x_2.*

1. *If $\xi \geq \rho\theta$, then*
   - (a) *$\widetilde{x}^+ \in (x_2, x^+)$ when*
     - $\{\rho \geq 0\}$,
     - $\left\{\rho \in (-0.5, 0), \frac{\theta}{\xi} \leq 2\rho - y_2\right\}$,
     - $\left\{\rho \in (-0.5, 0), \frac{\theta}{\xi} > 2\rho - y_2, t < t_2\right\}$, *or*
     - $\{\rho \leq -0.5, t < t_2\}$.
   - (b) *$\widetilde{x}^+ \in (1, x_2)$ when $\left\{\rho \in (-0.5, 0), \frac{\theta}{\xi} > 2\rho - y_2, t > t_2\right\}$ or $\{\rho \leq -0.5, t > t_2\}$.*
   - (c) *$\widetilde{x}^+ = x_2$ when $\left\{\rho \in (-0.5, 0), \frac{\theta}{\xi} > 2\rho - y_2, t = t_2\right\}$ or $\{\rho \leq -0.5, t = t_2\}$.*
2. *Suppose that $\xi < \rho\theta$. Note that $t_2 < \bar{t}$ ($\bar{t}$ is defined by formula (6.7)) because the function $\kappa(x_2; t)$ increases w.r.t. t and it is infinity for $\bar{t}$.*
   - (a) *If $t < t_2$, then $\widetilde{x}^+ \in (x_2, x^+)$.*
   - (b) *If $t = t_2$, then $\widetilde{x} = x_2$.*
   - (c) *If $t_2 < t$, then $1 < \widetilde{x}^+ < x_2 < x^+$.*

Proof: Suppose first that $\xi \geq \rho\theta$. The proof of the desired results can be obtained in a similar manner as in Theorem 6.2. First, we shall find when the function $\kappa(x; t)$ is less than $\frac{2\xi}{\theta^2}$. Note that $\kappa(x; t)$ increases w.r.t. t between $H(0) = 0$ and $H(+\infty) = \frac{x_2^2 - x_2}{\xi - \theta\rho x_2}$, where the function $H(\cdot)$ is defined as

$$H(t) = \frac{x_2^2 - x_2}{\frac{2}{t} + \xi - \theta\rho x_2}. \tag{6.22}$$

Hence, we need to find when $H(+\infty)$ is less than $\frac{2\xi}{\theta^2}$ or equivalently when $-\rho\theta x_2 < \xi$. We can immediately see that this inequality always holds when $\rho \geq 0$. On the other hand, if $\rho < 0$, then we have to find when $h\left(2\rho - \frac{\theta}{\xi}\right) < -2\frac{1-\rho^2}{\rho}$ – the function $h(\cdot)$ is defined in (6.21). The desired results follow the fact that the term $2\rho - \frac{\theta}{\xi}$ varies between $-\infty$ and 2ρ and thus $h\left(2\rho - \frac{\theta}{\xi}\right)$ is between $2(1-\rho)$ and $+\infty$.

Let us turn to the case $\xi < \rho\theta$. The first part in the second point is obvious. The rest cases follow the fact that function (6.22) increases from zero to infinity for $t \in \left(0, \bar{t}\right)$. Note that $\xi - \theta\rho x_2 < 0$, because $\xi < \theta\rho$ and $x_2 > 1$. □

6.3.2 Limiting case, $|\rho| = 1$

We shall discuss now the cases when the standard Brownian motions are perfectly correlated. Suppose first that $\rho = 1$ and $2\xi \neq \theta$. Thus the function (6.1) has unique root

$$\overline{x} = \frac{\xi^2}{\theta(2\xi - \theta)}. \tag{6.23}$$

If $2\xi < \theta$, then $x_1 = \overline{x}$ and $x_2 = \infty$. We can easily check that Theorem 6.2 holds having in mind that the constants y_1 and t_1 turn into $y_1 = 1$ and

$$t_1 = 4\frac{(2\xi - \theta)^2}{\xi(\theta - \xi)(3\xi - \theta)}. \tag{6.24}$$

Note that the important limit for $\frac{\theta}{\xi}$ is the number $y_1 + 2\rho = 3$. Also, $x_2 = \infty$ implies $t_2 = 0$ and thus Theorem 6.3 can be generalized in this sense.

If $2\xi > \theta$, then $x_1 = -\infty$ and $x_2 = \overline{x}$. We can easily check that $2\xi > \theta$ lead to $x_2 > 1$. Theorem 6.2 holds again in a generalized sense since t_1 turns to zero. Theorem 6.3 holds too since the critical value for the time t_2 turns into (6.24). Note that in Theorem 6.3, the cases $\xi > \theta$ and $\xi < \theta$ leads to different results. We have to mention that $y_2 = -1$ and thus the important boundary for $\frac{\theta}{\xi}$ is again the number $2\rho - y_2 = 3$.

The results for the case $2\xi = \theta$ are provided in the following theorem:

Theorem 6.4. *(Theorem 3.4 of Zaevski and Nedeltchev[187])*

If $\rho = 1$ *and* $2\xi = \theta$,[1] *then*

$$\widetilde{x}^{-,+} = \mp\sqrt{\frac{1}{2}\left(\coth\left(\frac{\xi t}{2}\right) + 1\right)}. \tag{6.25}$$

Proof: When $\rho = 1$ and $2\xi = \theta$, the function $P(\cdot)$ turns into the constant $P(x) = \xi$. Thus the equation $\kappa(x) = \frac{2\xi}{\theta^2}$ turns into a quadratic one which roots are given namely by formula (6.25). □

Let us discuss now briefly the case $\rho = -1$. The root of function (6.1) is $-\frac{\xi^2}{\theta(2\xi+\theta)}$. Note that it is negative and thus this is the smaller root x_1. Also, $x_2 = +\infty$. We can easily check Theorem 6.2 and 6.3 having in mind $\kappa(x_1) < \frac{2\xi}{\theta^2}$ and $t_2 = 0$.

[1] Let us mention that $x_1 = -\infty$ and $x_2 = \infty$ in this case.

Chapter 7

Entropy-based Value at Risk

Very often it is not sufficient for the market risk managers to compute the value under threat. Their agenda is full with questions like to find the most conservative VaR-based risk measure or to find the ultimate scenario that a portfolio should be ready to face. The traditional risk measures like the quantile VaR and the ES can't help in such queries. We need sophisticated risk measures like the $EVaR$ to face these challenges.

This chapter introduces and discusses the substance and the properties of the Entropic VaR. The measure is adjusted to the financial area and the dual representation is presented. The chapter contains a concrete way to derive the $EVaR$ via the MGF-related minimizer. Formulas for the MGF of the stochastic processes discussed in Chapter 3 are available. The volatility averaging discussed in Chapter 6 is leveraged to the $EVaR$ case.

7.1 Entropic VaR for stock returns

We shall introduce the $EVaR$ for financial assets. It quite differs from the traditional definition in the field of operation research provided by Ahmadi-Javid[7].

We need the lemma below which formalizes mathematically the fact that if $g_1(x) \leq g_2(x)$ are two monotonic functions, then their inversions change the positions, i.e. $g_1^{-1}(x) \geq g_2^{-1}(x)$.

Lemma 7.1. *Let $g_1(\cdot)$ and $g_2(\cdot)$ be two functions on the real numbers, $g_1(\cdot)$ be non-decreasing, $g_2(\cdot)$ be strictly increasing, $g_1(x) \leq g_2(\cdot)$, and the set A be the image of the real axes through the function $g_2(\cdot)$. We define the*

inversion of $g_1(x)$ *as* $g_1^{-1}(\alpha) = \inf\{x \in \mathbb{R} : g_1(x) > \alpha\}$. *If* $g_1(x) > \alpha$ *for all real* x *and some* $\alpha \in A$, *then* $g_1^{-1}(\alpha) = -\infty$. *Also, if* $g_1(x) < \alpha$ *for all* $x \in \mathbb{R}$ *and some* $\alpha \in A$, *then* $g_1^{-1}(\alpha) = +\infty$. *Under these assumptions,* $g_1^{-1}(\alpha) \geq g_2^{-1}(\alpha)$ *at the set* A.

Using the Chernoff inequality (Chernoff[47]), we restrict the CDF for a positive constant $z > 0$ by

$$\begin{aligned} F(a;\zeta) = P(\zeta < a) &= \mathbb{P}\left(e^{-z\zeta} > e^{-za}\right) \\ &\leq e^{az}\mathbb{E}\left[e^{-z\zeta}\right] = e^{az}M(-z;\zeta). \end{aligned} \tag{7.1}$$

Let us denote by $d(x,z;\zeta)$ the function

$$d(x,z;\zeta) := \frac{1}{z}\ln\left(\frac{M(-z;\zeta)}{x}\right). \tag{7.2}$$

Having in mind that the inversion w.r.t. the variable a of the right hand side of inequality (7.1) is $-d(\epsilon,z;\zeta)$ and applying Lemma 7.1, we deduce

$$VaR(\epsilon;\zeta) = -F^{-1}(\epsilon;\zeta) \leq -\sup_{z>0}(-d(\epsilon,z;\zeta)) = \inf_{z>0} d(\epsilon,z;\zeta). \tag{7.3}$$

We define the $EVaR$ in the financial area:

Definition 7.1. *The Entropic VaR at level* $\epsilon \in (0,1)$ *of the random variable* ζ *is defined as*

$$EVaR(\epsilon;\zeta) = \inf_{z>0} d(\epsilon,z;\zeta) \equiv \inf_{z>0}\frac{1}{z}\ln\left(\frac{M(-z;\zeta)}{\epsilon}\right). \tag{7.4}$$

We shall denote by a_ζ *the value at which the minimum occurs.*

Based on formula (7.3) and (7.4) we can say that the $EVaR$ is the upper bound of the quantile VaR.

Remark 7.1. *Definition 7.1 slightly deviates from the original one provided by Ahmadi-Javid[7]. The main difference stems from the fact that the left tail of the returns distribution is important in finance whereas the right one is used traditionally in the field of operation research. Thus Definition 7.1 measures in fact the opposite random variable in the sense of Ahmadi-Javid[7].*

Next we discuss the support of $EVaR$. Obviously, if $M(-\overline{z};\zeta) < \infty$ for every $z > 0$, then $EVaR$ is well defined. However, this is a quite strong restriction for many practical purposes. The following lemma motivates the set we use:

Lemma 7.2. *If $M(-\overline{z};\zeta) < \infty$ for some $\overline{z} > 0$, then $M(-z;\zeta) < \infty$ for every z such that $0 \leq z \leq \overline{z}$.*

Proof: We refer to Theorem 7.1.1. of Lukacs[127]. □

Based on Lemma 7.2, we define c_ζ as

$$c_\zeta = \arg\sup_{z>0} M(-z;\zeta) < \infty. \tag{7.5}$$

We shall say that $\mathcal{C}_\zeta = [0, c_\zeta)$ is the negative support of the moment generating function of ζ if $M(-c_\zeta;\zeta) = \infty$. If $M(-c_\zeta;\zeta) < \infty$, then $\mathcal{C}_\zeta = [0, c_\zeta]$. Thus we enlarged the support of $EVaR$ as these random variables for which $c_\zeta > 0$ – we shall denote this set by $\mathcal{B}$. A similar set is discussed also in Ahmadi-Javid and Pichler[9]. Thus we modify Definition 7.1 in the following way:

Definition 7.2. *For $\zeta \in \mathcal{B}$ and $\epsilon\,(0,1)$, the $EVaR$ is defined as*

$$EVaR(\epsilon;\zeta) = \inf_{0<z\leq c_\zeta} d(\epsilon, z;\zeta). \tag{7.6}$$

The following corollary stands:

Corollary 7.1. *If x is a constant, then $EVaR(\epsilon;\zeta + x) = EVaR(\epsilon;\zeta) - x$.*

Proof: Having in mind the relation $M(z;\zeta + x) = e^{xz}M(z;\zeta)$, we derive for the function $d(\epsilon, z;\zeta)$

$$d(\epsilon, z;\zeta + x) = \frac{1}{z}\ln\left(\frac{M(-z;\zeta + x)}{\epsilon}\right) = d(\epsilon, z;\zeta) - x. \tag{7.7}$$

We conclude that the minimum for the $EVaR$ is achieved at the same point a_ζ and it is downward shifted by x. Note that the domains of the MGFs of the random variables ζ and $\zeta + x$ coincide. □

To prove that the so-defined measure is coherent, we check the conditions for coherent risk measure (see Definition 2.1). The proof is similar to Theorem 3.1 of Ahmadi-Javid[7] and we omit it. Note that we need to consider intervals of the form $\mathcal{C}_\zeta$.

We shall provide now the dual presentation of the entropic VaR. It exists since $EVaR$ is a coherent risk measure – see above and also Delbaen[65]. Having in mind Remark 7.1 and Theorem 7 of Ahmadi-Javid[6] one can obtain the following result:

Proposition 7.1. *Let the set $\mathcal{S}$ consists of these equivalent to $\mathbb{P}$ measures $\mathbb{Q}$ for which*

$$\int \frac{d\mathbb{Q}}{d\mathbb{P}} \ln \frac{d\mathbb{Q}}{d\mathbb{P}} d\mathbb{P} \leq -\ln \epsilon. \tag{7.8}$$

We have

$$EVaR\left(\epsilon;\zeta\right) = -\inf_{\mathbb{Q}\in\mathcal{S}} \mathbb{E}^{\mathbb{Q}}\left[\zeta\right]. \tag{7.9}$$

We obtain the acceptance set for the $EVaR$ in the following proposition:

Proposition 7.2. *(Proposition 2.9 of Nedeltchev and Zaevski[141]) Let $\epsilon^*\left(\zeta\right)$ be defined for a random variable ζ as*

$$\epsilon^*\left(\zeta\right) = \inf_{0\leq z\leq c_\zeta} M\left(-z;\zeta\right) \tag{7.10}$$

The acceptance set for the $EVaR$ at the level ϵ is $\mathcal{A}_\epsilon = \{\zeta : \epsilon^*\left(\zeta\right) \leq \epsilon\}$.

Proof: First, suppose that ζ is such that $\epsilon^*\left(\zeta\right) \leq \epsilon$ and let $z^*\left(\zeta\right)$ be

$$z^*\left(\zeta\right) = \arg\inf_{0\leq z\leq c_\zeta} M\left(-z;\zeta\right). \tag{7.11}$$

Therefore Definition 7.2 leads to

$$\begin{aligned} EVaR\left(\epsilon;\zeta\right) &= \inf_{0<z\leq c_\zeta} \frac{1}{z} \ln\left(\frac{M\left(-z;\zeta\right)}{\epsilon}\right) \\ &\leq \frac{1}{z^*\left(\zeta\right)} \ln\left(\frac{M\left(-z^*\left(\zeta\right);\zeta\right)}{\epsilon}\right) \\ &= \frac{1}{z^*\left(\zeta\right)} \ln\left(\frac{\epsilon^*\left(\zeta\right)}{\epsilon}\right) \leq 0. \end{aligned} \tag{7.12}$$

Hence, $\zeta \in \mathcal{A}_\epsilon$. Inverse, suppose that $\zeta \in \mathcal{A}_\epsilon$. Therefore, $M(-z;\zeta) \leq \epsilon$ for some $0 < z \leq c_\zeta$. Hence, $\epsilon^*(\zeta) \leq \epsilon$ too. □

7.2 Deriving the Entropic VaR

We need the following statements before to continue with deriving the $EVaR$.

Lemma 7.3. *If the function $g(z)$ is monotone on a positive domain, then the function $\overline{g}(z) := g\left(\frac{1}{z}\right)$ is inverse monotone on the related set.*

Proposition 7.3. *(Proposition 3.2 of Nedeltchev and Zaevski[141]) For fixed ϵ and ζ, the function $g(z) := d(\epsilon, -z; \zeta)$ has no more than one local minimum in the interval $\mathcal{C}_\zeta$.*

Proof: Using similar arguments as in Lemma 3.1 of Ahmadi-Javid[7] we can prove that the function $\overline{g}(z) = g\left(\frac{1}{z}\right)$ is convex and continuous on the set $\left(\frac{1}{c_\zeta}, \infty\right)$. Hence, there exists a constant c, $\frac{1}{c_\zeta} \leq c \leq \infty$, such that $\overline{g}(z)$ is monotone decreasing in the interval $\left(\frac{1}{c_\zeta}, c\right)$ and monotone increasing in (c, ∞). Note that the cases $c = \frac{1}{c_\zeta}$ and $c = \infty$ lead to monotone function (increasing or decreasing, respectively) in the whole interval $\left(\frac{1}{c_\zeta}, \infty\right)$. Using Lemma 7.3 we conclude that the function $g(z)$ decreases in the interval $\left(0, \frac{1}{c}\right)$ and increases for $z \in \left(\frac{1}{c}, c_\zeta\right)$. This finishes the proof. □

We are ready to prove the main result for deriving the $EVaR$.

Theorem 7.1. *(Theorem 3.3 of Nedeltchev and Zaevski[141]) Let the functions $\phi(\cdot)$ and $h(\cdot)$ be defined through the MGF as*

$$\begin{aligned} \phi(z;\zeta) &= \ln M(-z;\zeta) \\ h(z,\epsilon;\zeta) &= \phi'(z)\, z - \phi(z) + \ln \epsilon. \end{aligned} \tag{7.13}$$

If $h(c_\zeta, \epsilon; \zeta) \leq 0$, then

$$EVaR(\epsilon;\zeta) = \frac{1}{c_\zeta} d(-c_\zeta, \epsilon; \zeta) \equiv \frac{1}{c_\zeta}\left(\phi(c_\zeta;\zeta) - \ln \epsilon\right) \tag{7.14}$$

Otherwise, if $h(c_\zeta, \epsilon; \zeta) > 0$*, then the equation* $h(z, \epsilon; \zeta) = 0$ *has a unique solution in the interval* $(0, c_\zeta)$ *which is* a_ζ *and thus*

$$EVaR(\epsilon; \zeta) = d(-a_\zeta, \epsilon; \zeta) \equiv \frac{1}{a_\zeta}(\phi(a_\zeta; \zeta) - \ln \epsilon). \tag{7.15}$$

Proof: First, we observe that $d(\epsilon, 0; \zeta) = +\infty$ because $M(0; \zeta) = 1$ and $\epsilon < 1$. Applying Proposition 7.3 we deduce that the function $d(\epsilon, -z; \zeta)$ is either decreasing w.r.t. the variable z in the interval $(0, c_\zeta)$ or first decreases and then increases having a global minimum. Using

$$\begin{aligned} d(\epsilon, -z; \zeta) &= \frac{1}{z}(\phi(z; \zeta) - \ln \epsilon) \\ \frac{\partial}{\partial z}(d(\epsilon, -z; \zeta)) &= \frac{h(z, \epsilon; \zeta)}{z^2}, \end{aligned} \tag{7.16}$$

we conclude that the function $h(z, \epsilon; \zeta)$ is always negative for $z \in (0, c_\zeta)$ or it has a unique root in this interval, $h(z, \epsilon; \zeta) < 0$ before it, and $h(z, \epsilon; \zeta) > 0$ after it. If $h(c_\zeta, \epsilon; \zeta) \leq 0$, then $h(z, \epsilon; \zeta) < 0$ in the whole interval $(0, c_\zeta)$ and thus $d(\epsilon, -z; \zeta)$ decreases w.r.t. z. Alternatively, if $h(c_\zeta, \epsilon; \zeta) > 0$, then equation $h(z, \epsilon; \zeta) = 0$ has a unique solution in $(0, c_\zeta)$ and it is the minimizer of $d(\epsilon, -z; \zeta)$. We finish the proof having in mind Definition 7.2. □

7.3 The MGF of the considered models

We shall consider the MGF of the models presented in Chapter 3 .

7.3.1 Black-Scholes model

The Gaussian moment generating function is always well-defined and it is

$$M(z) = e^{t\left(\left(\mu - \frac{\sigma^2}{2}\right)z + \frac{\sigma^2 z^2}{2}\right)}. \tag{7.17}$$

Hence, $c_{BS} = +\infty$. Thus functions (7.13) turn into

$$\begin{aligned} \phi(z; \zeta) &= t\left(-\left(\mu - \frac{\sigma^2}{2}\right)z + \frac{\sigma^2 z^2}{2}\right) \\ h(z, \epsilon; \zeta) &= \phi'(z)\, z - \phi(z) + \ln \epsilon. \end{aligned} \tag{7.18}$$

We conclude that the values of minimizer a_{BS} and the $EVaR$ are

$$\begin{aligned} a_{BS} &= \frac{1}{\sigma}\sqrt{-\frac{2\ln\epsilon}{t}} \\ EVaR\left(\epsilon; BS\right) &= \left(\frac{\sigma^2}{2} - \mu\right)t + \sigma\sqrt{-2t\ln\epsilon}. \end{aligned} \tag{7.19}$$

7.3.2 Exponential tempered stable model

The moment generating function is well defined in the interval $(-\lambda_1, \lambda_2)$ and thus $c_{ETS} = \lambda_1$. It can be written as

$$M_{TS}\left(z\right) = e^{t(\mu z + \psi_1(z) + \psi_2(z))}, \tag{7.20}$$

where

$$\begin{aligned} \psi_1\left(z\right) &= \begin{cases} \Gamma\left(-\alpha_1\right)\lambda_1^{\alpha_1}c_1\left(\left(1+\frac{z}{\lambda_1}\right)^{\alpha_1} - 1 - \frac{z\alpha_1}{\lambda_1}\right), & if \quad \alpha_1 \neq 1 \\ -zc_1 + c_1\left(\lambda_1 + z\right)\ln\left(1+\frac{z}{\lambda_1}\right), & if \quad \alpha_1 = 1 \end{cases} \\ \psi_2\left(z\right) &= \begin{cases} \Gamma\left(-\alpha_2\right)\lambda_2^{\alpha_2}c_2\left(\left(1-\frac{z}{\lambda_2}\right)^{\alpha_2} - 1 + \frac{z\alpha_2}{\lambda_2}\right), & if \quad \alpha_2 \neq 1 \\ zc_2 + c_2\left(\lambda_2 - z\right)\ln\left(1-\frac{z}{\lambda_2}\right), & if \quad \alpha_2 = 1. \end{cases} \end{aligned} \tag{7.21}$$

Hence, the function $\phi\left(\cdot; ETS\right)$ from (7.13) is $\phi\left(z; ETS\right) = t\left(-\mu z + \psi_1\left(-z\right) + \psi_2\left(-z\right)\right)$. Therefore, $\phi'\left(z; ETS\right) = -t\left(\mu + \psi_1'\left(-z\right) + \psi_2'\left(-z\right)\right)$, where

$$\begin{aligned} \psi_1{}'\left(z\right) &= \begin{cases} \Gamma\left(-\alpha_1\right)\lambda_1^{\alpha_1-1}c_1\alpha_1\left(\left(1+\frac{z}{\lambda_1}\right)^{\alpha_1-1} - 1\right), & if \quad \alpha_1 \neq 1 \\ c_1\ln\left(1+\frac{z}{\lambda_1}\right), & if \quad \alpha_1 = 1 \end{cases} \\ \psi_2'\left(z\right) &= \begin{cases} \Gamma\left(-\alpha_2\right)\lambda_2^{\alpha_2-1}c_2\alpha_2\left(\left(1-\frac{z}{\lambda_2}\right)^{\alpha_2-1} + 1\right), & if \quad \alpha_2 \neq 1 \\ -c_2\ln\left(1-\frac{z}{\lambda_2}\right), & if \quad \alpha_2 = 1. \end{cases} \end{aligned} \tag{7.22}$$

Several cases are available and we consider their results through the below Proposition:

Proposition 7.4. *(Proposition 3.4 of Nedeltchev and Zaevski[141])*

Let $D(x)$ be the digamma function and $D^{-1}(x)$ be its inversion in the interval $(-2,-1)$. Note that it exists because the digamma function increases between minus and plus infinity in this interval. Let the constant b be defined as $b = c_1\Gamma\left(d^{-1}\left(\ln\lambda_1\right)\right)\lambda_1^{-D^{-1}(\ln\lambda_1)}$. The following statements hold:

1. *If $b - \psi_2'(-\lambda_1)\lambda_1 - \psi_2(-\lambda_1) + \frac{\ln\epsilon}{t} > 0$, then $a_{ETS} < c_{ETS}$.*
2. *If $b - \psi_2'(-\lambda_1)\lambda_1 - \psi_2(-\lambda_1) + \frac{\ln\epsilon}{t} \leq 0$, then there exist two constants b_1 and b_2, $1 < b_1 < -d^{-1}(\ln\lambda_1) < b_2 < 2$, for which $a_{ETS} < c_{ETS}$ when $\alpha_1 \in (0, b_1) \cup (b_2, 2)$ and $a_{ETS} = c_{ETS}$ when $\alpha_1 \in [b_1, b_2]$.*

The $EVaR$ is obtained through Theorem 7.1.

Proof: Suppose first that $\alpha_1 < 1$. We have $-\lambda_1{\psi_1}'(-\lambda_1) = +\infty$ because $\lim_{z\to-\lambda_1}\left(1+\frac{z}{\lambda_1}\right)^{\alpha_1-1} = +\infty$ and $\Gamma(-\alpha_1) < 0$. Having in mind that the rest of the terms in $h(c_\zeta, \epsilon; \zeta)$ are finite, we conclude that $a_{ETS} < c_{ETS}$. If $\alpha_1 = 1$, the same result holds since $\lim_{z\to-\lambda_1}\ln\left(1+\frac{z}{\lambda_1}\right) = -\infty$.

Suppose now that $1 < \alpha_1 < 2$. Let us consider the part of $h(\lambda_1, \epsilon; \zeta)$ related to $\psi_1(\cdot)$ as a function of α_1, say $f(x)$. We can present the function and its derivative as

$$\begin{aligned} f(x) &= -\psi_1'(-\lambda_1)\lambda_1 - \psi_1(-\lambda_1) \\ &= c_1 x\Gamma(-x)\lambda_1^x + c_1(1-x)\Gamma(-x)\lambda_1^x \\ &= c_1\Gamma(-x)\lambda_1^x \\ f'(x) &= c_1\Gamma(-x)\lambda_1^x\left(\ln\lambda_1 - D(-x)\right), \end{aligned} \tag{7.23}$$

where $D(\cdot)$ is the digamma function. Having in mind that it increases between minus and plus infinity in the interval $(-2,-1)$, we conclude that $f'(x) < 0$ for $x \in (1, -D^{-1}(\ln\lambda_1))$ and $f'(x) > 0$ if $x \in (-D^{-1}(\ln\lambda_1), 2)$. Hence, $f(x)$ decreases when x belongs to the former interval and increases when x belongs to the latter interval. Thus the function $f(x)$ has minimum for $x = -D^{-1}(\ln\lambda_1)$ and its value is $f(-D^{-1}(\ln\lambda_1)) = b$ (see formulation of Proposition 7.4 for the value of b). We finish the proof using this behavior of $f(x)$ and the part of $h(\lambda_1, \epsilon; \zeta)$ coming from $\psi_2(\cdot)$ and $\ln\epsilon$. □

7.3.3 Heston model

We need the following result which is formulated as (7.16):

Proposition 7.5. *(Proposition 3.5 of Nedeltchev and Zaevski[141]) In the terms of Proposition 6.1, let x^* be the highest root of $f(\cdot)$ which is less than x_1. The abscissa of $EVaR$ is $c_{Heston} = -x^*$.[1] Functions (7.13) related to the MGF of the log-price in its domain can be written as*

$$\begin{aligned}
\phi(z;\xi) &= -x_0 z - \mu t z + \frac{2\xi\eta}{\theta^2}\left((\rho\theta z + \xi)\frac{t}{2} - \ln f(-z)\right) + v_0 \frac{z+z^2}{f(-z)} f_2(-z) \\
h(z,\epsilon;\xi) &= \phi'(z) z - \phi(z) + \ln\epsilon \\
&= \ln\epsilon + \frac{2\xi\eta}{\theta^2}\left(-\frac{\xi t}{2} + \frac{f'(-z)}{f(-z)} z + \ln f(-z)\right) \\
&\quad + v z^2 \left(\frac{f(-z) + (1+z) f'(-z)}{f^2(-z)} f_2(-z) - \frac{1+z}{f(-z)} f_2'(-z)\right) \\
f'(x) &= f_1'(x) - \rho\theta f_2(x) + (\xi - \rho\theta x) f_2'(x) \\
f_1'(x) &= \frac{t}{4} f_2(x) p'(x) \\
f_2'(x) &= \operatorname{sgn}(p(x)) \frac{p'(x)}{2P^2(x)}\left[\frac{t}{2} f_1(x) - f_2(x)\right] \\
p'(x) &= -2x\theta^2\left(1-\rho^2\right) + \theta(\theta - 2\rho\xi).
\end{aligned} \tag{7.24}$$

We obtain the minimizer that determines the value of $EVaR$ (a_ξ or c_ξ) through Theorem 7.1, more precisely via the sign of $h(c_\xi, \epsilon; \xi)$.

7.3.4 Stochastic volatility jump models

Let us consider first the Bates model. The MGF of the jump part is always well-defined and it is $M(z) = e^{t\psi_{CP}(z)}$, where $\psi_{CP}(u)$ is

$$\psi_{CP}(z) = \lambda\left(e^{\frac{\beta^2 z^2}{2} + \alpha z} - 1\right). \tag{7.25}$$

[1] In fact, x^* is the left abscissa of convergence of the MGF of the log-price in the Heston model. The right one is more variable – the complete exposition is provided in Theorem 3.1, points 1-3 of del Baño Rollin et al.[63].

We consider in addition the stochastic volatility jump model suggested by Zaevski et al.[188] – the jumps are presented by a tempered stable process discussed in Section 3.2. We can formulate the following results:

Proposition 7.6. *(Proposition 3.6 of Nedeltchev and Zaevski[141]) The domain of the MGF of the the log-returns of a stochastic volatility jump model is the intersection between the domains of the continuous and jump parts. Particularly, the support for the Bates model coincides with those for the Heston's one. Thus, we have for the abscissas* $c_{Bates} = c_{Heston}$ *and* $c_{SVTS} = \min\{c_{Heston}, \lambda_1\}$*, where the subscript* $SVTS$ *stands for the stochastic volatility model with tempered stable jumps.*

Proof: The proof is based on the fact that the MGF of the product of independent random variables is the product of their MGFs. □

Having in mind Proposition 7.6, we derive the minimizer for the $EVaR$ as well as its own value through Theorem 7.1. Functions (7.13) turn into

$$\begin{aligned} \phi(z;) &= \ln M_{Heston}(-z) + \ln M_J(-z;\xi) \\ h(z,\epsilon) &= [\phi'_{Heston}(z) + \phi'_J(z)]\, z - \phi_{Heston}(z) - \phi_J(z) + \ln\epsilon. \end{aligned} \tag{7.26}$$

The subscript J stands for the jump part. The terms for the Bates model are

$$\begin{aligned} \phi_J(z) &= t\lambda\left(e^{-\left(\frac{\delta^2 z^2}{2}+\left(k-\frac{\delta^2}{2}\right)z\right)} - 1\right) \\ h(z,\epsilon;\xi) &= [\phi'_{Heston}(z) + \phi'_J(z)]\, z - \phi_{Heston}(z) - \phi_J(z) + \ln\epsilon \\ \phi'_J(z) &= -t\lambda e^{-\left(\frac{\delta^2 z^2}{2}+\left(k-\frac{\delta^2}{2}\right)z\right)}\left(\delta^2 z + k - \frac{\delta^2}{2}\right). \end{aligned} \tag{7.27}$$

For the model of Zaevski et al.[188], we need to combine the results of Section 7.3.2 and 7.3.3.

7.4 Averaging w.r.t. the volatility

This section follows the approach applied and the conclusions drawn in Chapter 6 of the dissertation.

Several authors propose an approach for eliminating the initial value of the volatility that appears in MGF (6.4) – see Dragulescu and Yakovenko[71], Zaevski et al.[188], Zaevski and Nedeltchev[186], Zaevski and Nedeltchev[187]. This is necessary because the volatility is a hidden market parameter and there is no consensus between the practitioners and researchers how to extract it. On the other hand, the Cox-Ingersoll-Ross (CIR) process admits a Gamma stationary distribution with PDF given by equation (6.8). The above-mentioned authors suggest the volatility to be averaged w.r.t. this Gamma distribution and thus the averaged MGF turns into

$$\begin{aligned} M_{Heston}^{av}(z) &= \int_0^\infty M_{Heston}(z;v)\, g_\gamma(v)\, dv \\ &= \int_0^\infty e^{\omega(z)+\kappa(z)v} g_\gamma(v)\, dv \\ &= e^{\omega(z)} M_\gamma(\kappa(z)), \end{aligned} \tag{7.28}$$

where $M_\gamma(\cdot)$ is the MGF of the Gamma distribution

$$M_\gamma(u) = \left(1-\frac{u}{\alpha}\right)^{-\beta} \equiv \left(1-\frac{\theta^2 u}{2\xi}\right)^{-\frac{2\xi\eta}{\theta^2}} \tag{7.29}$$

and $\omega(z)$ and $\kappa(z)$ are defined by (6.5). Proposition 6.2 gives the existence of a random variable which MGF is given by formula (7.28) – we shall call it *averaged log-returns*. Following Theorem 6.1, we derive the left abscissa of convergence c_{av} of the MGF :

Proposition 7.7. *(Proposition 3.7 of Nedeltchev and Zaevski[141]) For a fixed t, the equation $\kappa(t,x) = \frac{2\xi}{\theta^2}$ has a unique root in the interval $(-c_{Heston}, 0)$. The boundary c_{av} is the opposite value of this root.*

The function $h(z,\epsilon;\zeta)$ that describes the minimizer of the $EVaR$ turns into

$$
\begin{aligned}
h\left(z,\epsilon;\xi\right) &= \phi'\left(z\right)z-\phi\left(z\right)+\ln\epsilon\\
\phi\left(z,\epsilon;\xi\right) &= \omega\left(-z\right)-\frac{2\xi\eta}{\theta^{2}}\ln\left(1-\frac{\theta^{2}\kappa\left(-z\right)}{2\xi}\right)\\
\phi'\left(z,\epsilon;\xi\right) &= -\omega'\left(-z\right)-\frac{2\xi\eta}{2\xi-\theta^{2}\kappa\left(-z\right)}\kappa'\left(-z\right)\\
\omega'\left(x\right) &= -\frac{2\xi\eta}{\theta^{2}}\left(\frac{\rho\theta t}{2}+\frac{f'\left(x\right)}{f\left(x\right)}\right)+t\mu\\
\kappa'\left(x\right) &= \frac{\left(2x-1\right)f_{2}\left(x\right)+\left(x^{2}-x\right)f_{2}'\left(x\right)}{f\left(x\right)}-\left(x^{2}-x\right)\frac{f_{2}\left(x\right)f'\left(x\right)}{f^{2}\left(x\right)}.
\end{aligned}
\tag{7.30}
$$

The derivatives $f'\left(x\right)$ and $f_{2}'\left(x\right)$ can be found in formulas (7.24).

Chapter 8

Computations and empirical results analysis

The dissertation would be incomplete if we had explored only the theoretical aspects of the contemporary risk measures. The material from the preceding chapters is challenged by applying it to real-life cases and drawing conclusions therefrom. In the financial mathematics we are biased to look at the losses but the downfall risk events happen rarely and hence only a few dots appear in the tails of the returns distribution. As any tail, the left tail (i.e. the losses) contains limited number of observations that jeopardizes the correctness, the completeness and the robustness of the analysis and the conclusions drawn. We remedy this drawback by applying stochastic processes that supply us sufficient number of loss observations.

8.1 Computations for the Expectile VaR

In this section we extract the risk measures from historical data set, we prepare the data set used, we elaborate the calibration methodology, we validate/compare the fits, and look at the calculated values of the VaR, ES, and ERM.

8.1.1 Extracting risk measures from historical sample

The purpose of this section is to extract the VaR, ES, and ERM from a historical sample of n observations of the log-returns r_i, $i = 1, 2, ..., n$.

We shall denote by r_{min} and r_{max} the smallest and the largest of them, respectively. The quantile function, and thus the measure VaR, can be obtained by the level which contains the $100\epsilon\%$ of observations in the left tail of the returns distribution (i.e., the losses). Usually, the ES is obtained by averaging the VaR. We derive the ERM through formula (5.3) – note that this method can be used for deriving the ES too via Proposition 4.1. The following lemma holds for the truncated expectations.

Lemma 8.1. *The truncated at the interval (a, b) expectation, if it exists, can be derived as*

$$\mathbb{E}\left[(\zeta - x)\, I_{a<\zeta<b}\right] = (b - x)\, F(b) - (a - x)\, F(a) - \int_a^b F(y)\, dy. \tag{8.1}$$

Proof: The desired result follows after an integration by parts. □

We estimate numerically the risk measures from the empirical data in the following way.

1. We calculate the empirical CDF at the point x as the number of observations lower than x divided by the total observations number

$$F_{empirical}(x) = \frac{\#\{r_i < x\}}{n}. \tag{8.2}$$

Note that

$$\begin{aligned} F_{empirical}(r_{min}) &= 0 \\ F_{empirical}(r_{max}) &= 1. \end{aligned} \tag{8.3}$$

2. Having in mind that the interval for the log-returns is (r_{min}, r_{max}) and using Lemma 8.1 and equations (8.3) we derive the truncated expectations

$$\begin{aligned}\mathbb{E}\left[(\zeta - x)^{+}\right] &= (r_{max} - x) - \int_{x}^{r_{max}} F_{empirical}\,(y)\,dy \\ \mathbb{E}\left[(\zeta - x)^{-}\right] &= \int_{r_{min}}^{x} F_{empirical}\,(y)\,dy.\end{aligned} \tag{8.4}$$

3. We obtain the quantile function, and as a consequence the VaR, as $q\,(x) = \inf\{y, F_{empirical}\,(y) < x\}$. The ES can be derived using Proposition 4.1 and the second part of equations (8.4). The expectile and thus the ERM can be derived through equation (5.3) having in mind equations (8.4).

We present in this section a numerical comparison between the theoretical models discussed in Chapter 3. We first calibrate these models to the empirical data and then we analyze the VaR, ES, and ERM they generate w.r.t. the empirical ones.

8.1.2 Historical data

We use historical data for the S&P500 index for the period between October 6, 2004 and July 01, 2022 – totally 4466 observations. We use the daily Adjusted Close values. We move the historical sample with length 1000 days from September 25, 2008 to July 01, 2022. That way the period between October 6, 2004 and September 24, 2008 is the first sample. The dates are chosen this way because the theoretical models are calibrated to the date September 25, 2008 in Zaevski et al.[188]. Thus we can use the derived parameters' values for the initial point for the calibrating minimization for the first sample – it is well known that the initial point is very important when we minimize a multivariate function. We use the derived parameters for the initial point when calibrate the models to the next day sample. That way we have totally 3466 samples.

8.1.3 Calibration methodology

Let the S&P500 index values for a particular sample are S_1, S_2,...,S_N, $i = 1, 2, ..., N-1$. We derive the log-returns in the usual manner $r_i = \ln(S_{i+1}) -$

$\ln(S_i)$. The empirical PDF is derived by the following standard algorithm. We divide the interval $(-0.25, 0.25)$ into $M = 250$ bins with length $\Delta = 0.002$. The interval is chosen this way because the higher deviation in the S&P500 index log-returns is -0.2290 at the Black Monday, October 19, 1987. Let n_i, $i = 1, 2, ..., 250$, be the number of log-returns belonging to each bin. The empirical PDF in the center of the i-th bin is approximated by $\frac{n_i}{N\Delta}$.

To calibrate the models we also need the theoretical PDF for the different models. Except for the Black-Scholes model, the PDFs in closed form are not available for the considered models, hence we must derive them through the characteristic functions. We invert the characteristic functions using the Fast Fourier transform (FFT) algorithm (see Chapter 5.3). To find a relatively good approximation, we derive the PDFs at 500 points uniformly taken at the interval $(-0.5, 0.5)$ – the length of the bins is again $\Delta = 0.002$. Finally, we derive the PDF using the cubic spline approach.

One more problem stands when we calibrate the three stochastic volatility models. They depend on an unobservable parameter, namely the initial volatility. To overcome this problem, we apply the approach presented in Chapter 6.

We calibrate via the least square errors (LSqE) approach. Let us denote by Υ the set of all possible values of the parameters of any theoretical model and by υ any realization, $\upsilon \in \Upsilon$. We modify the usual minimization LSqE criterion to

$$\min_{\upsilon \in \Upsilon} \left\{ \sum_{i=1}^{250} \left(\ln(p_{th,i} + 1) - \ln(p_{emp,i} + 1) \right)^2 \right\}, \tag{8.5}$$

where $p_{th,i}$ and $p_{emp,i}$ are the values of the theoretical PDF based on the parameter's set υ and the empirical PDF respectively. We use the logarithm to give relatively equal impact of the terms in the distribution's center and the tails. The unit is added to the PDFs because some of the empirical values may be equal to zero.

The optimization was done by running the *ASA* package available at https://www.ingber.com/#ASA.

8.1.4 Validation and comparison of the fits

Once we calibrated the models to the moving empirical data with length of 1000, we validate the goodness of the fit. The approach we suggest has some

Table 8.1: Deviations from the real values and forecast results

parameter	BS	ETS	Heston	Bates	SV/TS
averaged error	9.7756	4.3051	4.5368	4.3096	4.2394
whole data error	7.4516	1.1083	1.1845	1.1722	1.0809
averaged $VaR\,(0.05)$ error	0.0018	0.0009	0.0008	0.0007	0.0007
averaged $ES\,(0.05)$ error	0.0027	0.0020	0.0018	0.0047	0.0013
averaged $ERM\,(0.05)$ error	0.0028	0.0009	0.0008	0.0020	0.0011
one day forecast	9446.0785	10867.8194	10836.3136	10834.1492	10861.8049
averaged value – one day	29.5379	34.5787	34.3108	34.2134	34.6249
one week forecast	9473.2248	10842.6018	10820.1055	10815.7427	10830.1246
averaged value – one week	29.5231	34.5426	34.2752	34.1824	34.5881
one month forecast	9609.9859	10839.6393	10817.9633	10816.0895	10821.3718
averaged value – one month	29.5553	34.6076	34.3597	34.2527	34.6735

similarities with the maximum likelihood method but applied to forecasting. Let us denote by $p\,(x;i)$ the calibrated PDF for some model at the i-th date. We shall use the following forecast function

$$\prod_{i=1}^{N-j} p\,(r_{i+j},i) \tag{8.6}$$

or the related logarithmic one

$$\sum_{i=1}^{N-j} \ln\left(p\,(r_{i+j},i)\right). \tag{8.7}$$

This way we may validate the forecast of the fit at the date i for the value at the date $i+j$. We calculate the values which function (8.7) generates for $j=1$ (one day), 5 (one week), and 20 (approximately one month). The results are presented in Table 8.1. We provide in this table also the averaged non-logarithmic values calculated by the formula

$$\frac{\sum\limits_{i=1}^{N-j} p\,(r_{i+j},i)}{N-j}. \tag{8.8}$$

We can see that all models (except the Black-Scholes one) produce relatively equal forecasts. Note that a larger value means a better fit. Looking at

Table 8.2: ERM-related parameters for the considered models

parameter	BS	ETS	Heston	Bates	SV/TS
μ	-0.0252	0.0856	0.0526	0.0790	0.0885
ξ	-	-	2482.4726	161.1913	2.8933
η	-	-	0.0332	0.0248	0.0062
θ	-	-	47.4600	3.2837	0.2845
ρ	-	-	-0.2021	-0.4189	-0.6000
α_1	-	0.2154	-	-	0.0005
α_2	-	1.2755	-	-	1.3527
c_1	-	37.8024	-	-	67.7031
c_2	-	0.1425	-	-	0.0584
λ_1	-	69.1361	-	-	65.3019
λ_2	-	30.2549	-	-	14.2655
σ	0.1652	-	-	-	-
λ	-	-	-	9.5952	-
k	-	-	-	0.0022	-
δ	-	-	-	0.0332	-

the averaged values we see that the tempered stable models lead to a better forecast regardless of the presence or not of the stochastic volatility. The forecasts produced by different models are presented at Figure 8.1 – subfigures 8.1a-8.1e. On the axes are the support of the log-returns and the time presented by years. The surface presents the calibrated PDF's w.r.t. all days between September 25, 2008 to July 01, 2022, whereas the red points are the actually happened log-returns with one day lag.

The calibrated parameters for the different models based on the whole used data – from October 6, 2004 to July 01, 2022 – are presented in Table 8.2. The corresponding PDFs they lead to can be seen at Figure 8.1f. The conclusion that the models (except the Black-Scholes one) describe relatively similarly the empirical data is confirmed again. We can observe that the correlation coefficients for the stochastic volatility models are negative – -0.2021, -0.4189, and -0.6000 for the Heston, Bates and SV/TS models, respectively. This confirms the leverage effect is a stylized fact. We can see also that the normally distributed jumps in the Bates model have a relatively large intensity, 9.5952, but a low jump size and deviation – 0.0022 and 0.0332. This describes the infinite activity of a Lévy process rather than a compound

Figure 8.1: Forecasts and the calibrated PDFs

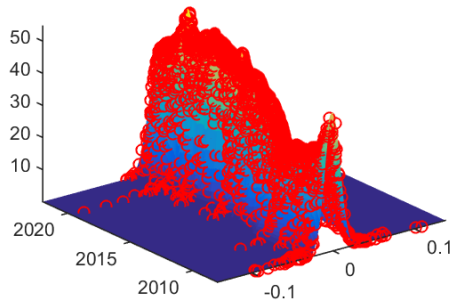

(a) Black-Scholes

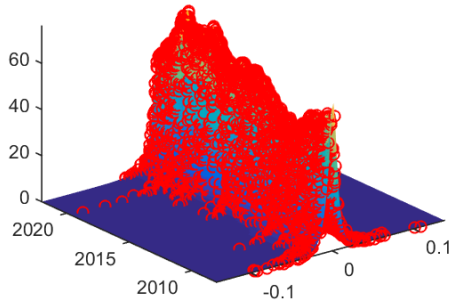

(b) Exponential tempered stable

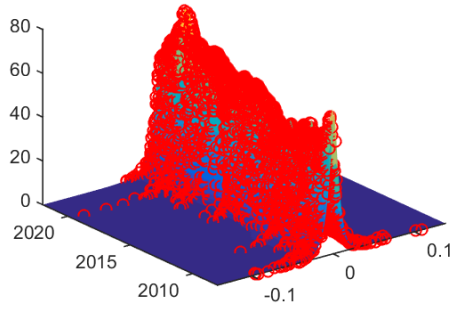

(c) Heston

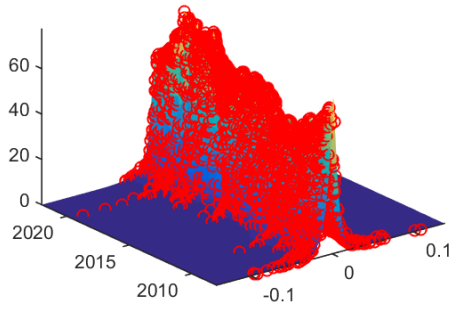

(d) Bates

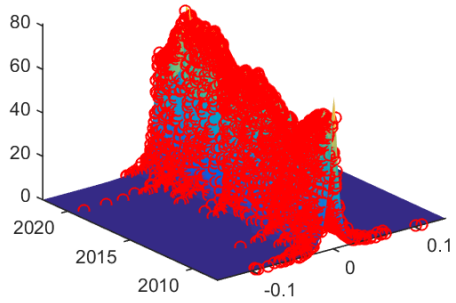

(e) SV/TS

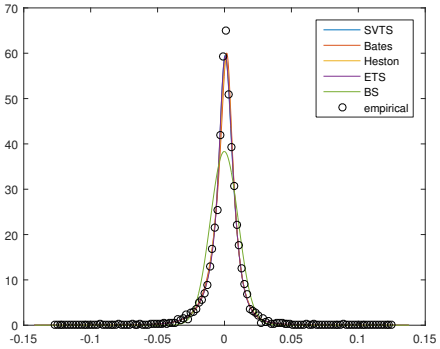

(f) total PDFs

Poisson process. Note also that the criterion we choose for our calibration methodology given in equation (8.5) leads to relatively large deviations in the distribution center but the fit is very strong in the tails. The errors that occurred are presented at the second line of Table 8.1. The models (except the Black-Scholes one which produces error = 7.4516) give errors near one. We can see again that the tempered stable process produces more realistic behavior. The error for the exponential tempered stable model is 1.1083 and for the stochastic volatility model with a tempered stable correction is 1.0809. For a comparison – the Heston and Bates deviations are 1.1845 and 1.1722, respectively.

The daily deviations which the models produced are presented at Figure 8.2d. Together we plot the values of the corresponding log-returns multiplied by 50 for a good visualization. Excluding the Black-Scholes model which produces higher deviations, the rest models have similar errors. The average errors are presented in the first line of Table 8.1. We can see that the stochastic volatility model with tempered stable jumps gives the smallest deviation: 4.2394. The other jump models, namely the Bates one and the exponential tempered stable model, have average errors of 4.3096 and 4.3051, respectively. The Heston model which exhibits continuous trajectories produces an averaged deviation with value of 4.5368. We can conclude that the jump models describe more realistically the empirical observations. In addition, the Black-Scholes's error is 9.7756 – hence we have validated the well-known stylized fact that the Gaussian assumption for the log-returns is not supported by the historical data.

Another conclusion we can make from Figure 8.2d is that the larger deviations appear in the periods of high volatility. This observation can be seen in the behavior of all models.

8.1.5 Calculated values of VaR, ES, and ERM

The approach to deriving the empirical values of the measures is considered in Section 8.1.1. Theoretical values are derived through the already calibrated PDFs. For the VaR we use the CDF obtained by the cubic spline method applied to the cumulative sum of the PDF and then invert it. The ES is obtained by averaging (integrating) the VaR function (see Definition 4.2). We find the ERM using Proposition 5.1.

As mentioned above, it is very important for the financial institutions different risk measures to return relatively close results. The currently adopted

Table 8.3: Empirical VaR, ES, ERM, and the corresponding ratios

parameter	VaR	ES	ERM	$k_1 = VaR/ES$	$k_2 = VaR/ERM$
$\epsilon = 0.01$	0.0366	0.0556	0.0290	0.6577	1.2634
$\epsilon = 0.02$	0.0295	0.0437	0.0225	0.6753	1.3148
$\epsilon = 0.03$	0.0244	0.0381	0.0190	0.6414	1.2837
$\epsilon = 0.04$	0.0210	0.0343	0.0167	0.6129	1.2548
$\epsilon = 0.05$	0.0186	0.0313	0.0150	0.5927	1.2335

method for this adjustment is based on changing the levels at which the measures are considered. The main disadvantage of this approach is that we loose (or add) a tail information changing the level. Alternatively, we suggest the use of correction coefficients between the VaR on the one hand and the ES and the ERM on the other. The coefficients we introduce are obtained as the ratios between the empirical VaR, ES and ERM calculated for the whole data. We shall denote them by $k_1 = VaR/ES$ and $k_2 = VaR/ERM$. The derived values of the risk measures together with the corresponding ratios are presented in Table 8.3. The used levels are $\epsilon \in \{0.01,\ 0.02,\ ,0.03,\ 0.04,\ 0.05\}$. We can see that the values of k_1 and k_2 are relatively stable w.r.t. the level ϵ and hence we assume that $k_1 = 0.6$ and $k_2 = 1.25$. Alternatively, the coefficients k_1 and k_2 can be considered as functions of ϵ. The exact values can be adjusted via additional tests based on many other indexes, assets, etc., if the suggested approach would be accepted in the financial practice.

The original values of the risk measures for the five models presented in Chapter 3 are compared at Figure 8.2. We can see that the models follow the empirical VaR-measure relatively closely. Let us note that the Bates model has a large deviation near the year 2018. A possible explanation is that this is due to a shortcoming of the calibration methodology. The same observation is applicable to the other models at a lesser extent. Nonetheless, it can be seen that the approach we suggest captures the empirical values after some time. On the other hand, we can restart the algorithm at the current moment, if it returns a large error since we re-calibrate daily. This is due to the large flexibility of our method and its weak time coherence. In such a way the new parameters may describe more efficiently the eventual new market realities. The same conclusion but strengthened can be made for the other two risk measures – the expected shortfall and the expectile-

based risk measure. This can be explained by the fact that (1) the ES is the integrated VaR and (2) the ERM is based on more information than the VaR. We have to mention that the Black-Scholes model follows the trend of all risk measures, but it leads to some underestimation. On the other hand, this model has a great advantage – it depends only on two parameters and thus its calibration is very easy. The averaged deviations for the models are reported in Table 8.1 – the third, fourth, and fifth line. We can confirm the observation made for the fits that the existence of tempered stable jumps leads to fine results in the presence or not of stochastic volatility. Also, the Heston model and the Bates model lead to good results too mentioning the large deviation in the ES for the Bates model – the explanation for it is provided above. Nonetheless, the stochastic volatility model with tempered stable jump correction produces best results. The price which we have to pay for this is the large number of the parameters and some calibration difficulties it leads to.

We present the corrected by the coefficients $k_1 = 0.6$ and $k_2 = 1.25$ risk measures at Figure 8.3. It can be seen that excluding the mentioned above rare discrepancies, which can be avoided by restarting the calibration algorithm when they happen, all models lead to a similar and parallel behavior of all risk measures. This observation is true for the Black-Scholes model too with the remark of its underestimation. All these findings strongly support our suggestion to introduce the correction coefficients between the VaR on the one hand and ES and ERM on the other. Finally, we calculate the risk measures which the already calibrated models for the period between October 6, 2004 and July 01, 2022 lead to. The parameters values are reported in Table 8.2 and the results for the levels 0.05, 0.025, and 0.01 are presented in Table 8.4. The left-hand values for the expected shortfall and the expectile risk measure are the original ones, whereas the right-hand values are corrected by the coefficients k_1 and k_2. We can see that the results for the VaR are very close to the real ones for all models except for the Black-Scholes one, which again produces significantly lower but predictable results. For the rest two measures the results are again admissible and confirm the previous conclusions.

The risk measures share a common pattern on Figure 8.2 and Figure 8.3: three regimes can be discerned. From the beginning of the observation period to late-2012 we witness the aftermath of the Global Financial Crisis of 2008. Since 2020 a new plateau is formed to reflect the COVID-19 impact on the financial markets, although at a lower level than the 2008 - 2012 period. In-

Table 8.4: Risk measures results for the whole data

parameter	empirical	BS	ETS	Heston	Bates	SV/TS
$VaR\,(0.05)$	0.0186	0.0173	0.0184	0.0184	0.0186	0.0186
$ES\,(0.05)$	0.0313/0.0188	0.0217/0.0130	0.0292/0.0175	0.0302/0.0181	0.0297/0.0178	0.0299/0.0179
$ERM\,(0.05)$	0.0150/0.0188	0.0121/0.0151	0.0142/0.0177	0.0147/0.0184	0.0144/0.0181	0.0145/0.0181
$VaR\,(0.025)$	0.0261	0.0206	0.0257	0.0260	0.0257	0.0260
$ES\,(0.025)$	0.0407/0.0244	0.0245/0.0147	0.0368/0.0221	0.0388/0.0233	0.0377/0.0226	0.0379/0.0227
$ERM\,(0.025)$	0.0205/0.0257	0.0148/0.0185	0.0191/0.0239	0.0199/0.0249	0.0194/0.0243	0.0195/0.0244
$VaR\,(0.01)$	0.0366	0.0245	0.0358	0.0373	0.0363	0.0368
$ES\,(0.01)$	0.0556/0.0334	0.0279/0.0167	0.0472/0.0283	0.0510/0.0306	0.0492/0.0295	0.0491/0.0294
$ERM\,(0.01)$	0.0290/0.0363	0.0181/0.0226	0.0262/0.0328	0.0278/0.0347	0.0269/0.0336	0.0270/0.0337

Figure 8.2: Risk measures, estimation errors, and log-returns

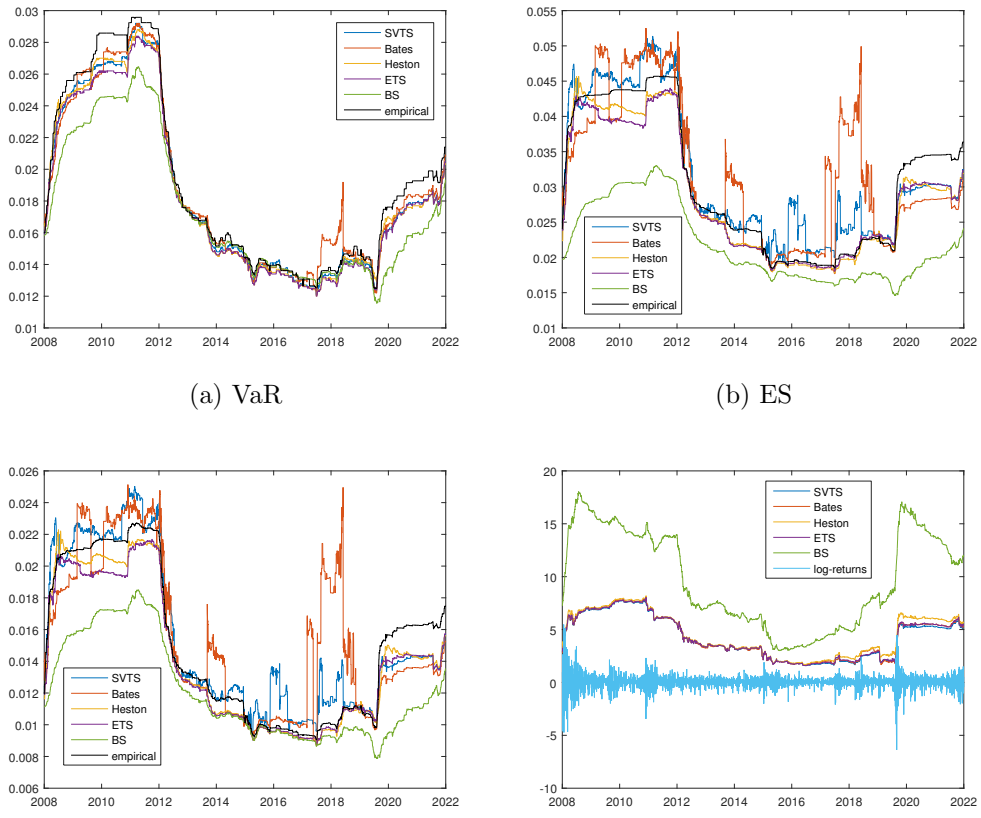

(a) VaR

(b) ES

(c) ERM

(d) Errors

between we observe the profile of a recovering market with a series of peaks that are reflected differently by the various models while the Bates one has the largest volatility among the risk measures.

8.2 Computations for the Entropic VaR

In this section we calibrate the models, we look at the calibration results, and we discuss the computational outcome for the Heston model.

Figure 8.3: Corrected risk measures

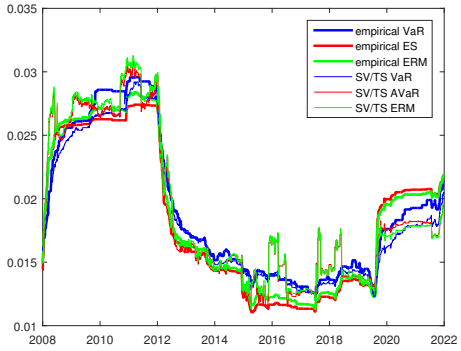

(a) SV/TS model

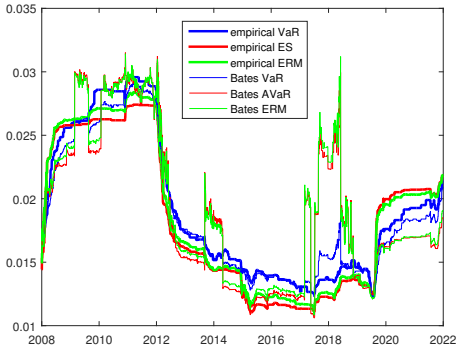

(b) Bates model

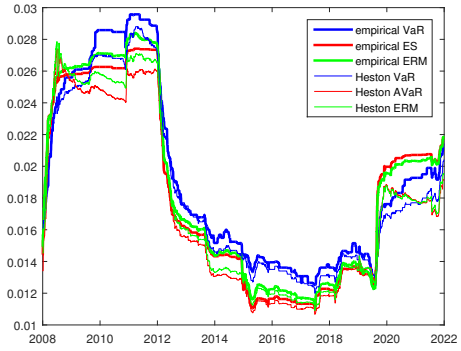

(c) Heston model

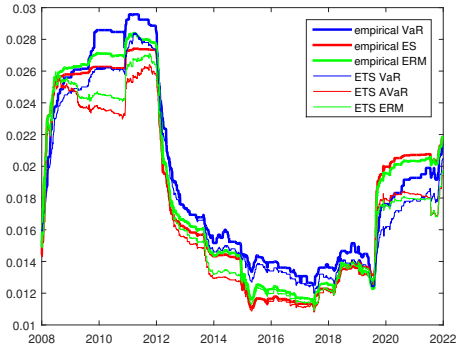

(d) ETS model

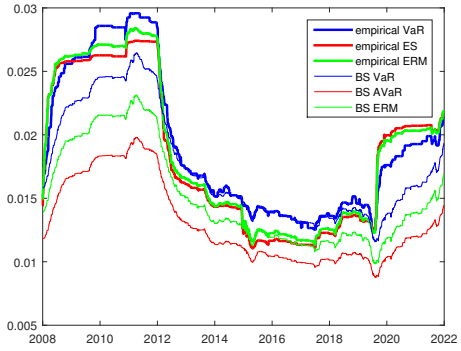

(e) Black-Scholes model

Table 8.5: EVaRs based on Table 2 of Zaevski and Nedeltchev[186]

parameter	empirical	BS	ETS	Heston	Bates	SV/TS
0.001	0.1144	0.0388	0.1139	0.1527	0.1061	0.1214
0.01	0.0857	0.0317	0.0795	0.1045	0.0762	0.0847
0.025	0.0726	0.0284	0.0657	0.0852	0.0638	0.0699
0.05	0.0212	0.0124	0.0179	0.0208	0.0184	0.0188
0.75	0.0116	0.0080	0.0100	0.0111	0.0103	0.0104
0.99	0.0015	0.0016	0.0013	0.0015	0.0014	0.0014

8.2.1 Models calibration

In Table 8.5, we provide the $EVaR$ for $\epsilon \in \{0.001, 0.01, 0.025, 0.05, 0.75, 0.99\}$ and the parameters reported in Table 8.2.

We can observe that there are similarities between the theoretical $EVaR$s and the empirical ones; nevertheless, the match is far from a good one. To have a more precise conclusion, we calculate the $EVaR$s that the calibrated models produced for the initial data window of 1000 observations. The calibration follows the pattern described in Section 8.1.2. The results are presented in Figure 8.4. We can see that although there are some similarities, the discrepancies are substantial. Several reasons may lead to this inaccuracy – the most likely one is the existence of over-fitting. To check this hypothesis, we recalibrate the models defining a cost functions consisting of two parts – one for the distribution's PDF and another one for the $EVaR$. Also, we update the historical sample considering the period between January 2, 2003 and February 19, 2025. We use the classical procedure for extracting the empirical PDF. The interval $(-0.23, 0.23)$ for the log-returns is divided into 230 bins with length 0.002. The interval is chosen in that way because the lowest log-return ever is -0.2290, observed at October 19, 1987 – the so-called Black-Monday. The empirical PDF values at the centers of the sub-intervals are obtained by counting the number of observations that fall in them. We obtain the empirical PDF values for the log-returns via the approach described in Section 8.1.3. As we mentioned in Section 7.4, the initial volatility for the stochastic volatility models is a hidden market parameter – we suggest to remove it from the calibration methodology by averaging w.r.t. its stationary distribution. We use the standard least square errors method to compare the theoretical and empirical PDFs. The second term

of the cost function is related to the deviations from the empirical $EVaR$s produced by the theoretical models. For a relative equalization of the weights of both components, we multiply the $EVaR$-part by 10^3. Thus we reach the minimization problem

$$\min_{\upsilon\in\Upsilon}\left\{\sum_{n=1}^{230}\left(p_{th,n}-p_{emp,n}\right)^2+10^3\sqrt{\sum_{n=1}^{6}\left(EVaR_{th}\left(\epsilon_n\right)-EVaR_{emp}\left(\epsilon_n\right)\right)^2}\right\}, \tag{8.9}$$

where Υ is the set of all possible parameters for the theoretical model, $\upsilon\in\Upsilon$, the symbol p is used for the PDFs, and by a subscript is marked the empirical and theoretical terms.

We derive the model's parameters without applying either penalization or regularization since we are not challenging the stability of the model performance over such large period. On the contrary, we would like to see how volatile are the parameters.

8.2.2 Calibration results

The calibrated parameters for the five models based on the whole data are reported in Table 8.6.

The generated PDFs can be compared to the empirical values in Figure 8.4b. The values of cost function (8.9) as well as its both components can be seen in the first part of Table 8.7. We conclude that all models except the Black-Scholes one capture the shape of the empirical PDF. The existing divergences can be explained by the challenges that stand in the multidimensional optimization. The value function during the period as well as its both components can be seen in Figures 8.5a, 8.5b, and 8.5c.

The reported in the second part of Table 8.7 values for the entropic VaR confirm that all non-lognormal models capture the risk profile of the S&P 500 index. Furthermore, we present the other discussed in the dissertation risk measures – VaR, ES, and ERM – in Table 8.7. We can see that despite some deviations, these measures are captured too. The $EVaR$s of the five models we deal with can be seen in Figure 8.4c. We use a moving window again with 1000 positions and thus the period consist of 4569 observations between December 21, 2006 and February 19, 2025. First, it is worth to underline that the profile of the empirical $EVaR$ very clearly differentiates

Figure 8.4: EVaR

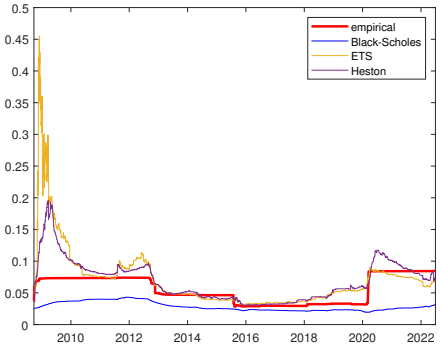

(a) EVaRs for data from Zaevski and Nedeltchev [186]

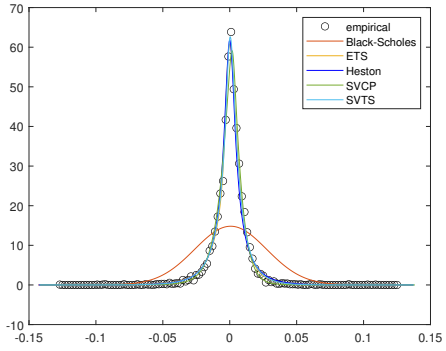

(b) calibrated PDFs

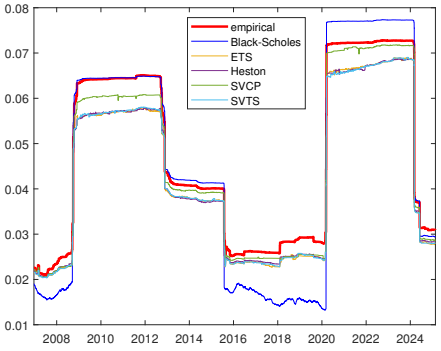

(c) calibrated EVaRs

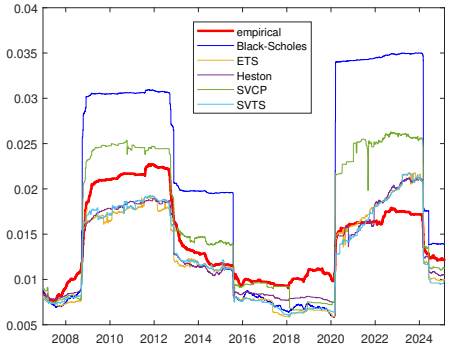

(d) ERMs

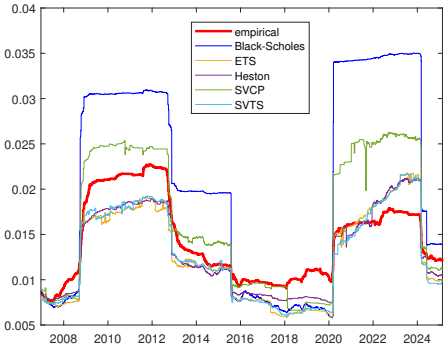

(e) ESs

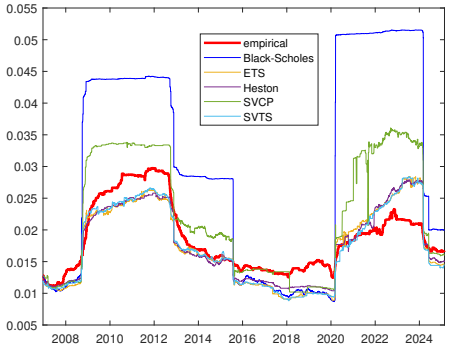

(f) VaRs

Figure 8.5: Some comparision

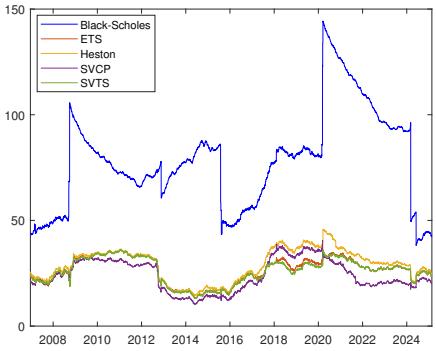

(a) Value function

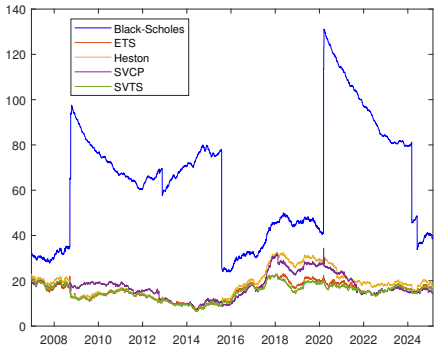

(b) Value function – PDFs

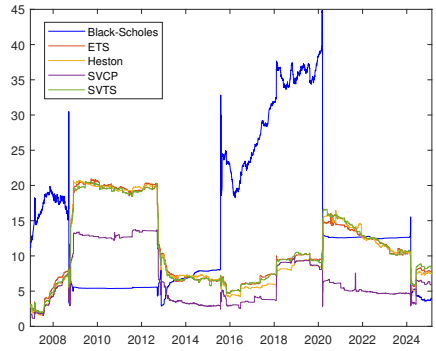

(c) Value function – EVaRs

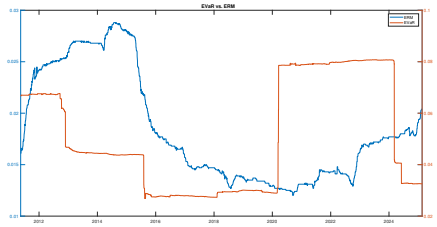

(d) ERM vs EVaR

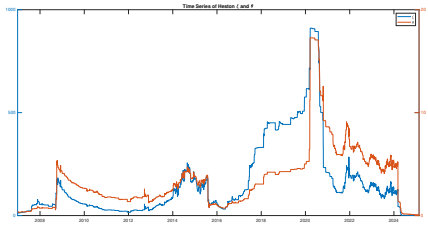

(e) Heston's ξ vs θ

Table 8.6: EVaR-related parameters for the considered models

parameter	BS	ETS	Heston	Bates	SV/TS
μ	0.2632	0.0767	0.1946	-0.0829	0.0616
ξ	-	-	142.7981	28.1853	37.4461
η	-	-	0.0419	0.0225	4.8209E-04
θ	-	-	5.6212	0.9738	0.0161
ρ	-	-	-0.0041	-0.7944	-0.2295
α_1	-	6.1266E-06	-	-	0.2402
α_2	-	1.0187	-	-	0.407
c_1	-	112.4077	-	-	37.3946
c_2	-	0.6192	-	-	18.7313
λ_1	-	71.5889	-	-	67.5161
λ_2	-	34.2866	-	-	79.1169
σ	0.4274	-	-	-	-
λ	-	-	-	3.5253	-
k	-	-	-	-0.0154	-
δ	-	-	-	0.0354	-

the zones with heightened level of market risk. Furthermore, all models except the Black-Scholes one more or less follow this behavior. This shows that the entropic VaR is a risk-measure that almost immediately indicates for market turbulence.

Next we calculate the VaR, the ES, and the ERM based on the calibrated parameters via the moving window and criteria (8.9). The results for the expectile risk measure can be viewed in Figure 8.4d, for the expected shortfall in Figure 8.4e, and for the VaR in Figure 8.4f. We can conclude that despite some deviations, the calibrated models follow the behavior of the ERM, ES, and VaR in addition to the entropic VaR. Hence, the calibration method we suggest captures not only the distributions and $EVaR$s, but also other properties coming from the expectile risk measure, expected shortfall, and VaR. All these results confirm that the approach can be used for avoiding over-fitting as well as for capturing the intrinsic features of the financial data.

Table 8.7: Deviations,Expectile Risk Measures, Expected Shortfall, VaR

deviations	empirical	BS	ETS	Heston	Bates	SV/TS
total	—	108.5314	14.4035	16.7178	19.0651	15.1364
PDF	—	92.9494	8.0434	9.6454	14.0027	7.5923
EVaR	—	15.5820	6.3601	7.0724	5.0624	7.5441
EVaR	empirical	BS	ETS	Heston	Bates	SV/TS
0.001	0.1121	0.0994	0.1164	0.1168	0.1158	0.1173
0.01	0.0835	0.0810	0.0821	0.0820	0.0827	0.0821
0.025	0.0706	0.0724	0.0682	0.0680	0.0690	0.0679
0.05	0.0602	0.0652	0.0576	0.0572	0.0583	0.0571
0.75	0.0539	0.0606	0.0512	0.0508	0.0519	0.0506
0.99	0.0014	0.0031	0.0015	0.0012	0.0021	0.0015
ERM	empirical	BS	ETS	Heston	Bates	SV/TS
0.001	0.0564	0.0649	0.0507	0.0496	0.0510	0.0489
0.01	0.0271	0.0456	0.0288	0.0277	0.0252	0.0276
0.025	0.0192	0.0370	0.0211	0.0202	0.0183	0.0202
0.05	0.0141	0.0300	0.0157	0.0149	0.0139	0.0151
ES	empirical	BS	ETS	Heston	Bates	SV/TS
0.001	0.1055	0.0889	0.0785	0.0773	0.0841	0.0760
0.01	0.0518	0.0711	0.0515	0.0502	0.0467	0.0495
0.025	0.0380	0.0624	0.0404	0.0392	0.0348	0.0388
0.05	0.0293	0.0550	0.0322	0.0310	0.0275	0.0309
VaR	empirical	BS	ETS	Heston	Bates	SV/TS
0.001	0.0792	0.0828	0.0683	0.0670	0.0706	0.0659
0.01	0.0347	0.0622	0.0395	0.0381	0.0322	0.0378
0.025	0.0248	0.0523	0.0285	0.0273	0.0234	0.0273
0.05	0.0174	0.0438	0.0205	0.0195	0.0177	0.0197

8.2.3 Analyzing Heston Model Calibration

We choose to comment the parameters inferred for the Heston model because it is based on the stochastic volatility which we observe on the financial markets while the Black-Scholes one is based on the assumption of a constant volatility. Also, the model is well-known among the academic circles and the practitioners, and this secures a solid ground to compare our results with previous studies and large enough target group for the chapter. Heston model paves the way to understanding the more sophisticated models elaborated in Chapter 3.

A general observation is that the Global Financial Crisis 2008 (the GFC) and COVID19 left footprints on the profile of every parameter. Figure 8.6 confirms that Heston parameters for the $EVaR$ reacted to the GFC and to the COVID19 pandemia. The most important observation regarding μ is that it changes its sign; it reaches the lowest values during the COVID19 pandemia and has record high values from the end-2012 to the end-2016. The speed of the mean reversion ξ is a very volatile parameter with min value of 0.3279 at the very last day of the considered period and max value of 910.3188 observable from March 20, 2020 to April 21, 2020. The parameter η is of very low value until the break of the GFC; also, from August 2015 till the break of the COVID19; its value decreases from end of 2012 to the mid-2015 and increases steadily during the remaining periods. We observe that the profile of ξ and θ are surprisingly identical although of different scale - see Figure 8.5e. The correlation coefficient ρ has a very stable behavior through the calm market periods and is significantly volatile in the turbulence. Let us also consider the impact of Heston parameters evolution on the distribution of the log-returns in light of Rouah[(169)]. We know that the log-returns are positively skewed when ρ is positive and negatively when ρ is negative. Hence, we anticipate that the related distribution is negatively skewed except in the period after March 2024. We know that a high θ results in high distribution kurtosis. Hence, we anticipate fat tails for the whole period except the first quarter after the beginning of the COVID19 pandemia.

Last but not least, we compare the market risk measured by the expectile risk measure and the entropic VaR through the results presented in section 8.1.1. We take into account that the empirical data for this investigation consists of the daily observations of the S&P500 index between September 25, 2008 to July 1, 2022 – totally of 3466 log-returns. We use namely this data to equalize the historical samples. First, we can observe that the entropic

Figure 8.6: EVaR Heston Parameters

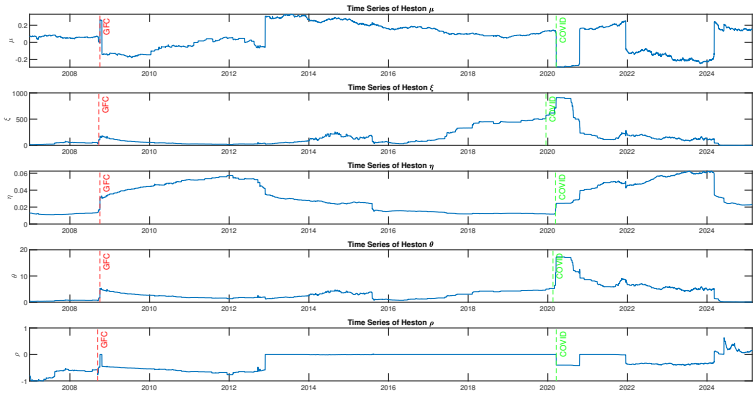

VaR better reacts to exogenous events like the GFC and the COVID19 – see Figure 8.5d. On the other hand, Figure 8.8 presents the joint plot of the parameters. We see a good match for the time drift μ. Also, we note that ξ and θ are of very different scale. The variance volatility θ is the same from the second half of 2015 to the begin of COVID19. During the rest of the period, we see opposite values. Furthermore, we see that the correlation coefficient for the entropic VaR is rather stable whereas it is more volatile for the expectile risk measure.

Figure 8.8: Comparing Heston parameters for ERM and EVaR

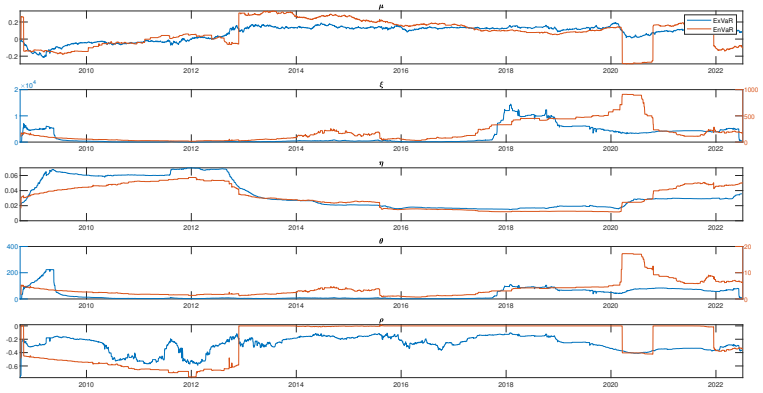

Chapter 9

Rough Volatility: A New Stylized Fact

The dissertation applies various models for asset price dynamics. Such models are developed and selected for use based on their capability to capture the market realities called "stylized facts" (see Section 1.5.4). The better a model reflects the stylized facts, the more the model is preferred. The financial market keeps evolving in a fast pace and new stylized facts crystalize constantly. This presses the academic community and the practitioners to keep inventing models for the new type of stylized facts. Among the recently established stylized facts is the rough volatility. For this reason we shall describe the features of the rough volatility.

The stylized facts play a key role in the way the humans comprehend the complicated and vibrating reality around them. The reality complexity is reduced to a degree that matches the current cognitive capacities. This simplification is needed and justifiable until it preserves some reality pivots called *stylized facts*. Actually, the stylized facts is what we decided *a priori* to find in the mirrored simplification of the reality. Hence, any bias in defining and enumerating the stylized facts results in a distorted image of the reality.

Some knowledge branches (like model validation) developed the epistemological concept of stylized facts, ways to establish new stylized facts, and thus secure dynamics of the stylized facts set (see for example Meyer[136]). Other areas (like the Financial Mathematics for example) do not have such toolkit; the academic community attempts to identify which features a financial model should not miss.

The establishment of stylized facts is important *per se* and also since it

unlocks further activities, like developing financial models (see for example Kim and Shin[114]), volatility forecasting (Malmsten and Teräsvirta[130]), and portfolio optimization (Karmous et al.[113]). Financial models are developed to reduce the financial market complexity to a limited number (one or two but no more than that) of already established and agreed upon stylized facts; for example, a model is developed to reflect the jumps observed on the market, to capture the stochasticity of the volatility or both of them. Consequently, the model is rated on its capacity to capture this or that aspect of market activities.

The preceding chapters indicate the main research directions of the dissertation:

- the *pros* and the *cons* of applying different risk measures;
- the importance of describing the returns via a model that captures the needed stylized fact(s).

Section 1.5.4 of the dissertation presented the emergence of a new academic and practitioner's understanding of the rough volatility as a contemporary stylized fact. This chapter borrows from Nedeltchev and Zaevski[140] and delves into some theoretical aspects of the rough volatility, proposes a particular approach for calculating it, and derives empirical evidences of it. It leaves open the question whether it is convenient to apply any of the available risk measures to the rough volatility or the new stylized fact requires the elaboration of a new risk measures type.

9.1 Theoretical Background.

Let us begin with an admitted stylized fact related to the at-the-money volatility skew (ATMVS). The ATMVS is described as follows:

$$\psi(\tau) := |\frac{\partial}{\partial k}\sigma_{BS}(k,\tau)|_{k=0}, \tag{9.1}$$

where σ_{BS} is the implied Black-Scholes volatility, k is the log-moneyness, and τ is time to expiry. To present the case in a more convenient for the reader way we attach below Figure 2 of Gatheral et al.[88] which exemplifies the ATMVS reads a curve that reaches infinity as time reaches zeros. On the volatility side, various approaches are developed to estimate the volatility

both on the long-term end of the curve and on the short-term end; these methods differ in their capability to capture the above stylized fact.

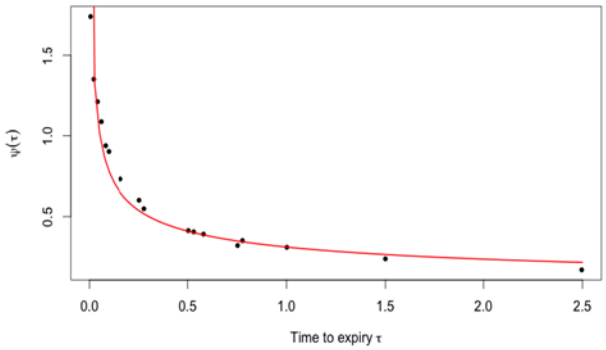

Figure 1.2: The black dots are non-parametric estimates of the S&P ATM volatility skews as of June 20, 2013; the red curve is the power-law fit $\psi(\tau) = A\,\tau^{-0.4}$.

On the returns side, models are developed with the purpose to adjust the basic Black-Scholes model to the contemporary realities and hence jump component is added to the models to reflect the infinity-reaching short-term end of the ATMVS curve (an example for such models is the Merton jump diffusion model for the constant volatility, the Bates model for the stochastic volatility (see Section 3.4), and the Stochastic Volatility Tempered Stable model (see Section 3.5)). Such model augmentation comes at the costs of calibration troubles - for example, the Bates model calibration requires that eight parameters were inferred, while the Stochastic Volatility Tempered Stable model is governed by 11 parameters.

Recent researches reveal that the ATMVS curve might be fitted by a power-law of certain parameters; for concrete fit parameters see Gatheral et al.[88]. This finding opens the door to generalize the standard Brownian Motion (for the sBM and its properties see Section 2.2.1) with the fractional Brownian Motion (for the fBM and its properties see Section 2.2.2). An adequately calibrated fBM-based model would pass the reality-checks without the burdensome jump component (see Gatheral et al.[88] and Rømer[168]).

9.2 Estimating the Hurst index value.

The application of a fBM-based model requires the estimation of the Hurst index value. A challenge for the Hurst index calibration is the lack of a unified approach to follow (see Beran[29], Berzin et al.[30], Rao[163]). This challenge might be cured by leveraging the following approaches:

- run regression to exploit the monofractal property of the fBM (the fBM monofractal property considered by Gatheral et al.[88] is equivalent to the self-similarity of the fBM (see the fourth bullet point of Property 2.1) and a sole scaling factor) which has been criticized by some authors for committing estimation error (for example see Cont and Das[52] and Fukasawa et al.[84]). Such implementation includes calculating the moments of the log-volatility differences:

$$m\left(q,\Delta\right)=\frac{1}{N}\sum_{k=1}^{N}|\ln\sigma_{k\Delta}-\ln\sigma_{(k-1)\Delta}|^{q}, \tag{9.2}$$

  where m is the moment of order q, Δ is the time lag (days), and σ is the volatility. Given the fBM monofractal property for various q, we anticipate to observe that $m\left(q,\Delta\right)\propto\Delta^{\zeta_q}$, where ζ_q is the scaling factor. Hence, we can derive the Hurst index value by running regression

$$\zeta_q\approx q\hat{H}. \tag{9.3}$$

- Run regression to exploit the auto-correlation function of the volatility (see Bennedsen et al.[27] for details). Let us present the volatility as $y_t=\ln\sigma_t=B_t^H$. Then, the variance is $var\left[y_t\right]=t^{2H}$ and the covariance is $cov\left[y_t,y_{t+1}\right]=\frac{1}{2}\{|t|^{2H}+|t+\Delta|^{2H}-\Delta^{2H}\}$. We get the following auto-correlation function

$$\kappa\left(\Delta\right)=\frac{1}{2}\left\{1+\left(1+\frac{\Delta}{t}\right)^{2H}-\left(\frac{\Delta}{t}\right)^{2H}\right\}. \tag{9.4}$$

  For sufficiently small $\frac{\Delta}{t}$, we get $\ln\left(1-\kappa\left(\Delta\right)\right)=a+2H\ln\Delta$ which is the base for the regression.

Figure 9.1: Realized Variance Series and Their Monofractal Property.

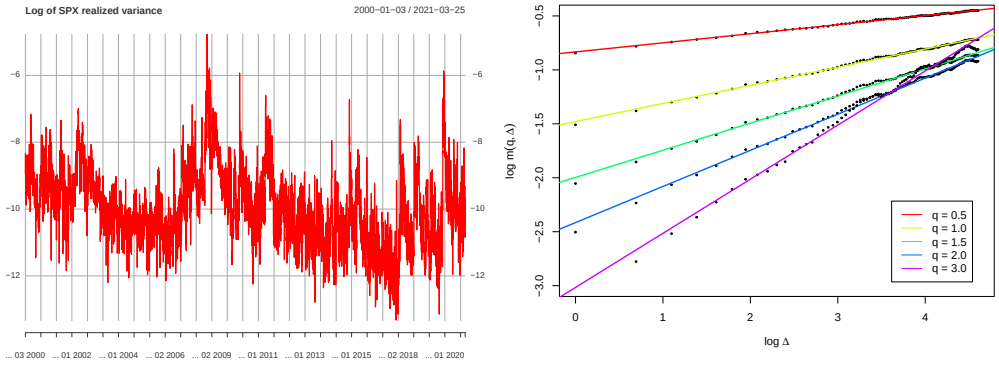

(a) Log 5-min Realized Variance for S&P500 Index with Tukey-Hanning Kernel.

(b) Monofractal Property Check.

9.3 Hurst Index Value During the COVID19 Period.

We attach high importance to the Rough Volatility model capability to correctly reflect the market realities during tranquil periods as well as turmoils. This is why we shall explore the model during the most recent period of financial uncertainty: the COVID19 Period. We model the volatility as $\sigma_t = c \exp\left(vB_t^H\right)$, where c, v are positive constants and B_t^H is a fBM.

We use the data set available online from the Oxford-Man library (https://oxford-man.ox.ac.uk/research/realized-library/). It includes 31 indexes that cover the Americas (the USA, and a couple of Emerging Markets), Europe, and Asia (incl. some Emerging Markets). The time ranges from January 2000 to March 2021; in other words, data for the COVID19 pandemic period is available to us. We are talking of high-frequency series for 5-min realized variance (RV), 10-min RV, and various kernels (Tukey-Hanning, Two-Scale/Bartlett, and Non-Flat Parzen) are applied to integrate the RV. For more details about the features of the data, see https://impa.br/en_US/eventos-do-impa/eventos-2018/research-in-options-2018/. Figure 9.1a exemplifies the data subset for S&P500 Index and 5-min integration of the RV via the Tukey-Hanning kernel.

Exploring the data, we observe that data for the STI index is missing for

Table 9.1: Quadratic Fit Coefficients.

$FitCoefficient$	$S\&P500$	$STOXX50E$	KSE	$FTSE$
$intercept$	-0.0006898	0.01819	-0.002272	0.001306
$coef1$	0.1693142	0.1631	0.13306	0.162386
$coef2$	-0.0006323	-0.03238	-0.00948	-0.009459

the period 2008 – 2015 and for this reason the index is excluded from our research. The DJI data contain negative values for a couple of days. We removed from the data 10 dates with variance of 0. We believe the steps taken to secure the data quality cover a limited portion of the data set and thus do not compromise our conclusions.

We challenged the approach defined by formula (9.2) and confirmed the monofractal property $m(q, \Delta) \propto \Delta^{\zeta_q}$ which is compatible with Gatheral et al.[88] – see Figure 9.1b. Also, we questioned the link between ζ_q and the empirically derived Hurst index value $\hat{H}$ for several indexes: S&P500 (Figure 9.2a), STOXX50E (Figure 9.2b), FTSE (Figure 9.2c), and KSE (Figure 9.2d). We find that the link between ζ_q and $\hat{H}$ for the latter 3 indexes is far from being linear. Table 9.1 reads the coefficients of a parabolic fit.

Hence, there are no arguments to estimate the H-index by running the *linear* regression in formula (9.3). This failure drove us to use the approach defined by formula (9.4). Figure 9.3a reads the Hurst index series of S&P500. Next, we checked whether the same observations apply to other indexes; we find that the Hurst index series for $STOXX50E$ (for example) follow the same patterns (see Figure 9.3b). We double check this result by drawing the two series S&P500 vs. STOXX50E (see Figure 9.3c). We would like to exclude any role of the integrating kernel; hence, we run the same checks for the Parzen kernel (see Figure 9.3d). Figure 9.3e presents the Hurst index series for the COVID19 period only.

Figure 9.2: Derived Hurst index Values

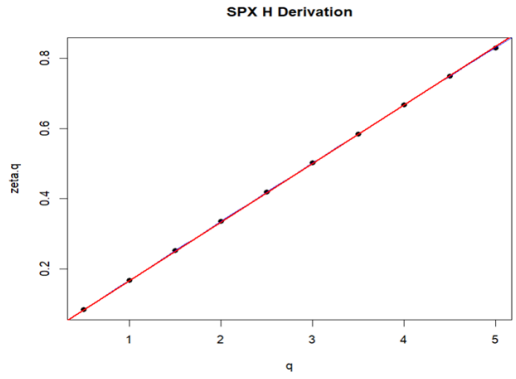

(a) Hurst index Derivation for S&P500 Index.

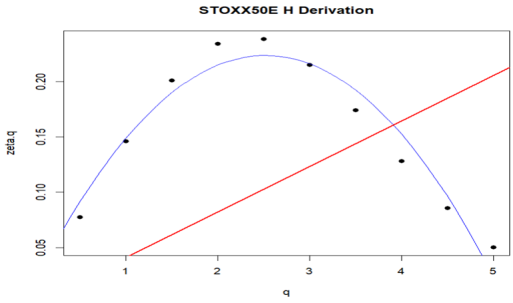

(b) Hurst index Derivation for STOXX50E Index.

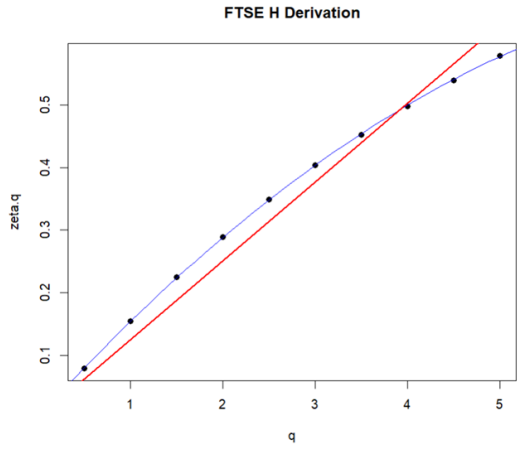

(c) Hurst index Derivation for FTSE Index.

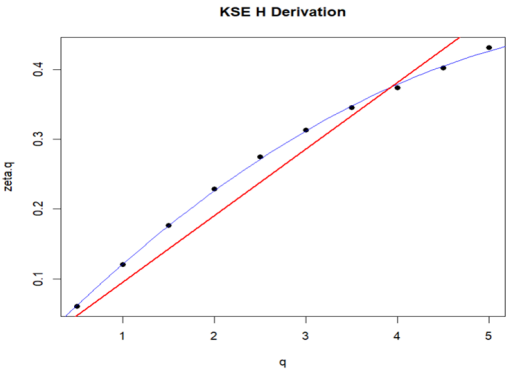

(d) Hurst index Derivation for KSE Index.

Figure 9.3: Hurst index Series.

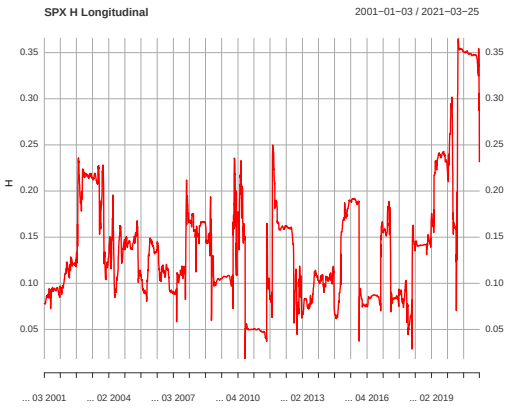

(a) Hurst index Series for S&P500 Index.

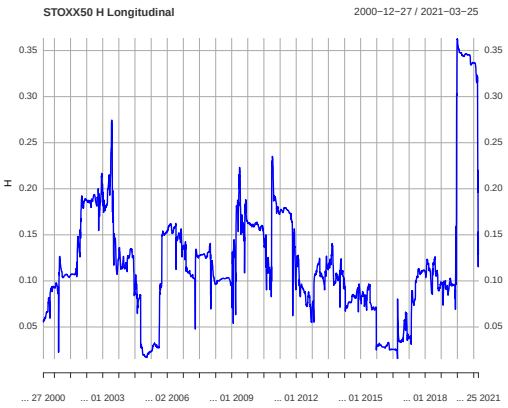

(b) Hurst index Series for STOXX50E Index.

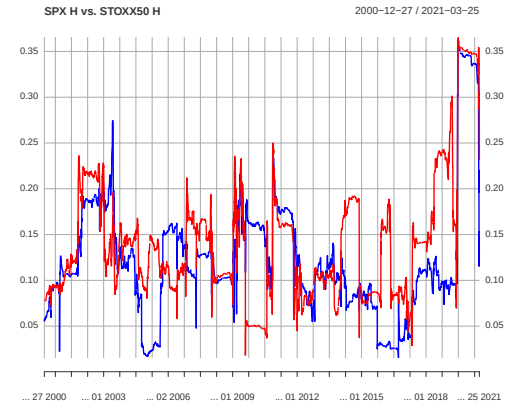

(c) Comparison Hurst index S&P500 vs. STOXX50E.

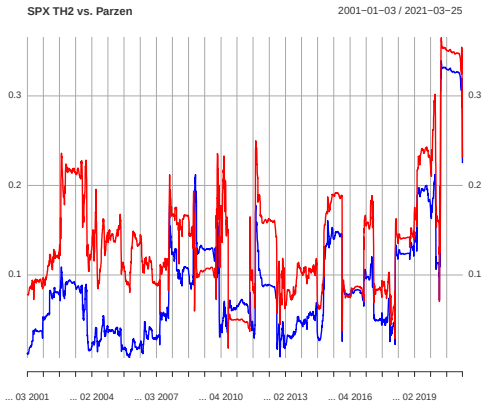

(d) Comparison Tukey-Hanning vs. Parzen Kernel for S&P500 Index.

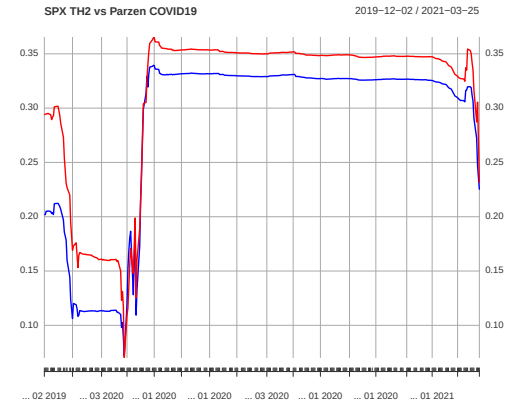

(e) Hurst index Series During COVID19 Period.

Chapter 10

Concluding remarks and further works

The dissertation tackles the ERM as a risk measure that is the opposite to the expectile which on its turn is found via a square optimization. It has the advantage to be the only risk measure that is both coherent and elicitable when certain constraints on its significance level are met.

We present the CDF via the characteristic function which is later used to derive the VaR by inverting the CDF. Also, we suggest to compute truncated expectation via the characteristic function and later apply it to derive the ES as well as the ERM.

The dissertation's computations include S&P500 index data set of the daily Adjusted Close price ranging from October 6, 2004 to July 01, 2022. We applied a moving window of 1000 observations. We select the start date and the window width in a way to use the calibration results from previous studies.

We found a satisfactory good match between the theoretical and the empirical values of the VaR, ES, and ERM. The theoretical - empirical comparison leverages a coefficient that corrects the VaR/ES ratio and the VaR/ERM ratio. This innovation better preserves the information available at the returns distribution when changing the measurement level. We suggest value of 0.6 for the former coefficient and 1.25 for the latter one. We observe that all models (except the Black-Scholes one) match the empirical VaR and the tempered stable jumps model reaches the best match.

The theoretical PDFs were received by minimizing the least square error between the empirical and the theoretical values of the function. The lack of

PDFs for the considered models (except for the Black-Scholes model) needed us to derive the PDF by applying Fast Fourier Transform to the characteristic functions of the models. The theoretical VaR values were computed as a quantile of the CDF; on its turn, the CDF was computed as the inverse value of cubic splines applied to the cumulative sum of the theoretical PDFs. The theoretical ES values were obtained by integrating the VaR values. Formula 5.3 was used to compute the theoretical ERM values.

We verified how well the PDF values are calibrated. To this end, we applied an approach that resembles the maximum likelihood estimation. We found a relatively good fit of all models; the best fit is achieved by the tempered stable model, while the Black-Scholes model produced the worst fit. The check we undertook confirmed the leverage effect as a stylized fact. Also, we found that the Bates model produces results of a relatively large intensity and a low jump size. We see that the calibrated results are marked with relatively large deviations in the distribution center and a strong fit in the tails.

The dissertation transforms the initial way of presenting the $EVaR$ from the right-hand distribution tail (i.e., the profit) to the left-hand one (i.e., the losses) which is of interest for the finance. This risk measure is defined as a minimization of a MGF-related function which requires us to determine the diapason where the MGF is defined, since contrary to the CDF, the MGF is not defined everywhere.

The dissertation presents the $EVaR$ as a coherent risk measure. Hence, its dual representation is described. A contribution of the dissertation is the derivation of the $EVaR$'s acceptance set.

The $EVaR$ is derived via a minimizer of a MGF-related function. The dissertation elaborates the MGF for the 5 models considered and the value of the MGF-related minimizer. Also, the text indicates the interval where the MGF is defined for the 5 models.

In the case of the Heston model and models that incorporate it (like the Bates model or the Stochastic Volatility Tempered Stable) we deal with the initial volatility as an unobservable parameter of the model and hence enters the MGF formula. To solve this issue, we take advantage of the fact that the volatility is described by a Cox-Ingersoll-Ross process that has a Gamma stationary distribution. We average the volatility over it and we solve the challenge to define the diapason of the averaged MGF. This approach reduces the number of the model's variables/parameters but shrinks the diapason where the MGF is defined.

The dissertation computes the $EVaR$ values for 6 confidence levels and we see discrepancies between the theoretical and the empirical values. We dive deeper by calculating the $EVaR$ via the calibration approach used for ERM purposes. Again we observe gaps that we attribute to over-fitting and this is why we add $EVaR$-related part to the cost function. After calibrating the models, we compared the generated PDFs with the empirical ones; the gaps we see stem from over-fitting. We find satisfactory ability of the $EVaR$ to capture the risk profile of the S&P500 index: the zones of higher market risk are well visible while the Black-Scholes model is the worst performing among the models.

Next, the dissertation summarizes the capacity of the calibrated models to generate reliable values of the VaR, ES, ERM, and $EVaR$. The results confirm that the applied approach produces satisfactorily good results.

Last but not least, we analyze the time series of the parameters of the calibrated Heston model. We see that the parameters change qualitatively its behaviour during turmoils (the Global Financial Crisis and the COVID19 period). We see an identical profile for ξ and θ. We note that the volatility of the parameter ρ increases during financial crises.

The dissertation compares the calibrated results for the ERM and the $EVaR$ by drawing a joint plot of the parameters. We conclude that the $EVaR$ better reflects the financial crises.

The theoretical aspects discussed in the dissertation and the empirical computations done allow us to perform the following comparison of the ERM and the $EVaR$:

1. The ERM is both coherent (under the condition we deal with a significance level below 0.5) and elicitable, while for the $EVaR$ matters only the coherence property;

2. the ERM is well defined only for random variables with finite second moments;

3. we can apply the whole quantile-related toolkit to the expectile;

4. once computed, the truncated expectation value can be used for calculating both the $EVaR$ and the ES;

5. the $EVaR$ value is calculated by minimizing a MGF-related function. Hence, we have to identify the diapason where the MGF is defined and keep in mind that averaging the volatility reduces this diapason;

6. the $EVaR$ better reacts to financial crises.

Regarding the Rough Volatility, the dissertation was launched from the ubiquitous position where the dominant way to estimate volatility (as the standard deviation of asset log-returns) complicates the derivation of volatility-related stylized facts. We are facing lack of commonly adopted algorithm to reveal volatility-related stylized facts nor short-list of them and the admitted volatility-related stylized facts lag behind the current market hypothesis. Another obstacle for us is the under-exploration of market turbulence; stylized facts of market crisis are mimicked as Market Inefficiency (i.e. a deviation from the Efficient Market Hypothesis), Market Failures, etc. Stylized facts for the historic/realized volatility are better researched than the features of the implied volatility.

Based on a representative data set for an extensive time period, we observe scaling property of the log-volatility for a large pool of market indexes. Also, we confirmed there is a non-linear link between the scaling factor and the value of the Hurst index. Our calculations read a material increase of the Hurst index values during the COVID19 period; we do not spot similar increase during the Global Financial Crisis 2008. We distinguish several sub-periods of the COVID19 pandemic that match the timing split discovered by other authors (see for example Curto and Serrasqueiro[55], Bentes[28]).

We can summarize the key contributions of this chapter of the dissertation as a couple of new stylized volatility-related facts. We find that the log-volatility is rough since the Hurst index value is $H < \frac{1}{2}$. Additionally, the Hurst index value varies within a range and moves in packages with transition period between the packages. We noted that the log-volatility becomes smoother during market misbehavior. We observe that the choice of the kernel type determines the Hurst index value but preserves the above conclusions.

We started the rough volatility chapter from one stylized fact (namely handling the at-the-money volatility skew) and we established a couple of stylized facts. We suggest further researches to create eco-system of the volatility-related stylized facts that would unleash new findings of academic and practical merits. Additional efforts are necessary to separate the volatility studies from the returns series and hence a new generation of volatility-estimation methods is needed; new ways of volatility estimation might inspire a new generation of rough volatility models in addition to the existing ones, like the rough-Heston (see Euch and Rosenbaum[75], the extended rough-

Heston, the rough-Bergomi model (see Bayer et al.[21]). The next explorations in this area of the Financial Mathematics might derive the Hurst index value by running non-linear regression from the scaling factor with the fit coefficients from Table 9.1.

What is imminent for the risk measures is their backward-looking usage. It means they summarize risk information about what has already happened, i.e. what was the risk profile of a portfolio for the last reporting period. Market participants sometimes need forward-looking risk indicators. Some financial instruments (mainly derivatives, like the options) serve this purpose (see Jarrow and Chatterjea[108], Dempsey[66], Johnson[110]).

Options allow the investor to mitigate the market risk. Various combinations option-underlying (like Covered Call or Protective Put) are able to neutralize inconvenient moves of the underlying. Dynamic hedging is possible for the risk factors covered by the pricing model. For example, the Black-Scholes model introduces exposure to the underlying price, the time, the interest rate, and the volatility. In other words, the option holder can dampen the impact of the underlying shocks or the volatility moves on the option price until the option becomes neutral w.r.t the underlying price or the volatility respectively (for the role of the Greek Letters in market risk management see Anand and Manu[12]). This is why the option market reallocates the market risk from risk aversive players to risk tolerant ones (see Chapter 1-5a of Chance[43]).

Another way to mitigate risk via options is to enter option strategies (see Vine[179] and Sinclair[171]). Spreads, straddles, strangles, butterfly, condors and other figures reduce the risks accompanying the option investments, in exchange of the fee payed to enter the trade.

The option market plays another important role. The chain of options with different time to expiration and strike price on the same underlying reflects the market expectations via the so-called volatility surface (see Gatheral[86]). This construct reads the market fears or the optimism about the underlying price until the expiration. The shape of the implied volatility brings valuable information about the expected amplitude of the underlying changes (see Fengler[78]). Various operationalizations of using the implied volatility are possible, like the Implied Volatility Rank, the Implied Volatility Percentile, etc.

Option markets produce also sentiment indicators, like the Put/Call Ratio (see Houlihan and Creamer[101]). Decoding this signal indicates how the short/long side estimates the underlying market risks.

Other financial instruments, like the bonds, are used to derive the yield curve which indicates the market expectation about the interest rate dynamics. The shape of the curve (contango, humped, etc.) summarizes the fears of pending malign market developments (see Choudhry[48] and Nymand-Andersen[146]).

These relationships between financial instruments and the market risk motivate us to launch further researches in this area.

Chapter 11

Scientific Contributions

- The main contribution is the application of stochastic models (the Black-Scholes model, the Heston model, the Bates model, the exponential tempered stable model, the model with stochastic volatility and tempered stable process) to various risk measures (the Value at Risk, the Expected Shortfall, the Expectile Risk Measure, the Entropic VaR).

- The Truncated Expectation is derived through the characteristic function of the process (Proposition 5.4). On this basis, the Expected Shortfall and the Expectile Risk Measure are calculated via the Truncated Expectation (Theorem 5.2).

- The logarithm of the Heston returns are presented as random variables (Proposition 6.2) by averaging on the stationary distribution of the volatility process. Their convergence abscissas are identified as a subset of the abscissas of the initial process (Lemma 6.2 and Theorem 6.1). All possible positioning of the abscissas are discussed (Lemma 6.4, Theorem 6.2, Theorem 6.3, and Theorem 6.4). The same approach is applied also to models that upgrade the Heston model, like the Bates model and the model with stochastic volatility / tempered stable process.

- The dissertation derives the Acceptance Set of the Entropic VaR (Proposition 7.2). It proves a theorem regarding the calculation of the value of the EVaR by minimizing an MGF-related function (Theorem 7.1). The text provides formulas for the EVaR of all the 5 models: the Black-Scholes model (formulas (7.18) and (7.19)), the Heston model

(Proposition 7.5), the Bates model (Proposition 7.6), the exponential tempered stable mode (Proposition 7.4), model with stochastic volatility / modified stable process (Proposition 7.7).

- The dissertation empirically investigates the 4 risk measures applied to the 5 stochastic models for the S&P500 index for the last 23 years that include periods of normal market functioning as well as financial crises. The main conclusion in this part of the dissertation is that the EVaR reacts more adequately to market crises; the models with stochastic volatility and jumps outperform the rest of the models.

- The value of the Hurst index is calculated for 4 leading indexes (S&P500, STOXX50E, FTSE, and KSE). The calculations read a linear relationship between the scaling coefficient and the value of the Hurst index for the S&P500 index. For the rest of the indexes the relationship is non-linear. The results show that the Hurst index is less than 0.5 for the last 21 years, i.e. the volatility is rough. The value of the Hurst index varies within certain borders and evolves in packages. During financial turbulences the value of the Hurst index increases, i.e. the volatility gets smoother.

Bibliography

[1] C. Acerbi. Spectral measures of risk: A coherent representation of subjective risk aversion. *Journal of Banking & Finance*, 26(7):1505–1518, 2002.

[2] C. Acerbi and B. Szekely. Back-testing expected shortfall. *Risk*, 27 (11):76–81, 2014.

[3] C. Acerbi and D. Tasche. On the coherence of expected shortfall. *Journal of banking & finance*, 26(7):1487–1503, 2002.

[4] M.D. Adegbola, A.E. Adegbola, P. Amajuoyi, L.B. Benjamin, and K.B. Adeusi. Quantum computing and financial risk management: A theoretical review and implications. *Computer science & IT research journal*, 5(6):1210–1220, 2024.

[5] D. Ahelegbey, P. Giudici, and F. Mojtahedi. Tail risk measurement in crypto-asset markets. *International Review of Financial Analysis*, 73: 101604, 2021.

[6] A. Ahmadi-Javid. An information-theoretic approach to constructing coherent risk measures. In *2011 IEEE International Symposium on Information Theory Proceedings*, pages 2125–2127. IEEE, 2011.

[7] A. Ahmadi-Javid. Entropic value-at-risk: A new coherent risk measure. *Journal of Optimization Theory and Applications*, 155:1105–1123, 2012.

[8] A. Ahmadi-Javid and M. Fallah-Tafti. Portfolio optimization with entropic value-at-risk. *European Journal of Operational Research*, 279(1): 225–241, 2019.

[9] A. Ahmadi-Javid and A. Pichler. An analytical study of norms and Banach spaces induced by the entropic value-at-risk. *Mathematics and Financial Economics*, 11(4):527–550, 2017.

[10] D. Ahmed, F. Soleymani, M.Z. Ullah, and H. Hasan. Managing the risk based on entropic value-at-risk under a normal-rayleigh distribution. *Applied Mathematics and Computation*, 402:126129, 2021.

[11] C. Alexander. *Market risk analysis, value at risk models*. John Wiley & Sons, 2009.

[12] U. Anand and KS Manu. Role of options greeks in risk management. *International Journal of Management Studies*, 3:33–45, 2021.

[13] O.M. Ardakani. Coherent measure of portfolio risk. *Finance Research Letters*, 57:104222, 2023.

[14] C. Argyropoulos and E. Panopoulou. Backtesting var and es under the magnifying glass. *International Review of Financial Analysis*, 64: 22–37, 2019.

[15] P. Artzner, F. Delbaen, J.-M. Eber, and D. Heath. Coherent measures of risk. *Mathematical Finance*, 9(3):203–228, 1999.

[16] H. Assa, M. Morales, and H. Omidi Firouzi. On the capital allocation problem for a new coherent risk measure in collective risk theory. *Risks*, 4(3):30, 2016.

[17] M.G. Avci and M. Avci. An empirical analysis of the cardinality constrained expectile-based VaR portfolio optimization problem. *Expert Systems with Applications*, 186:115724, 2021.

[18] A. Axelrod and G. Chowdhary. A dynamic risk form of entropic value at risk. In *AIAA Scitech 2019 Forum*, page 0392, 2019.

[19] R.T. Baillie, F. Calonaci, D. Cho, and S. Rho. Long memory, realized volatility and heterogeneous autoregressive models. *Journal of Time Series Analysis*, 40(4):609–628, 2019.

[20] D. Bates. Jumps and stochastic volatility: The exchange rate processes implicit in deutschemark options. *Review of Financial Studies*, 9:69–107, 1996.

[21] C. Bayer, P. Friz, and J. Gatheral. Pricing under rough volatility. *Quantitative Finance*, 16(6):887–904, 2016.

[22] F. Bellini and E. Di Bernardino. Risk management with expectiles. *The European Journal of Finance*, 23(6):487–506, 2017.

[23] F. Bellini and V. Bignozzi. On elicitable risk measures. *Quantitative Finance*, 15(5):725–733, 2015.

[24] F. Bellini, B. Klar, A. Müller, and E.R. Gianin. Generalized quantiles as risk measures. *Insurance: Mathematics and Economics*, 54:41–48, 2014.

[25] F. Bellini, F. Cesarone, Ch. Colombo, and F. Tardella. Risk parity with expectiles. *European Journal of Operational Research*, 291(3): 1149–1163, 2021.

[26] F. Bellini, T. Fadina, R. Wang, and Y. Wei. Parametric measures of variability induced by risk measures. *Insurance: Mathematics and Economics*, 106:270–284, 2022.

[27] M. Bennedsen, A. Lunde, and M. Pakkanen. Decoupling the short- and long-term behavior of stochastic volatility. *Journal of financial econometrics*, 20(5):961–1006, 2022.

[28] S.R. Bentes. How covid-19 has affected stock market persistence? evidence from the g7's. *Physica A: Statistical Mechanics and its Applications*, 581:126210, 2021.

[29] J. Beran. *Statistics for long-memory processes*. Routledge, 2017.

[30] C. Berzin, A. Latourn, and J.R. León. *Inference on the Hurst parameter and the variance of diffusions driven by fractional Brownian motion*, volume 216. Springer, 2014.

[31] A. Bhattacharjee, M. Nandy, and S. Lodh. Covid-19 and persistence in the stock market: a study on a leading emerging market. *International Journal of Disclosure and Governance*, pages 1–12, 2024.

[32] F. Biagini, Y. Hu, B. Øksendal, and Th. Zhang. *Stochastic calculus for fractional Brownian motion and applications*. Springer, 2008.

[33] M.L. Bianchi, St.V. Stoyanov, G.L. Tassinari, F.K. Fabozzi, and S.M. Focardi. *Handbook of heavy-tailed distributions in asset management and risk management*. World Scientific, 2019.

[34] A. Biglova, S. Ortobelli, S. Rachev, and S. Stoyanov. Different approaches to risk estimation in portfolio theory. *Journal of Portfolio Management*, 31(1):103, 2004.

[35] F. Black and M. Scholes. The pricing of options and corporate liabilities. *Journal of Political Economy*, 81(3):637–654, 1973.

[36] G. Bormetti, V. Cazzola, G. Livan, G. Montagna, and O. Nicrosini. A generalized Fourier transform approach to risk measures. *Journal of Statistical Mechanics: Theory and Experiment*, 2010(01):P01005, 2010.

[37] M. Brandtner, W. Kürsten, and R. Rischau. Entropic risk measures and their comparative statics in portfolio selection: Coherence vs. convexity. *European Journal of Operational Research*, 264(2):707–716, 2018.

[38] E. Del Brio, A. Mora-Valencia, and J. Perote. Risk quantification for commodity etfs: Backtesting value-at-risk and expected shortfall. *International Review of Financial Analysis*, 70:101163, 2020.

[39] M. Burzoni, C. Munari, and R. Wang. Adjusted expected shortfall. *Journal of Banking & Finance*, 134:106297, 2022.

[40] J. Cai and K.S. Tan. Optimal Retention for a Stop-loss Reinsurance Under the VaR and CTE Risk Measures. *ASTIN Bulletin*, 37(1):93–112, 2007.

[41] I. Cascos and M. Ochoa. Expectile depth: Theory and computation for bivariate datasets. *Journal of Multivariate Analysis*, 184:104757, 2021.

[42] L. Catania and A. Luati. Quasi maximum likelihood estimation of value at risk and expected shortfall. *Econometrics and Statistics*, 2021.

[43] D.M. Chance. *An introduction to derivatives and risk management*. Cengage Learning, 2016.

[44] J.M. Chen. On exactitude in financial regulation: Value-at-risk, expected shortfall, and expectiles. *Risks*, 6(2):61, 2018.

[45] Zh. Chengli and Ch. Yan. Coherent risk measure based on relative entropy. *Applied Mathematics & Information Sciences*, 6(2):233–238, 2012.

[46] S. Chennaf and J.B. Amor. Entropic value at risk to find the optimal uncertain random portfolio. *Soft Computing*, 27(20):15185–15197, 2023.

[47] H. Chernoff. A measure of asymptotic efficiency for tests of a hypothesis based on the sum of observations. *The Annals of Mathematical Statistics*, pages 493–507, 1952.

[48] M. Choudhry. *Analysing and interpreting the yield curve*. John Wiley & Sons, 2019.

[49] P. Christoffersen. *Elements of financial risk management*. Academic press, 2011.

[50] Basel Committee et al. Fundamental review of the trading book: A revised market risk framework. *Consultative Document, October*, 2013.

[51] R. Cont. Empirical properties of asset returns: stylized facts and statistical issues. *Quantitative finance*, 1(2):223, 2001.

[52] R. Cont and P. Das. Rough volatility: fact or artefact? *Sankhya B*, 86 (1):191–223, 2024.

[53] R. Cont and P. Tankov. *Financial modelling with jump processes*. Chapman and Hall/CRC, 2003.

[54] J.C. Cox, J.E.Jr Ingersoll, and S.A. Ross. A theory of the term structure of interest rates. *Econometrica*, 53:385–407, 1985.

[55] J. D. Curto and P. Serrasqueiro. The impact of covid-19 on s&p500 sector indices and fatang stocks volatility: An expanded aparch model. *Finance Research Letters*, 46A, 2022.

[56] J.D. Curto and P. Serrasqueiro. The impact of covid-19 on s&p500 sector indices and fatang stocks volatility: An expanded aparch model. *Finance Research Letters*, 46:102247, 2022.

[57] Zh. Dai, J. Kang, and F. Wen. Predicting stock returns: A risk measurement perspective. *International Review of Financial Analysis*, 74: 101676, 2021.

[58] J. Daníelsson. *Financial risk forecasting: The theory and practice of forecasting market risk with implementation in R and Matlab*. John Wiley & Sons, 2011.

[59] J. Daníelsson, P. Embrechts, Ch. Goodhart, C. Keating, F. Muennich, O. Renault, H. Shin, et al. An academic response to basel ii, 2001.

[60] J. Daníelsson, B. Jorgensen, G. Samorodnitsky, M. Sarma, and C.G. de Vries. Fat tails, var and subadditivity. *Journal of econometrics*, 172 (2):283–291, 2013.

[61] A. Daouia, S. Girard, and G. Stupfler. Expecthill estimation, extreme risk and heavy tails. *Journal of Econometrics*, 221(1):97–117, 2021.

[62] A.C. Davison, S.A. Padoan, and G. Stupfler. Tail risk inference via expectiles in heavy-tailed time series. *Journal of Business & Economic Statistics*, pages 1–34, 2022.

[63] S. del Baño Rollin, A. Ferreiro-Castilla, and F. Utzet. On the density of log-spot in the Heston volatility model. *Stochastic Processes and their Applications*, 120(10):2037–2063, 2010. ISSN 0304-4149. doi: https://doi.org/10.1016/j.spa.2010.06.003. URL https://www.sciencedirect.com/science/article/pii/S0304414910001560.

[64] F. Delbaen. *Remark on the Paper "Entropic Value-at-Risk: A New Coherent Risk Measure" by Amir Ahmadi-Javid, J. Optim. Theory Appl., 155(3) (2001) 1105–1123*, chapter Chapter 7, pages 151–158. World Scientific, 2001.

[65] F. Delbaen. Coherent risk measures on general probability spaces. *Advances in finance and stochastics: essays in honour of Dieter Sondermann*, pages 1–37, 2002.

[66] M. Dempsey. *Financial risk management and derivative instruments*. Routledge, 2021.

[67] D. Dentcheva and A. Ruszczynski. *Risk-averse optimization and control*. Springer, 2024.

[68] D. Dentcheva and G. Stock. On the price of risk in a mean-risk optimization model. *Quantitative Finance*, 18(10):1699–1713, 2018.

[69] D. Dentcheva, S. Penev, and A. Ruszczyński. Statistical estimation of composite risk functionals and risk optimization problems. *Annals of the Institute of Statistical Mathematics*, 69(4):737–760, 2017.

[70] T. Dimitriadis and J. Schnaitmann. Forecast encompassing tests for the expected shortfall. *International Journal of Forecasting*, 37(2):604–621, 2021.

[71] A. Dragulescu and V. Yakovenko. Probability distribution of returns in the heston model with stochastic volatility. *Quantitative finance*, 2 (6):443, 2002.

[72] S. Drapeau and M. Tadese. Dual representation of expectile based expected shortfall and its properties. *arXiv preprint arXiv:1911.03245*, 2019.

[73] E. Dri, A. Yomi, M. Vetrivelan, C. Kuassivi, and I.D. Exposito. Exploring quantum-enhanced estimation of financial risk metrics with quantum rng. *arXiv preprint arXiv:2502.02125*, 2025.

[74] P. Embrechts and R. Wang. Seven proofs for the subadditivity of expected shortfall. *Dependence Modeling*, 3(1):000010151520150009, 2015.

[75] O. El Euch and M. Rosenbaum. The characteristic function of rough heston models. *Mathematical Finance*, 29(1):3–38, 2019.

[76] E. Fama. Efficient capital markets: A review of theory and empirical work. *The journal of Finance*, 25(2):383–417, 1970.

[77] W. Feller. Two singular diffusion problems. *Annals of mathematics*, pages 173–182, 1951.

[78] M. R. Fengler. *Semiparametric modeling of implied volatility*. Springer, 2005.

[79] H. Föllmer and T. Knispel. Entropic risk measures: Coherence vs. convexity, model ambiguity and robust large deviations. *Stochastics and Dynamics*, 11(02n03):333–351, 2011.

[80] H. Föllmer and T. Knispel. Convex risk measures: Basic facts, law-invariance and beyond, asymptotics for large portfolios. In *Handbook of the fundamentals of financial decision making: Part II*, pages 507–554. World Scientific, 2013.

[81] H. Föllmer and A. Schied. Convex measures of risk and trading constraints. *Finance and stochastics*, 6:429–447, 2002.

[82] H. Föllmer and A. Schied. *Stochastic finance: an introduction in discrete time*. Walter de Gruyter, 2004.

[83] S. Fuchs, R. Schlotter, and K. Schmidt. A review and some complements on quantile risk measures and their domain. *Risks*, 5(4):59, 2017.

[84] M. Fukasawa, T. Takabatake, and R. Westphal. Is volatility rough? *arXiv preprint arXiv:1905.04852*, 2019.

[85] L. Gao, W. Ye, and R. Guo. Jointly forecasting the value-at-risk and expected shortfall of bitcoin with a regime-switching caviar model. *Finance Research Letters*, 48:102826, 2022.

[86] J. Gatheral. *The volatility surface: a practitioner's guide*. John Wiley & Sons, 2011.

[87] J. Gatheral. Rough volatility. *Eventos do IMPA*, 2018. URL https://impa.br/en_US/eventos-do-impa/eventos-2018/research-in-options-2018/.

[88] J. Gatheral, T. Jaisson, and M. Rosenbaum. Volatility is rough. In *Commodities*, pages 659–690. Chapman and Hall/CRC, 2022.

[89] P. Georgieva and I. Popchev. Application of q-measure in real time fuzzy system for managing financial assets. *IJSC*, 3(4):21–38, 2012.

[90] P. Georgieva and I. Popchev. Fuzzy logic q-measure model for managing financial investments. *COMPTES RENDUS DE L ACADEMIE BULGARE DES SCIENCES*, 66(5):651–658, 2013.

[91] H.U. Gerber, E.S.W. Shiu, and H. Yang. A constraint-free approach to optimal reinsurance. *Scandinavian Actuarial Journal*, 2019(1):62–79, 2019.

[92] B. Ghosh, E. Bouri, J.B. Wee, and N. Zulfiqar. Return and volatility properties: Stylized facts from the universe of cryptocurrencies and nfts. *Research in International Business and Finance*, 65:101945, 2023.

[93] T. Gneiting. Making and evaluating point forecasts. *Journal of the American Statistical Association*, 106(494):746–762, 2011.

[94] S. Goncalves and M. Guidolin. Predictable dynamics in the s&p 500 index options implied volatility surface. *The Journal of Business*, 79 (3):1591–1635, 2006.

[95] Michael Grabchak and Gennady Samorodnitsky. Do financial returns have finite or infinite variance? a paradox and an explanation. *Quantitative Finance*, 10(8):883–893, 2010.

[96] M. Gulliksson, S. Mazur, and A. Oleynik. Minimum var and minimum cvar optimal portfolios: The case of singular covariance matrix. *Results in Applied Mathematics*, 26:100557, 2025.

[97] M. Hallin and C. Trucíos. Forecasting value-at-risk and expected shortfall in large portfolios: A general dynamic factor model approach. *Econometrics and Statistics*, 2021.

[98] A. Hamel. Monetary measures of risk. *arXiv preprint arXiv:1812.04354*, 2018.

[99] M. Herdegen and C. Munari. An elementary proof of the dual representation of expected shortfall. *Mathematics and Financial Economics*, 17(4):655–662, 2023.

[100] S. Heston. A closed-form solution for options with stochastic volatility with applications to bond and currency options. *Review of Financial Studies*, 6(2):327–343, 1993.

[101] P. Houlihan and G. Creamer. Leveraging a call-put ratio as a trading signal. *Quantitative Finance*, 19(5):763–777, 2019.

[102] J. Hu, Y. Chen, and K. Tan. Estimation of high conditional tail risk based on expectile regression. *ASTIN Bulletin*, 51(2):539–570, 2021.

[103] W. Hu and Zh. Zheng. Expectile capm. *Economic Modelling*, 88:386–397, 2020.

[104] J. Hull. *Risk management and financial institutions*. John Wiley & Sons, 2023.

[105] F. Ielpo and G. Simon. Mean-reversion properties of implied volatilities. *The European Journal of Finance*, 16(6):587–610, 2010.

[106] N.P. Indah and A. Fadilla. Assessing Optimal Retention With Quantile and Expectile Risk Measure. In *Brawijaya International Conference on Multidisciplinary Sciences and Technology (BICMST 2020)*, pages 11–14. Atlantis Press, 2020.

[107] T. Jalal. Stable and tempered stable distributions and processes: an overview toward trajectory simulation. *arXiv preprint arXiv:2412.06374*, 2024.

[108] R. Jarrow and A. Chatterjea. *Introduction To Derivative Securities, Financial Markets, And Risk Management, An*. World Scientific, 2024.

[109] L. Jia. A new coherent risk measure of entropic value at risk for uncertain systems. *Journal of Uncertain Systems*, 17(01):2350013, 2024.

[110] R.S. Johnson. *Derivatives markets and analysis*. John Wiley & Sons, 2017.

[111] M.C. Jones. Expectiles and M-quantiles are quantiles. *Statistics & Probability Letters*, 20(2):149–153, 1994.

[112] E. Kamal and E. Bouri. Green bond, stock, cryptocurrency, and commodity markets: a multiscale analysis and portfolio implications. *Financial Innovation*, 11(1):100, 2025.

[113] A. Karmous, H. Boubaker, and L. Belkacem. Forecasting volatility for an optimal portfolio with stylized facts using copulas. *Computational Economics*, 58(2):461–482, 2021.

[114] D. Kim and M. Shin. Volatility models for stylized facts of high-frequency financial data. *Journal of Time Series Analysis*, 44(3):262–279, 2023.

[115] Y.S. Kim, S. Rachev, M. Bianchi, and F. Fabozzi. Computing var and avar in infinitely divisible distributions. *Probability and Mathematical Statistics*, 30(2):223–245, 2010.

[116] I. Koponen. Analytic approach to the problem of convergence of truncated lévy flights towards the gaussian stochastic process. *Physical Review E*, 52(1):1197, 1995.

[117] Ch.M. Kuan, J.H. Yeh, and Y.Ch. Hsu. Assessing value at risk with CARE, the Conditional Autoregressive Expectile models. *Journal of Econometrics*, 150(2):261–270, 2009.

[118] U. Küchler and S. Tappe. Exponential stock models driven by tempered stable processes. *Journal of Econometrics*, 181(1):53–63, 2014.

[119] E. Lazar and X. Xue. Forecasting risk measures using intraday data in a generalized autoregressive score framework. *International Journal of Forecasting*, 36(3):1057–1072, 2020.

[120] A. Leccadito, A. Staino, and P. Toscano. A novel robust method for estimating the covariance matrix of financial returns with applications to risk management. *Financial Innovation*, 10(1):116, 2024.

[121] H. Li and R. Wang. PELVE: Probability Equivalent Level of VaR and ES. *Journal of Econometrics*, pages –, 2022.

[122] H. Lin, D. Saunders, and Ch. Weng. Mean-expectile portfolio selection. *Applied Mathematics & Optimization*, 83(3):1585–1612, 2021.

[123] F. Liu and R. Wang. A Theory for Measures of Tail Risk. *Mathematics of Operations Research*, 46(3):1109–1128, 2021.

[124] W. Liu, L. Yang, and B. Yu. Distributionally robust optimization based on kernel density estimation and mean-entropic value-at-risk. *INFORMS Journal on Optimization*, 5(1):68–91, 2023.

[125] A. Lo. *Adaptive markets: Financial evolution at the speed of thought*. Princeton University Press, 2017.

[126] A. Lo and A.C. MacKinlay. A non-random walk down wall street. In *A Non-Random Walk Down Wall Street*. Princeton University Press, 2011.

[127] E. Lukacs. *Characteristic Functions 2nd edn.* Griffin, London, 1970.

[128] Y. Lyu, F. Qin, R. Ke, M. Yang, and J. Chang. Forecasting the var of the crude oil market: A combination of mixed data sampling and extreme value theory. *Energy Economics*, 133:107500, 2024.

[129] B.G. Malkiel. *A random walk down Wall Street: the time-tested strategy for successful investing.* WW Norton & Company, 2019.

[130] H. Malmsten and T. Teräsvirta. Stylized facts of financial time series and three popular models of volatility. *European Journal of pure and applied mathematics*, 3(3):443–477, 2010.

[131] B. Mandelbrot and R. Hudson. *The Misbehavior of Markets: A fractal view of financial turbulence.* Basic books, 2007.

[132] B. Mandelbrot and J.W. Van Ness. Fractional brownian motions, fractional noises and applications. *SIAM review*, 10(4):422–437, 1968.

[133] P. Marcin and T. Schmidt. Estimating and backtesting risk under heavy tails. *Insurance: Mathematics and Economics*, 104:1–14, 2022.

[134] Ph. Masset. Volatility stylized facts. *Available at SSRN 1804070*, 2011.

[135] A.J. McNeil, R. Frey, and P. Embrechts. *Quantitative risk management: concepts, techniques and tools-revised edition.* Princeton university press, 2015.

[136] M. Meyer. How to use and derive stylized facts for validating simulation models. In *Computer Simulation Validation: Fundamental Concepts, Methodological Frameworks, and Philosophical Perspectives*, pages 383–403. Springer, 2019.

[137] A. Mihoci, W.K. Härdle, and Ch.Y.H. Chen. TERES: Tail Event Risk Expectile Shortfall. *Quantitative Finance*, 21(3):449–460, 2021.

[138] Y. Mishura, K. Ralchenko, P. Zelenko, and V. Zubchenko. Properties of the entropic risk measure evar in relation to selected distributions. *Modern Stochastics: Theory and Applications*, 11(4):373–394, 2024.

[139] S. Mozumder, M.K. Hassan, and M.H. Kabir. An evaluation of the adequacy of lévy and extreme value tail risk estimates. *Financial Innovation*, 10(1):100, 2024.

[140] D. Nedeltchev and T.S. Zaevski. Volatility structure during financial turbulence. *IMEA 2024 - Informatics, Mathematics, Education and their Applications*, 1(1):1–12, 2024. URL https://imea2024.fmi-plovdiv.org/wp-content/uploads/2025/01/2_2_Nedeltchev_Zaevski_47_60.pdf.

[141] D. Nedeltchev and T.S. Zaevski. Measuring market risk through entropic var. *Working Paper*, x:y, 2025.

[142] M. Neisen and St. Röth. *Basel IV: The next generation of risk weighted assets*. John Wiley & Sons, 2018.

[143] W.K. Newey and J.L. Powell. Asymmetric least squares estimation and testing. *Econometrica: Journal of the Econometric Society*, pages 819–847, 1987.

[144] N.Q.A. Nguyen and T.N.T. Nguyen. Risk measures computation by Fourier inversion. *The Journal of Risk Finance*, 18(1):76–87, 2017.

[145] N. Nolde and J.F. Ziegel. Elicitability and backtesting: Perspectives for banking regulation. *The Annals of Applied Statistics*, 11(4):1833–1874, 2017.

[146] P. Nymand-Andersen. *Yield curve modelling and a conceptual framework for estimating yield curves: evidence from the European Central Bank's yield curves*. Number 27 in ECB Statistics Paper. ECB Statistics Paper, 2018.

[147] B. Oksendal. *Stochastic Differential Equations: an Introduction with Aplication*. Springer-Verlag, 2003.

[148] Committee on Banking Regulations and Switzerland) Supervisory Practices (Basel. *International convergence of capital measurement and*

capital standards. Committee on Banking Regulations and Supervisory Practices (Basel, Switzerland), 1988.

[149] Basle Committee on Banking Supervision. *Revisions to the Basel II Market Risk Framework: Updated as of 31 December 2010*. Bank for International Settlements, 2011.

[150] A. Opschoor and A. Lucas. Observation-driven models for realized variances and overnight returns applied to value-at-risk and expected shortfall forecasting. *International Journal of Forecasting*, 37(2):622–633, 2021.

[151] P. Ortega-Jiménez, F. Pellerey, M.A. Sordo A, and A. Suárez-Llorens. Probability equivalent level for covar and var. *Insurance: Mathematics and Economics*, 115:22–35, 2024.

[152] Y.-H. Park. The effects of asymmetric volatility and jumps on the pricing of VIX derivatives. *Journal of Econometrics*, 192(1):313–328, 2016.

[153] E. Peters. *Fractal market analysis: applying chaos theory to investment and economics*. John Wiley & Sons, 1994.

[154] E. Peters. *Chaos and order in the capital markets: a new view of cycles, prices, and market volatility*. John Wiley & Sons, 1996.

[155] A. Pichler and R. Schlotter. Entropy based risk measures. *European Journal of Operational Research*, 285(1):223–236, 2020.

[156] J. Pitman and M. Yor. A decomposition of Bessel bridges. *Zeitschrift für Wahrscheinlichkeitstheorie und verwandte Gebiete*, 59(4):425–457, 1982.

[157] I. Popchev and N. Velinova. Application of monte carlo simulation in pricing of options. *Cybernetics and Information Technologies*, 3(2): 74–91, 2003.

[158] I. Popchev, I. Radeva, and I. Nikolova. Aspects of the evolution from risk management to enterprise global risk management. *Engineering sciences: journal of science department engineering sciences at the Bulgarian academy of sciences*, 1(1):16–30, 2021.

[159] Zh. Qiu, E. Lazar, and K. Nakata. Var and es forecasting via recurrent neural network-based stateful models. *International Review of Financial Analysis*, 92:103102, 2024.

[160] S. Rachev, S. Stoyanov, and F. Fabozzi. *Advanced Stochastic Models, Risk Assessment, and Portfolio Optimization: The Ideal Risk, Uncertainty, and Performance Measures*. Wiley, New York, 2008.

[161] S. Rachev, Y. Kim, M. Bianchi, and Fr.J. Fabozzi. *Financial models with Lévy processes and volatility clustering*. John Wiley & Sons, 2011.

[162] S. Rachev, S. Stoyanov, and F. Fabozzi. *A Probability Metrics Approach to Financial Risk Measures*. Wiley-Blackwell, 2011.

[163] BLS P. Rao. *Statistical inference for fractional diffusion processes*. John Wiley & Sons, 2011.

[164] R. Ren, M.-J. Lu, Y. Li, and W. Härdle. Financial risk meter frm based on expectiles. *Journal of Multivariate Analysis*, 189:104881, 2022.

[165] M. Righi, F. Müller, and M. Moresco. On a robust risk measurement approach for capital determination errors minimization. *Insurance: Mathematics and Economics*, 95:199–211, 2020.

[166] S. Roccioletti. *Backtesting value at risk and expected shortfall*. Springer, 2015.

[167] R.T. Rockafellar, S. Uryasev, and M. Zabarankin. Generalized deviations in risk analysis. *Finance and Stochastics*, 10:51–74, 2006.

[168] S.E. Rømer. Empirical analysis of rough and classical stochastic volatility models to the spx and vix markets. *Quantitative Finance*, 22(10): 1805–1838, 2022.

[169] F.D. Rouah. *The Heston model and its extensions in Matlab and C*. John Wiley & Sons, 2013.

[170] A. Ruszczyński and A. Shapiro. Optimization of risk measures. In *Probabilistic and randomized methods for design under uncertainty*, pages 119–157. Springer, 2006.

[171] E. Sinclair. *Option trading: Pricing and volatility strategies and techniques*. John Wiley & Sons, 2010.

[172] E. Sinclair. *Volatility trading*. John Wiley & Sons, 2013.

[173] G. Storti and C. Wang. Nonparametric expected shortfall forecasting incorporating weighted quantiles. *International Journal of Forecasting*, 38(1):224–239, 2022.

[174] M. Tadese and S. Drapeau. Relative bound and asymptotic comparison of expectile with respect to expected shortfall. *Insurance: Mathematics and Economics*, 93:387–399, 2020.

[175] D. Tasche. Expected shortfall is not elicitable. so what, 2014.

[176] W. Thomson. Eliciting production possibilities from a well-informed manager. *Journal of Economic Theory*, 20(3):360–380, 1979.

[177] B. Tong, X. Diao, and X. Li. Forecasting vars via hybrid evt with normal and non-normal filters: A comparative analysis from the chinese stock market. *Pacific-Basin Finance Journal*, 83:102271, 2024.

[178] J.E. Vera-Valdés. The persistence of financial volatility after covid-19. *Finance Research Letters*, 44:102056, 2022.

[179] S. Vine. *Options: trading strategy and risk management*, volume 288. John Wiley & Sons, 2011.

[180] J. Wang, S. Wang, M. Lv, and H. Jiang. Forecasting var and es by using deep quantile regression, GANs-based scenario generation, and heterogeneous market hypothesis. *Financial Innovation*, 10(1):36, 2024.

[181] C. Wen, J. Zhai, Y. Wang, and Y. Cao. Implied volatility is (almost) past-dependent: Linear vs non-linear models. *International Review of Financial Analysis*, 95:103406, 2024.

[182] J. Xia. Optimal investment with risk controlled by weighted entropic risk measures. *SIAM Journal on Financial Mathematics*, 15(1):54–92, 2024.

[183] B. Yang and Y. Ma. Value at risk, mispricing and expected returns. *International Review of Financial Analysis*, 78:101902, 2021.

[184] H. Yoshioka and Y. Yoshioka. Statistical evaluation of a long-memory process using the generalized entropic value-at-risk. *Environmetrics*, 35(4):e2838, 2024.

[185] T.S. Zaevski and O. Kounchev. A jump moment as a stopping time and defaultable derivatives. *Comptes rendus de l'Académie bulgare des Sciences*, 71(9):1186–1191, 2018. ISSN 2367-6248 (print),2603-4832 (online).

[186] T.S. Zaevski and D. Nedeltchev. From BASEL III to BASEL IV and beyond: Expected shortfall and expectile risk measures. *International Review of Financial Analysis*, 87:102645, 2023. ISSN 1057-5219. doi: https://doi.org/10.1016/j.irfa.2023.102645. URL https://www.sciencedirect.com/science/article/pii/S1057521923001618.

[187] T.S. Zaevski and D. Nedeltchev. Moment generating function of the averaged log-returns in the heston's stochastic volatility model. In *Proceedings of the Bulgarian Academy of Sciences*, volume 78, pages 321–330, 2025.

[188] T.S. Zaevski, Y. S. Kim, and F. J. Fabozzi. Option pricing under stochastic volatility and tempered stable lévy jumps. *International Review of Financial Analysis*, 31:101 – 108, 2014. ISSN 1057-5219. doi: https://doi.org/10.1016/j.irfa.2013.10.004. URL http://www.sciencedirect.com/science/article/pii/S1057521913001403.

[189] T.S. Zaevski, O. Kounchev, and M. Savov. Two frameworks for pricing defaultable derivatives. *Chaos, Solitons & Fractals*, 123:309–319, 2019. ISSN 0960-0779. doi: https://doi.org/10.1016/j.chaos.2019.04.025. URL http://www.sciencedirect.com/science/article/pii/S0960077919301365.

[190] S. Zhang and W. Fang. Multifractal behaviors of stock indices and their ability to improve forecasting in a volatility clustering period. *Entropy*, 23(8):1018, 2021.

[191] W. Zhong. Portfolio optimization under entropic risk management. *Acta Mathematica Sinica, English Series*, 25(7):1113–1130, 2009.

[192] R. Zhou, X. Liu, M. Yu, and K. Huang. Properties of risk measures of generalized entropy in portfolio selection. *Entropy*, 19(12):657, 2017.

[193] J.F. Ziegel. Coherence and elicitability. *Mathematical Finance*, 26(4): 901–918, 2016.

[194] Zh. Zou, Q. Wu, Z. Xia, and T. Hu. Adjusted rényi entropic value-at-risk. *European Journal of Operational Research*, 306(1):255–268, 2023.

[195] Zh. Zou, Zh. Xia, and T. Hu. Tsallis value-at-risk: generalized entropic value-at-risk. *Probability in the Engineering and Informational Sciences*, 38(1):1–20, 2024.

[196] G. Zumbach. *Discrete time series, processes, and applications in finance*. Springer Science & Business Media, 2012.